NATIONAL BUREAU OF STANDARDS REPORT

10 571

Progress Report

on

NOBLE METAL CONSTITUTION DIAGRAMS

U.S. DEPARTMENT OF COMMERCE

NATIONAL BUREAU OF STANDARDS

NATIONAL BUREAU OF STANDARDS

The National Bureau of Standards [1] was established by an act of Congress March 3, 1901. Today, in addition to serving as the Nation's central measurement laboratory, the Bureau is a principal focal point in the Federal Government for assuring maximum application of the physical and engineering sciences to the advancement of technology in industry and commerce. To this end the Bureau conducts research and provides central national services in four broad program areas. These are: (1) basic measurements and standards, (2) materials measurements and standards, (3) technological measurements and standards, and (4) transfer of technology.

The Bureau comprises the Institute for Basic Standards, the Institute for Materials Research, the Institute for Applied Technology, the Center for Radiation Research, the Center for Computer Sciences and Technology, and the Office for Information Programs.

THE INSTITUTE FOR BASIC STANDARDS provides the central basis within the United States of a complete and consistent system of physical measurement; coordinates that system with measurement systems of other nations; and furnishes essential services leading to accurate and uniform physical measurements throughout the Nation's scientific community, industry, and commerce. The Institute consists of an Office of Measurement Services and the following technical divisions:

Applied Mathematics—Electricity—Metrology—Mechanics—Heat—Atomic and Molecular Physics—Radio Physics [2]—Radio Engineering [2]—Time and Frequency [2]—Astrophysics [2]—Cryogenics.[2]

THE INSTITUTE FOR MATERIALS RESEARCH conducts materials research leading to improved methods of measurement standards, and data on the properties of well-characterized materials needed by industry, commerce, educational institutions, and Government; develops, produces, and distributes standard reference materials; relates the physical and chemical properties of materials to their behavior and their interaction with their environments; and provides advisory and research services to other Government agencies. The Institute consists of an Office of Standard Reference Materials and the following divisions:

Analytical Chemistry—Polymers—Metallurgy—Inorganic Materials—Physical Chemistry.

THE INSTITUTE FOR APPLIED TECHNOLOGY provides technical services to promote the use of available technology and to facilitate technological innovation in industry and Government; cooperates with public and private organizations in the development of technological standards, and test methodologies; and provides advisory and research services for Federal, state, and local government agencies. The Institute consists of the following technical divisions and offices:

Engineering Standards—Weights and Measures — Invention and Innovation — Vehicle Systems Research—Product Evaluation—Building Research—Instrument Shops—Measurement Engineering—Electronic Technology—Technical Analysis.

THE CENTER FOR RADIATION RESEARCH engages in research, measurement, and application of radiation to the solution of Bureau mission problems and the problems of other agencies and institutions. The Center consists of the following divisions:

Reactor Radiation—Linac Radiation—Nuclear Radiation—Applied Radiation.

THE CENTER FOR COMPUTER SCIENCES AND TECHNOLOGY conducts research and provides technical services designed to aid Government agencies in the selection, acquisition, and effective use of automatic data processing equipment; and serves as the principal focus for the development of Federal standards for automatic data processing equipment, techniques, and computer languages. The Center consists of the following offices and divisions:

Information Processing Standards—Computer Information — Computer Services — Systems Development—Information Processing Technology.

THE OFFICE FOR INFORMATION PROGRAMS promotes optimum dissemination and accessibility of scientific information generated within NBS and other agencies of the Federal government; promotes the development of the National Standard Reference Data System and a system of information analysis centers dealing with the broader aspects of the National Measurement System, and provides appropriate services to ensure that the NBS staff has optimum accessibility to the scientific information of the world. The Office consists of the following organizational units:

Office of Standard Reference Data—Clearinghouse for Federal Scientific and Technical Information [3]—Office of Technical Information and Publications—Library—Office of Public Information—Office of International Relations.

---

[1] Headquarters and Laboratories at Gaithersburg, Maryland, unless otherwise noted; mailing address Washington, D.C. 20234.
[2] Located at Boulder, Colorado 80302.
[3] Located at 5285 Port Royal Road, Springfield, Virginia 22151.

NATIONAL BUREAU OF STANDARDS REPORT

NBS PROJECT		NBS REPORT
311.05-11-3110561	April 20, 1971	10 571

Progress Report

on

NOBLE METAL CONSTITUTION DIAGRAMS

by

R. M. Waterstrat and R. C. Manuszewski*

* Research Associates, American Dental Association
Research Program in the Dental Research Section,
National Bureau of Standards, Washington, D. C. 20234

This investigation was supported in part by Research Grant DE02455 to the American Dental Association from the National Institute of Dental Research and is part of the dental research program conducted by the National Bureau of Standards, in cooperation with the American Dental Association; the Dental Research Division of the U. S. Army Medical Research and Development Command; the Dental Sciences Division of the School of Aerospace Medicine, USAF; the National Institute of Dental Research; and the Veterans Administration.

U.S. DEPARTMENT OF COMMERCE

NATIONAL BUREAU OF STANDARDS

October 15, 1970

NOBLE METAL CONSTITUTION DIAGRAMS

by

R. M. Waterstrat and R. C. Manuszewski*

*Research Associates, American Dental Association Research Program in the Dental Research Section, National Bureau of Standards, Washington, D. C. 20234

This investigation was supported in part by Research Grant DE02455 to the American Dental Association from the National Institute of Dental Research and is part of the dental research program conducted by the National Bureau of Standards, in cooperation with the American Dental Association; the Dental Research Division of the U. S. Army Medical Research and Development Command; the Dental Sciences Division of the School of Aerospace Medicine, USAF; the National Institute of Dental Research; and the Veterans Administration.

NBS PROGRESS REPORT 10 571

NOBLE METAL CONSTITUTION DIAGRAMS

R. M. Waterstrat and R. C. Manuszewski

SEPTEMBER 1970

Performed under
NIDR Research Grant DE02455 to
The American Dental Association.

Conducted at the
National Bureau of Standards
Washington, D. C. 20234

FOREWORD

This investigation was supported primarily by Research Grant DE02455 to the American Dental Association from the National Institute of Dental Research. The research was conducted at the National Bureau of Standards during the period from September 1, 1966 to August 31, 1970.

The electron probe microanalyses of two-phase alloys was performed at the National Bureau of Standards by Mr. Don Vieth, Mr. Barry Hammond, Mr. Robert Myklebust and Mr. Charles Fiore under the direction of Dr. Kurt Heinrich.

ABSTRACT

Four binary constitution diagrams involving the noble metals are presented. These diagrams include the Cr-Pt, Cr-Ir, Cr-Rh and V-Pt alloy systems.

Experimental alloys were prepared from starting materials having a nominal purity of at least 99.9% and precautions were taken to insure that no significant contamination was introduced during alloy preparation and heat-treatment. Temperatures were measured to an accuracy within ± 20°C.

TABLE OF CONTENTS

TABLE OF CONTENTS (Cont'd.)

LIST OF ILLUSTRATIONS

LIST OF ILLUSTRATIONS (Cont'd.)

LIST OF TABLES

I. SUMMARY

A. Constitution Diagrams

The constitution diagrams which have been determined are presented in Figure 1.

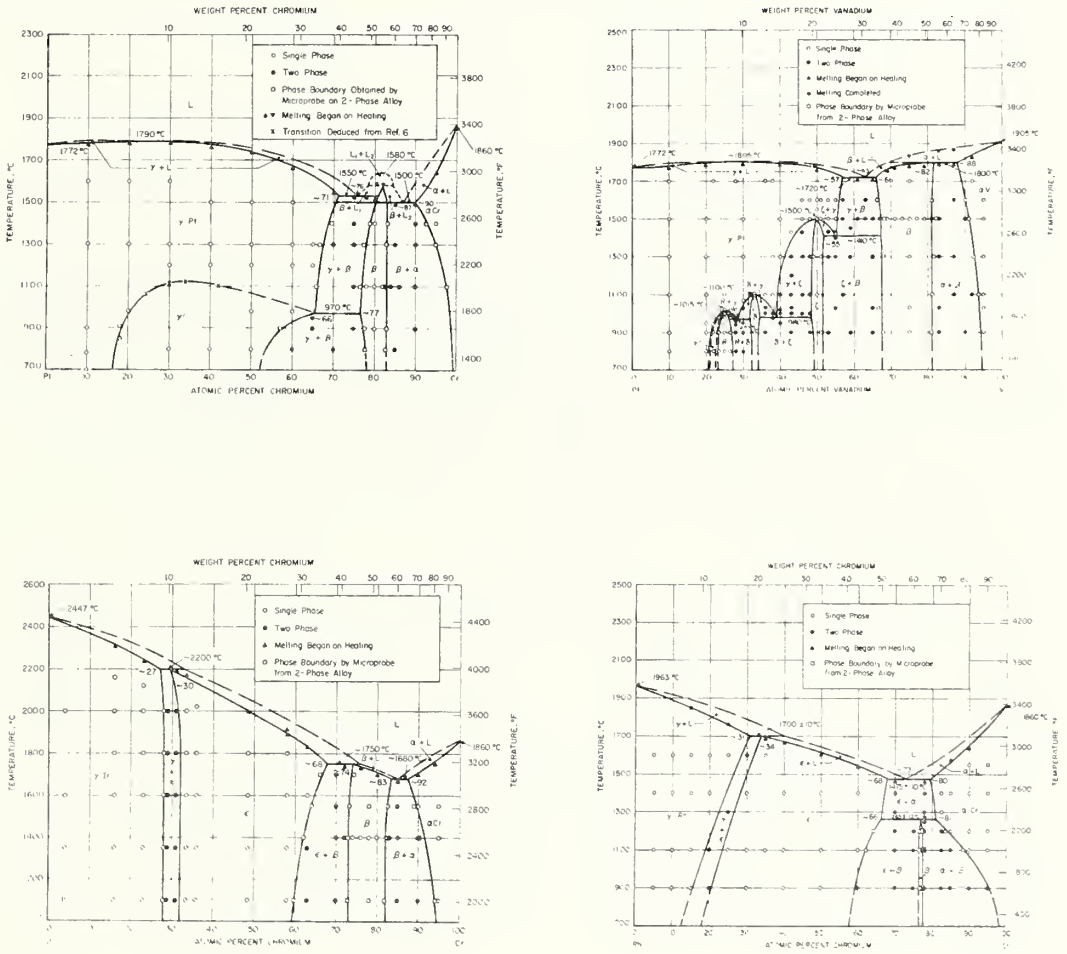

Fig. 1 - Constitution diagrams of chromium-platinum; vanadium-platinum; chromium-iridium; and chromium-rhodium.

B. Experimental Method

1. Materials

The purity of all the starting materials used in this study was at least 99.9%. This purity was considered to be adequate to insure a reliable constitution diagram within the accuracy limits imposed by uncertainties in temperature and composition measurements.

2. Alloy Preparation

The experimental alloys were prepared by non-consumable arc melting of the pure metals. The pure metals were submitted to melting in various forms. Chromium was in the form of fused droplets of about 1/8-inch diameter. Vanadium was in the form of electrolytic dendrites which were compacted into 1/2-inch diameter cylinders of the appropriate weight. Iridium and rhodium powder or sponge was also compressed into 1/2-inch diameter cylinders. Platinum was in the form of 1/32-inch sheet cut to an appropriate size.

3. Composition Determination

The primary method of establishing the compositions of the experimental alloys was by monitoring weight changes at various stages of the alloy preparation. In addition, compositions were checked by wet chemical analysis, electron probe microanalysis, and lattice parameter measurements whenever these techniques were appropriate.

4. Temperature Measurement

Temperatures below 1500°C were measured using platinum versus platinum-10% rhodium thermocouples. Temperatures between 1500°C and 2200°C were measured using tungsten versus

tungsten-26% rhenium thermocouples. These thermocouples were calibrated against a standard platinum-6% rhodium versus platinum-30% rhodium thermocouple up to 1600°C. The standard thermocouple had been calibrated at the National Bureau of Standards. Secondary melting point standards were used to check the calibration of the tungsten versus tungsten-26% rhenium thermocouples at higher temperatures and to assist in extrapolating a furnace current versus temperature plot. The secondary melting point standards were high purity wires of nickel, platinum, rhodium, and iridium. The accuracy of the temperature measurements was believed to be within ± 20°C.

5. Phase Boundary Determinations

a. Solidus - A technique was developed to allow direct observation of a melting specimen and to obtain its temperature reliably. This technique was suitable for solidus determinations in alloys which melt congruently or are close to a eutectic composition. It is also reliable for alloys having a relatively small temperature increment between their solidus and liquidus temperatures. For other alloys, the technique of metallographic examination of quenched alloys to detect incipient fusion is a more accurate method and was used to supplement the method of direct observation.

b. Phase Boundaries - The methods used to locate phase boundaries include metallographic examination, x-ray diffraction studies, and electron probe microanalysis of equilibrated two-phase alloys. In each case the specimens were rapidly cooled or quenched from the equilibration temperature. The methods used detect changes in microstructure, crystal structure, and chemical composition which occur when an alloy is equilibrated at various temperatures or when its composition is varied at a fixed temperature.

II. INTRODUCTION

A. Background

The existing metallurgical literature concerning binary or ternary constitution diagrams contains only a relatively small percentage of alloy combinations involving the noble metals (i.e., those metals which are exceptionally resistant to chemical corrosion or oxidation, such as gold and metals of the platinum group). The restricted industrial usage of the noble metals due to their limited availability and high cost may partly account for the scarcity of constitution diagrams. Another deterrent to such studies is the prohibitive cost of experimental samples, which should be of a sufficient number and size to permit measurements having the desired accuracy. It is probably not surprising, therefore, that the available noble metal constitution diagrams are sometimes inaccurate and in a few cases may even be considered to be essentially incorrect.

The importance of obtaining reliable constitution diagrams is widely recognized among those who are familiar with their uses. These diagrams may be directly used to predict equilibrium phase relationships and alloy microstructures for any given conditions of temperature, pressure, and alloy composition. With training and experience it is also possible to use these diagrams to predict the non-equilibrium microstructures which are produced when the alloy is cast, heat-treated, or subjected to various mechanical operations such as forging, drawing, rolling, etc. The existing microstructure is a highly important factor in determining the physical properties of an alloy.

The constitution diagram may be used to reveal other useful information. It is of considerable importance to know the temperature at which an alloy begins to melt (solidus temperature). A knowledge of the solidus temperature permits one to estimate recovery temperatures, recrystallization temperatures, and the rates of atomic

diffusion during annealing treatments. Accurate constitution diagrams may be used to determine various thermodynamic functions since the slopes of the phase boundaries are related to free energy relationships between the coexisting phases. Constitution diagrams are also helpful in studying the kinetics of phase transformations.

In recent years, there has been a considerable effort by alloy theorists to develop methods for predicting the extent of terminal solid solutions and the occurrence of intermediate phases having various crystal structures. Some attempts have been made to construct the entire binary constitution diagram on the basis of theoretical calculations. It appears that significant progress is being made in this direction, but such studies must continue to rely on experimental data in order to check the reliability of the theoretical calculations and to suggest new ways to improve their accuracy.

In order to obtain reliable experimental data, it is necessary to take many precautions during the preparation and examination of the experimental alloys. Starting materials should be of high purity and care must be taken to insure that the alloys are not contaminated during melting or heat-treating. Particular attention must be given to the problems of temperature measurement and composition determination since the accuracy of these measurements is a major factor in the production of a reliable constitution diagram.

Temperatures below 1500°C were measured with platinum versus platinum-10% rhodium thermocouples because of the high accuracy and reproducibility associated with this type of thermocouple. These thermocouples were periodically checked for accuracy against a standard platinum-6% rhodium versus platinum-30% rhodium thermocouple which had been calibrated at the National Bureau of Standards to 1600°C.

Temperatures above 1600°C are usually measured with an optical pyrometer, but this method did not yield satisfactory results in this study due to the formation of metallic films on the viewing windows. These films formed quite rapidly during the relatively brief time necessary for a temperature measurement, particularly when the experimental alloys contained chromium. It was impossible to make reliable corrections for this film absorption even by using a two-color pyrometer. Difficulties were also encountered in obtaining black-body radiation from within the hot zone of the furnace at a position which would yield a temperature corresponding to that of the experimental samples. Cylindrical black-bodies were fabricated of tantalum and designed to produce the necessary depth to diameter ratios, but it was found that these objects were unavoidably positioned within rather sharp temperature gradients and were, therefore, not at the uniform temperature which is essential for such black-body radiators.

In view of these difficulties with optical pyrometry, it was necessary to consider using high-temperature thermocouples for measuring the temperature between 1500°C and 2200°C. This method entails the risk of introducing errors due to thermocouple contamination by metal vapors. Metal vapors, in some cases, may even penetrate the refractory ceramics normally used to insulate the thermocouple, and for this reason it was decided to obtain thermocouples having an outer metallic sheath. Sheathed thermocouples are commercially available in a variety of sizes and also with several alternative combinations of ceramic insulators and metallic sheaths. The combination selected as being most suitable under the conditions of this investigation was a tungsten versus tungsten-26% rhenium thermocouple insulated with beryllium oxide and having a tantalum sheath. The size of the thermocouple wires was 0.005" diameter and the entire assembly was enclosed in a sheath having a diameter of 0.040", thus minimizing errors due to heat conduction along the axis of the thermocouple.

The tungsten versus tungsten-26% rhenium thermocouples were calibrated against the standard platinum-6% rhodium versus platinum-30% rhodium thermocouple to 1600°C under the same experimental conditions used in the actual measurements on the alloy samples. Simultaneous readings of current in the furnace heating elements were obtained during the calibration runs so that a plot of temperature versus current was also obtained. This plot could be extended to higher temperatures with the help of standard emf versus temperature data for the tungsten versus tungsten-26% rhenium thermocouples, together with secondary fixed points obtained by observing the melting of high purity wires of nickel (1455°C), platinum (1772°C), rhodium (1963°C), and iridium (2447°C). In addition, many experimental runs were accompanied by an appropriate determination of a secondary fixed point obtained just prior to the temperature determination. This procedure is explained in greater detail in Section III, G-1.

Alloy compositions were checked at various stages throughout this investigation. Considerable reliance was placed in the use of electron probe microanalysis to determine the compositions of coexisting phases in equilibrated two-phase alloys. In order to check the reliability of the probe data, however, it is desirable to submit certain alloys to a complete wet chemical analysis. Alloys selected for this purpose were given a homogenization anneal at a temperature intended to produce a single phase sample. The compositions selected in each system usually included the equiatomic composition. The alloys were checked for homogeneity using the electron probe and then submitted to wet chemical analysis. The result of this chemical analysis was used not only to check the probe data, but also to check the nominal composition of the alloy and the feasibility of determining alloy compositions by monitoring weight losses during melting. Careful consideration was given to the possibility of alloy contamination during melting and annealing. Metallographic studies, particularly at the surfaces of the experimental samples, were quite helpful in detecting contamination.

Many other difficulties were encountered which posed a continual challenge to the success of these studies. Some of these problems are common to all such investigations while others are unique to a particular alloy system. These problems are discussed in connection with each system.

III. CHROMIUM-PLATINUM CONSTITUTION DIAGRAM

A. Previous Studies

Chromium-platinum alloys have been studied in several previous investigations [1-6] but the results have been contradictory. In reviewing these studies, [1-5] Hansen and Anderko [7] have concluded that the data "are still insufficient to establish the exact constitution of the system."

Melting point data obtained by Müller [1] have indicated that the addition of chromium to pure platinum produces a broad maximum in the liquidus but thermal analysis data from three chromium-rich alloys [4] has led Gebhardt and Köster to conclude that Müller's melting curve is much too high. Hansen and Anderko [7] have also concluded that Müller's melting points "are certainly too high."

The present study contradicts these conclusions and establishes a location of the solidus which is in substantial agreement with Müller's results. The solidus temperatures are found to be significantly higher than those reported by Gebhardt and Köster. [4] Other results of Gebhardt and Köster have been contradicted by Raub and Mahler [5] who reported that the platinum solid solution and the chromium solid solution are separated by an intermediate phase, $PtCr_3$, having the A15 (β-W) crystal structure. Gebhardt and Köster [4] apparently did not detect this intermediate phase and consequently they erroneously concluded that the two terminal solid solutions coexist in the region between 80 and 100 atomic percent Cr. The present results are in agreement with those reported by Raub and Mahler [5] except that the intermediate phase is found to occur only for compositions on the Cr-rich side of the "ideal" ($PtCr_3$) stoichiometry.

B. Materials

The chromium metal used in this investigation was obtained from Leico Industries, Incorporated in the form of small droplets of about 1/8-inch diameter which were quite suitable for arc-melting. It's nominal purity was 99.999% with respect to nongaseous impurities. A spectrographic analysis of this material is shown in Table 1. The gaseous impurities were determined by vacuum fusion analyses and these results are also given in Table 1. It is apparent that the major impurity in this material is oxygen, which is present at a rather high concentration of over two atomic percent. This is an appreciable impurity content, and one must consider whether it can be responsible for significant changes in the location of phase boundaries. This problem was dealt with in two different ways.

One approach was to melt the alloys using the chromium with high oxygen content and then to deoxidize these alloys by annealing them in dry hydrogen at temperatures of 1400° or above. The effect of such a deoxidation anneal is quite visible in the microstructures of these alloys. It is manifested by a removal of oxide particles (presumably Cr_2O_3) from the microstructure. The oxide particles apparently contain most of the oxygen in these alloys. It has been reported that oxygen is not very soluble in chromium at low temperatures. One may therefore conclude that those samples which were relatively free of oxide inclusions were also essentially free of oxygen and that they can be used to establish the location of phase boundaries in the binary system. A comparison of experimental data obtained from the hydrogen-treated alloys with data obtained from the oxygen-containing alloys revealed that the location of phase boundaries was essentially unchanged by the observed oxygen contamination.

Table 1

Chemical and Spectrographic Analyses of the Materials Used in Preparing the Experimental Alloys †

	Chromium	Platinum
Impurity	Leico Metals Inc.	Stock supply
Ag	ND	<10
Ca	<10	ND
Cu	ND	<100
Fe	<10	<10
Mg	<10	<100
Ni	<10	ND
Pb	<10	ND
Pd	ND	<1000
Ru	ND	<100
Si	<10	<100
C	16	
H*	295	
O*	6540	
N*	6	

† Values are given in ppm.

ND Not detected spectrographically.

* Values obtained by vacuum fusion analysis.

No other elements were detected spectrographically.

Another approach to the problem of oxygen contamination was to submit the pure chromium pellets to a heat-treatment in dry hydrogen prior to melting the experimental alloys. These heat-treatments were performed over various time intervals ranging from three hours at 1700°C to three days at 1400°C. Alloys prepared from the deoxidized chromium pellets yielded results similar to those obtained from samples prepared from untreated chromium. For example, the microstructure of our untreated alloy, $Cr_{80}Pt_{20}$, in the "as-cast" condition (Fig.11b) has been largely responsible for our conclusion that a syntectic reaction occurs in the chromium-platinum system. This same microstructure has been obtained in "as-cast" alloys prepared using deoxidized chromium.

We have therefore concluded that oxygen contamination to the extent of up to two atomic percent does not change the location of the phase boundaries within the experimental error of our measurements.

The platinum metal was available from a stock supply whose original source was unknown. Spectrographic analysis, shown in Table 1, indicates a purity of about 99.9% with the major impurity being palladium. The platinum metal was in the form of 1/32-inch thick sheet which could be readily cut and bent to a shape which is suitable for arc-melting.

C. Alloy Preparation

The experimental alloys were prepared by weighing the appropriate amount of each elemental constituent and then melting these constituents in an arc furnace under an inert atmosphere. Further details are given below.

1. Weighing.

Samples were weighed out in 10 atom percent intervals across the entire phase diagram except in the vicinity of the anticipated phase boundaries where additional compositions were prepared. The components of each alloy were weighed to an accuracy of ± 0.01 gram and the total weight of each sample was approximately 20 grams. It was therefore possible to establish the nominal compositions of our alloys to within ± 0.05 weight percent. The weights were checked to this accuracy at various stages in the sample preparation in order to obtain a material balance for each alloy which would permit the establishment of maximum uncertainties in the alloy compositions.

2. Melting

The samples were arc melted on a water-cooled copper hearth using a non-consumable tungsten electrode. All melting was done in an atmosphere of 50% helium and 50% argon. These inert gases were of a special ultra-pure grade for which the gas analyses shown in Table 2 were provided by the manufacturer. No further purification of these gases was attempted but careful precautions were taken to insure that gas lines and regulators were clean and leak-tight in order to prevent contamination. The single-hearth melting chamber was evacuated and flushed several times with the inert gas mixture and the final evacuation was extended to a pressure of 10^{-3} mm or less. This pressure corresponds to a residual impurity level of less than 3.0 ppm which is comparable to the residual impurity levels in our ultra-pure inert gases as shown in Table 2.

Each sample was melted at least four times and was inverted in the hearth between each melt. Special precautions were taken with brittle alloys to insure that no fragments of the alloy were lost if a sample shattered under the arc. It was found that brittle alloys were much less susceptible to such losses if the

Table 2

Analyses of Inert Gases Used for
Arc-melting the Experimental Alloys †

Impurity	Argon		Helium
	Matheson Co.		Matheson Co.
CO_2	ND*	0.5	0.0
O_2		1.0	0.3
H_2	ND*	1.0	0.0
CO	ND*	0.5	--
N_2	<	2.0	1.0
CH_4	<	0.4	0.0
H_2O		3.5	1.5
Ne	---		9.2
A	---		0.0

† Impurities are given in ppm.

* None detected less than.

alloys were broken up into irregular lumps of about 1/4-inch thickness prior to any subsequent remelting. This was done using a hardened steel rod in a deep cylindrical hardened steel container so that none of the alloy fragments were lost. For most of the brittle alloys, only a light sharp blow was necessary to fracture the sample and no contamination from the steel container was detected.

D. Composition Determination of the Melts

The alloy compositions were established by chemical analyses, electron probe microanalyses, weight balances and lattice parameter measurements. Weight losses which occurred during melting of the platinum-rich alloys were always less than 1% but some chromium-rich alloys exhibited weight losses as high as 1.2% after four melts, or 1.7% after six melts. It was subsequently found that good agreement with the chemical analyses of our alloys was obtained if these weight losses were attributed entirely to losses of chromium.

Table 3

Chemical Analyses of Experimental Alloys

Intended Composition	Chromium atomic %	Platinum atomic %
$Cr_{10}Pt_{90}$	9.7	90.2
$Cr_{20}Pt_{80}$	20.0	80.0
$Cr_{30}Pt_{70}$	29.7	70.4
$Cr_{40}Pt_{60}$	39.5	60.4
$Cr_{50}Pt_{50}$	49.7	50.2
$Cr_{60}Pt_{40}$	59.4	40.5

The chemical analyses, shown in Table 3, were obtained from alloy samples which had been given a prior homogenization anneal in vacuum at elevated temperatures. The annealing treatment produced small weight losses and a metallographic

study revealed that these losses were essentially confined to a very thin layer on the surface of the sample which had been depleted of chromium. The homogenization anneal was given prior to chemical analysis in order that the chemical analysis results could be correlated with the electron probe data. The electron probe microanalyzer measures areas of about one micron diameter so the data would be unreliable if segregation occurred on a larger scale than this. However, it was subsequently found by line scanning that our platinum-rich alloys were quite homogeneous, even in the "as-cast" condition. This may be due to the existence of a congruent melting maximum in the platinum solid solution region.

Each of the alloys shown in Table 3 was cut in half after the homogenization anneal. One half was submitted to chemical analysis and the other half was used to obtain electron microprobe data. The results of the chemical analyses thus established the compositions of the standard samples which were used in calibrating the electron probe data on a quantitative basis.

The lattice parameters of alloys within the range of the platinum solid solution are plotted as a function of composition in Fig. 6, and the chemically analyzed alloys are included in this plot. The variation of the lattice parameters with composition is linear and the experimental data is in excellent agreement with data reported by Raub and Mahler [5] which is also plotted in Fig. 6.

E. Temperature Measurement

A platinum versus platinum-10% rhodium thermocouple was used to measure temperatures up to 1500°C. Temperatures above 1500°C were measured with a tungsten versus tungsten-26% rhenium thermocouple. Both of these thermocouples were periodically calibrated against a standard platinum-6% rhodium versus

platinum-30% rhodium thermocouple at temperatures up to 1600°C. The standard thermocouple had been calibrated at the National Bureau of Standards. In addition, the thermocouples were calibrated against secondary standards such as the melting points of pure nickel or pure platinum, particularly in connection with the determination of solidus or liquidus temperatures. Details of this procedure are given in Section III, G.

F. Thermal Treatments

1. Homogenization

Most of the samples used in this study were initially homogenized by heating to within about 200°C of the solidus temperature for about three hours. The homogenization treatment was conducted with all the precautions normally used in the equilibration treatments so that the samples could be considered as being equilibrated at the homogenization temperature.

Samples to be homogenized were placed in tantalum buckets suspended by tantalum wire within the hot zone of a tantalum strip resistance furnace operating at a pressure of between 5×10^{-6} and 5×10^{-7} mm Hg. No reaction between the samples and the tantalum was detected, and it is probable that any small reaction with Ta is insignificant in the temperature ranges which were used in this study.

The degree of homogenization was checked by means of the electron probe microanalyzer, metallographic examination, and by the sharpness of x-ray powder patterns obtained from the homogenized samples. In all cases, the samples appeared to be adequately homogenized.

2. Equilibration

Equilibration anneals at temperatures up to 1100°C were conducted by sealing the samples in quartz tubes (previously baked-out and evacuated) under a partial pressure of pure argon and then placing these tubes in a platinum-wound resistance furnace capable of being controlled within a temperature range of ± 1°C. For temperatures above 1100°C, the samples were equilibrated in a tantalum-strip resistance furnace operating at a pressure of 5×10^{-6} to 5×10^{-7} mm Hg. The samples were suspended in tantalum buckets but no tantalum pickup was detected in the alloy samples. Temperatures in this furnace were normally controlled to within ± 10°C, but could be maintained within ± 5°C over relatively short periods of time. This was verified by measuring temperature profiles through the hot zone using thermocouples which were inserted both vertically and horizontally. The temperature profiles were also used to establish the location of various temperature gradients within the hot zone. The alloy samples could then be located within the constant-temperature region.

Samples annealed in the tantalum-strip furnace were cooled rapidly from the annealing temperature by turning off the power to the heating elements. Samples annealed in the quartz tubes were quenched in cold water. In each case, the cooling rates were sufficient to permit retention of the phases which existed at the annealing temperature. However, atomic ordering in the Pt terminal solid solution region occurs very rapidly and it was not possible to retain the disordered condition for alloys containing over 20 atomic percent Cr.

G. Methods for Determination of Phase Boundaries

1. Solidus Temperatures

The accurate measurement of solidus temperature by conventional thermal analysis was found to be extremely

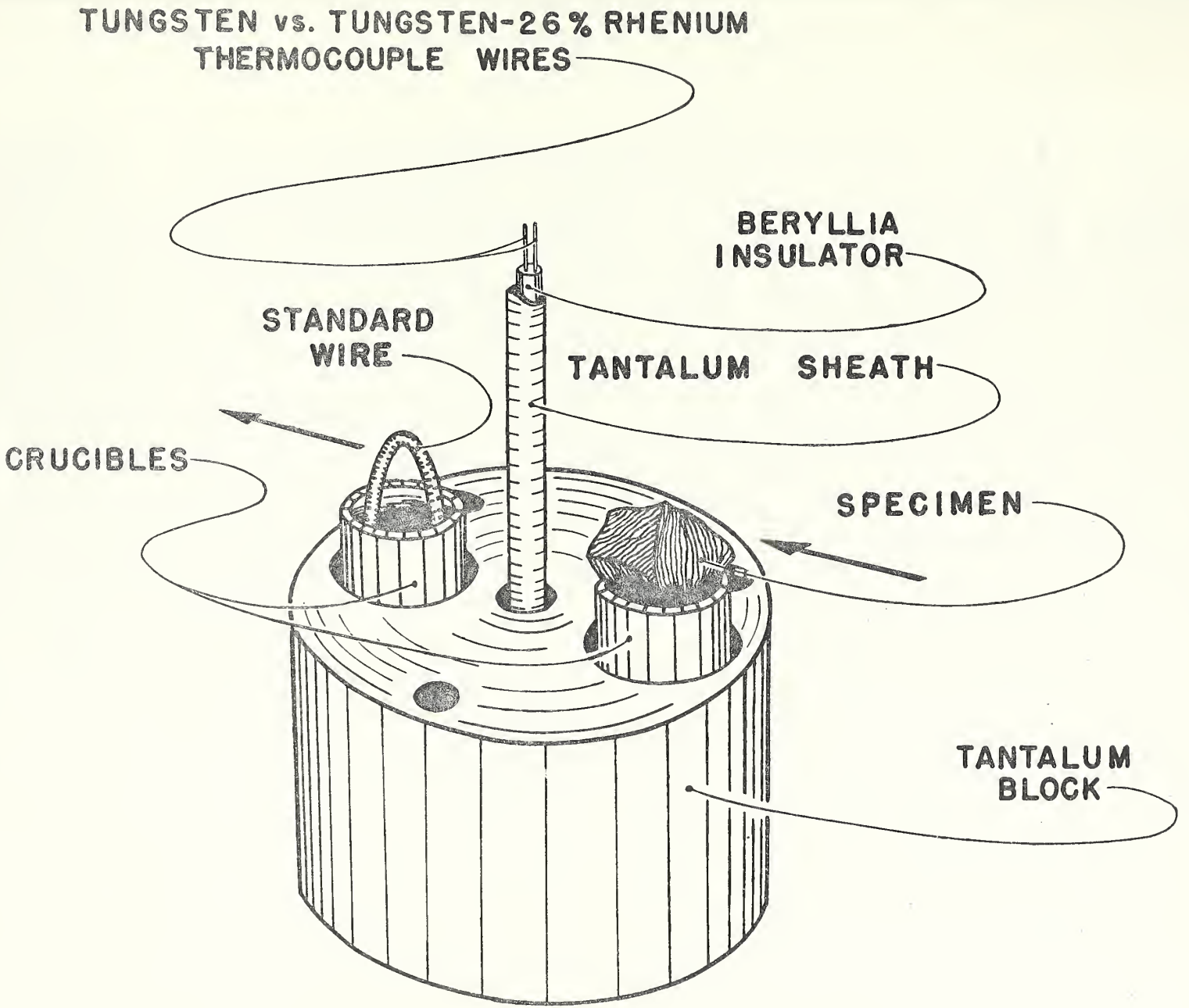

Fig. 2 - Apparatus used in the determination of solidus temperatures.

difficult due to the high vapor pressures and chemical activity of chromium when it is heated to relatively high temperatures. Thermocouples tend to become contaminated by Cr vapor, which may even penetrate the refractory tubes used as insulators for the thermocouple. Many refractories are chemically attacked by molten chromium alloys with a consequent serious contamination of the alloy. Optical pyrometry techniques are unreliable due to a rapid condensation of Cr vapor on the glass windows through which the optical measurements are made. The use of window shields, which are removable during the time interval necessary for a temperature measurement, helps to reduce fogging of the windows but does not appreciably alleviate the problems of temperature measurement due to the rapid rate at which the vapors are deposited. We were, therefore, unable to use conventional methods of thermal analysis in most cases, and were forced to utilize a method which is more suited to these severe experimental conditions.

A schematic drawing illustrating the technique which was used is shown in Fig. 2. A previously homogenized alloy specimen, together with a pure metal of known melting temperature, were placed in suitable refractory crucibles (alumina or thoria) in a manner such as to expose the upper portion of each metal to direct visual observation along the direction indicated by the arrows in Fig. 2. The crucibles are inserted into cylindrical holes drilled part-way into a tantalum cylinder of 1-1/4-inch diameter and about 7/8-inch height. The tantalum cylinder is suspended vertically within the constant temperature region of the vacuum furnace by means of tantalum wire which is inserted into three holes drilled through the tantalum cylinder near its periphery. At the center of the cylinder a vertical hole drilled part-way through the cylinder admits a sheathed thermocouple of tungsten versus tungsten-26% rhenium which can be used to measure temperatures at least up to about 2300°C in vacuum. The tantalum thermocouples sheath has a diameter of about 0.040", and is

closed at its lower end thus acting to protect the thermocouple from attack by metal vapors. The beryllia insulator serves to provide electrical insulation at high temperatures and is chemically inert to the thermocouple.

The alloy sample, which preferably has a jagged edge, and the standard wire are visible against a relatively cool background as viewed between the tantalum strips comprising the heating element of the furnace. Melting is readily detected by visual observation using dark glasses at the higher temperatures. The upper portions of the standard wires were found to melt before the lower portions melted. It was necessary to increase the furnace temperature by about 10°C in order to melt the lower portions of the wires. The alloy samples, however, extend only a short distance into the crucibles and when an alloy sample has melted, one generally observes that the entire sample suddenly falls down into the crucible and solidifies. The tip of the thermocouple is located within the tantalum cylinder near the base of the crucibles, however, and will probably measure a temperature approximately 10°C lower than that of the alloy samples which are visible above the rim of the crucibles. This correction, however, is included in our temperature calibration procedure since a thermocouple reading is obtained as the top of the standard wire begins to melt. The top of the wire is probably at a temperature nearly equal to that of the alloy specimen. Measurement of a vertical temperature profile can also be made by raising and lowering the thermocouple. This procedure also helps in establishing the temperature difference between the sample and the normal location of the thermocouple.

Losses of metal by vaporization during a solidus determination occurred mainly at the surface of the alloy specimens. Lattice parameter measurements on the bulk sample after a run usually indicated a composition change of about 1% or less. It appears that appreciable losses due to vaporization occur only after

the formation of a liquid phase. Our samples are usually in the liquid condition for only a few seconds during the run, thus minimizing metal losses. The use of a high vacuum during solidus determinations, therefore, seems justified since the avoidance of possible sample contamination by gaseous impurities prevents more serious errors than are introduced by the metal losses.

When making a melting temperature determination, the temperature of the furnace was raised in increments of about 5°C as the solidus point was approached. Between each increment, the temperature was allowed to equilibrate by waiting for the temperature-sensitive thermocouple to indicate a constant temperature.

This usually required less than a minute near the solidus temperature. Meanwhile, the metal samples are checked visually for signs of melting. The pure metals and many of the alloy samples melted very suddenly, but some of the alloy samples showed only slight rounding of sharp edges or changes in brightness as the solidus temperature was exceeded. Any question as to whether the sample had actually begun to melt could usually be settled by metallographic examination of the sample after its removal from the furnace. The thermocouple wires were of 0.005" diameter and it is, therefore, assumed that the temperature reading is not greatly affected by heat losses along the thermocouple wires.

A possible source of error in using pure metals with known melting points as temperature standards may arise if the pure metals become contaminated during the calibration procedure. We found no evidence for any significant contamination of the pure metal wires. Wires melted with and without the chromium alloy specimens melted at nearly the same temperature as indicated by the thermocouple readings and values of furnace current at tne melting point.

Our standard platinum-6% rhodium versus platinum-30% rhodium thermocouple was inserted in the furnace under standard operating conditions and a calibration of temperature versus furnace current was obtained up to 1700°C. This calibration was extended to higher temperatures by obtaining furnace current readings at the melting points of pure platinum (1772°C), pure rhodium (1963°C), and pure iridium (2447°C). The pure metal wires were of special high purity (99.99%) and had unusually low Fe and Si contents (<100 ppm). The use of furnace current as an indication of the temperature in the hot zone was considered fairly reliable. The method yielded good reproducibility under standard operating conditions and reasonable accuracy resulted owing to the fact that furnace temperature is a fairly sensitive function of furnace current as shown in Fig. 3.

The technique of visual observation of melting was considered to be best suited for pure elements and alloys melting isothermally. Thus, it is most reliable in the vicinity of congruent melting maxima and near eutectic compositions. For alloys melting over a wide temperature range, however, this method may yield erroneous results since such alloys may show no visual evidence of melting, even though much melting may have occurred. In such cases, the technique of "incipient melting" was used to obtain more accurate solidus temperatures. In this technique, an alloy sample is heated for a few minutes at a selected temperature. The furnace power is then turned off and the sample is removed and examined metallographically. If the solidus temperature has been exceeded, one usually observes rounded primary grains with a network of fine grains at the prior grain boundaries of the larger primary grains. Comparison of this structure with structures obtained by heating at lower temperatures enables one to determine the solidus temperature to the desired accuracy within the limits of the temperature calibration.

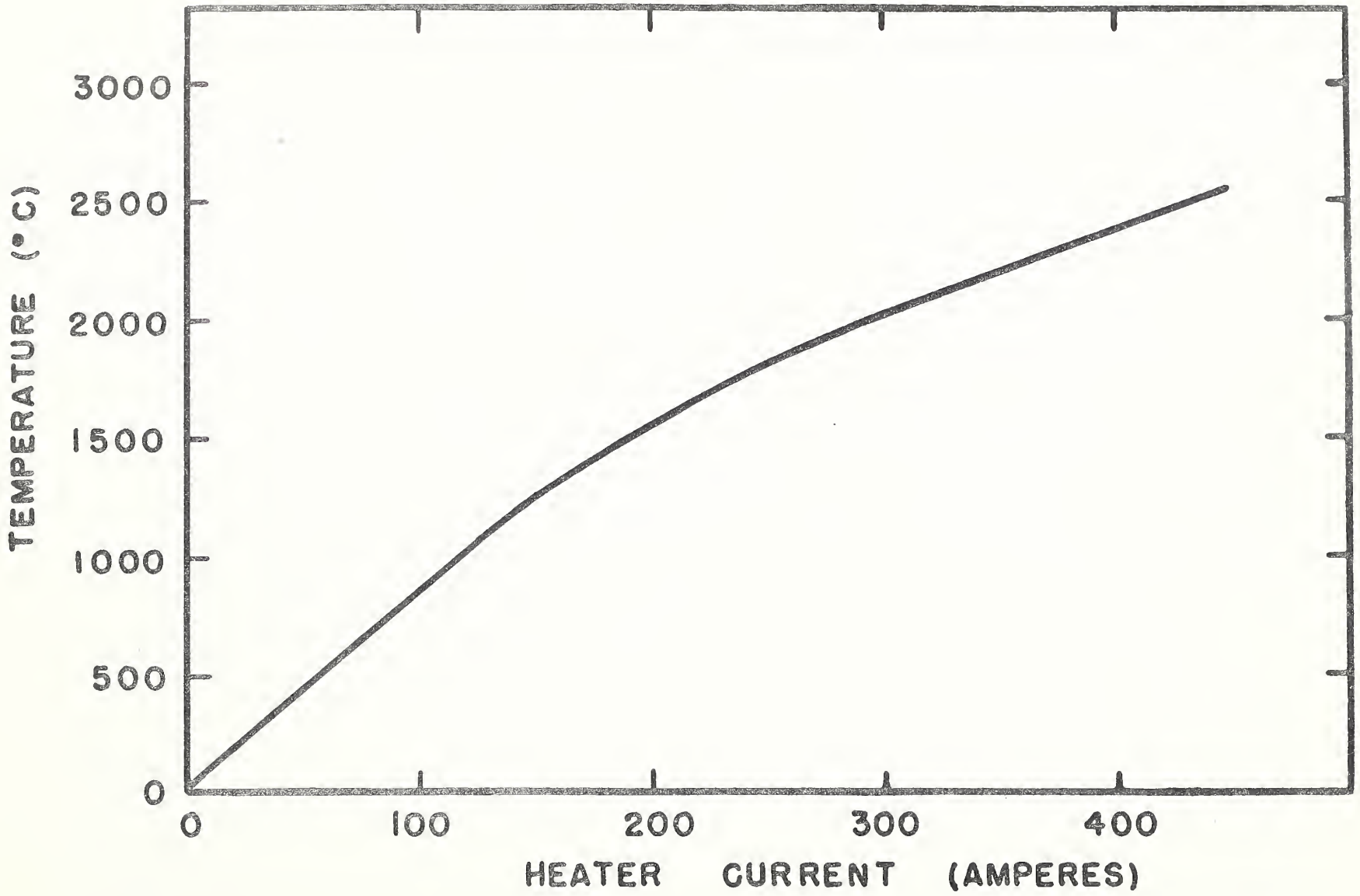

Fig. 3 - Vacuum furnace hot-zone temperature as a function of heater current.

2. Liquidus Temperatures

Due to the previously mentioned experimental difficulties of conducting thermal analyses on chromium alloys at high temperatures, we have not obtained direct measurements of liquidus temperatures. The approximate liquidus temperatures were estimated from the metallographic appearance of samples quenched from above the solidus. Given the form of the solidus and the temperature at which the specimen was held, one can estimate the liquidus composition by applying the lever rule after estimating the relative amount of solid and liquid phases as revealed by metallographic examination.

3. Invariant Reactions

The phases existing at various temperatures were determined by metallographic examination and Debye-Scherrer x-ray examination of alloys which had been annealed at these temperatures followed by rapid cooling. From such studies, one may characterize the structure existing above a given transformation temperature and then compare this structure with those obtained for alloys which have been annealed below the transformation temperature. This technique can be used to bracket the transformation temperature by choosing successive annealing temperatures above and below the transformation temperature. Such a procedure converges fairly rapidly and one can usually determine the transformation temperature to within the accuracy of the temperature measurement itself. By using this technique, one may avoid the supercooling effects which are a complicating factor when conventional thermal analysis methods are employed.

Eutectic transformation temperatures may also be determined using the methods described for the determination of the solidus temperatures (Section III, G-1). After the solidus

determination the experimental sample is examined metallographically. One can then estimate the eutectic composition by observing the amount of any typical eutectic structure relative to the amount of coexisting phases of known compositions. The observation of a typical eutectic structure also helps to verify that the transformation is indeed a eutectic transformation.

4. Other Phase Boundaries

The solvus lines and the phase boundaries of intermediate phases were obtained by electron probe microanalysis whenever it was possible to use this method. Details of the experimental procedures are given in the Appendix. In some instances, it was not possible to use this method due to the presence of fine particles of precipitated phases or other finely decomposed structures. In such cases, the diameter of the electron beam is too large to permit its impingement entirely within a single phase region and metallographic examination is, therefore, used to determine the location of the phase boundary.

H. Experimental Results

1. General

The proposed constitution diagram for the chromium-platinum system is presented in Fig. 4. The various features of this diagram are discussed below. All alloys were inspected either metallographically or by means of x-ray, Debye-Scherrer powder patterns, or both. In general, good agreement exists among the metallographic, Debye-Scherrer, and electron microbeam probe data.

2. Solidus

The solidus was determined mainly by using the technique of direct observation of melting using the cylindrical

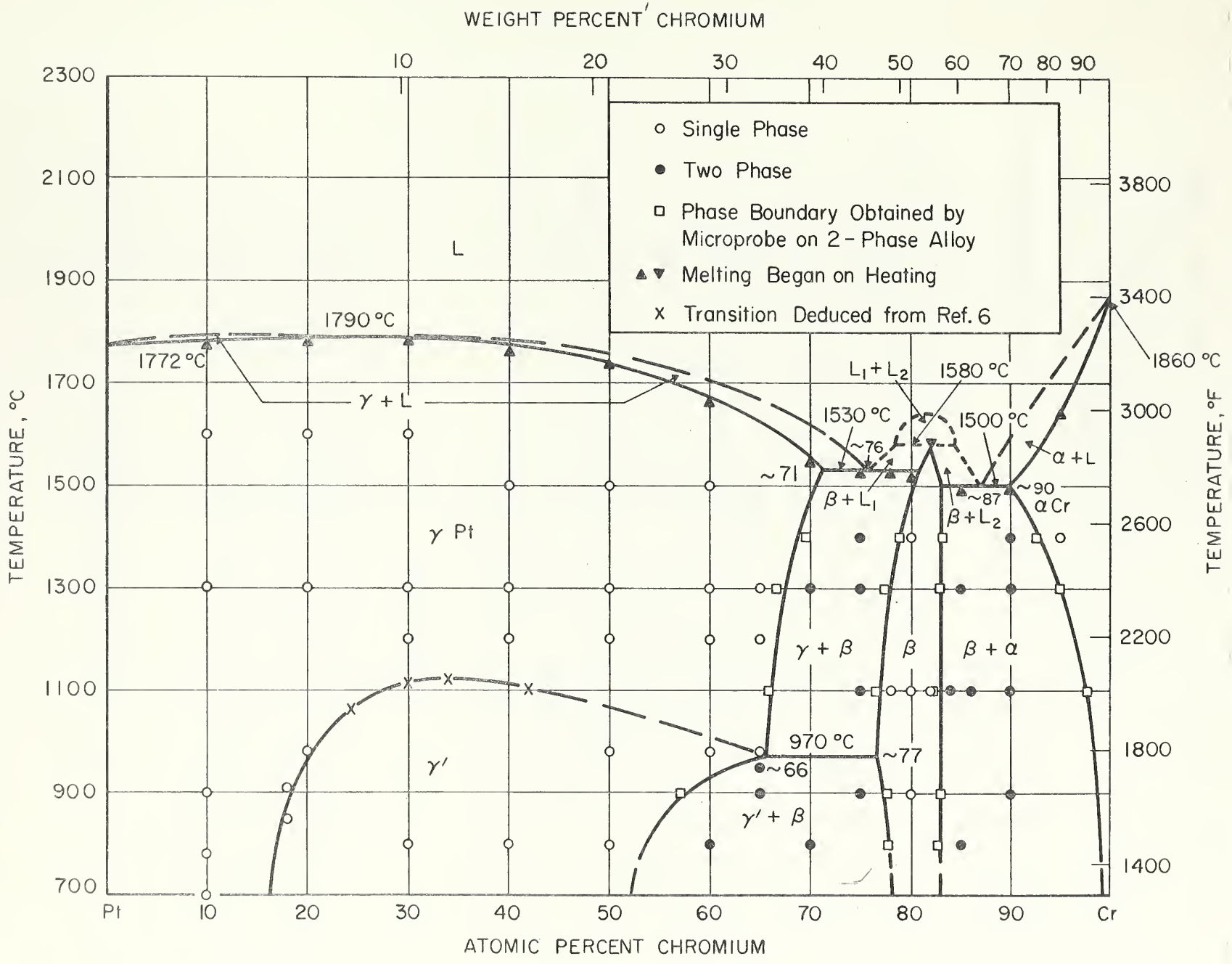

Fig. 4 - Chromium-platinum constitution diagram

tantalum holder as shown in Fig. 2, and described in Section III, G-1. In most cases, melting occurred quite rapidly at a definite temperature level, particularly in the γ solid solution region where a congruent melting maximum presumably exists. Each solidus determination included an alloy sample and also a piece of high purity platinum wire so that a simultaneous temperature calibration was obtained at the Pt-point.

This technique seems quite reliable since the Pt-point calibration is done during the course of the actual solidus determination and under identical experimental conditions. The sheathed thermocouple is quite sensitive to temperature changes of the order of 1°C or less, and it was, therefore, quite easy to detect the small temperature difference which usually existed between the observed melting point of the platinum wires and those of the alloy samples. High purity ΔRR alumina crucibles were used in these experiments. The crucibles appeared to resist any chemical attack except in the case of Cr-rich alloys where a slight green discoloration was detected. These samples were rerun using thoria crucibles, but we observed no significant differences in our results between the use of alumina versus thoria crucibles for the Cr-rich alloys.

3. Equilibration

Preliminary homogenization was accomplished for each sample by heating in a high vacuum to a temperature about 200°C below the solidus temperature for at least three hours. Electron microprobe data and x-ray diffraction patterns were used to establish that the samples were satisfactorily homogenized.

A summary of the equilibration treatments for the alloys in this system is given in Table 4.

Table 4

Summary of Equilibration Treatments for Chromium-Platinum Alloys

Temperatures (°C)	Time	Alloys (atomic % Cr)
1600°	3 hrs.	10, 20, 30
1500°	3 hrs.	40, 50, 60
1400°	12 hrs.	75, 80, 90, 95
1300°	2 days	10, 20, 30, 40, 50, 60, 65 70, 75, 85, 90
1200°	3 hrs.	30, 40, 50, 60, 65
1100°	30 days	30, 76, 78, 80, 82, 84, 86
1100°	14 days	75, 90
980°	17 hrs.	20, 50, 60, 65
970°	38 days	65
950°	27 days	18
910°	3 hrs.	10
900°	3 hrs.	10
900°	42 days	65, 75, 80, 90
850°	3 hrs.	18
800°	1 day	30, 40, 50
800°	60 days	50, 60, 70, 85
780°	3 hrs.	10
700°	3 hrs.	10
600°	3 days	10

4. Platinum Terminal Solid Solution - γ and γ'

It has been established in previous studies that chromium will dissolve in face-centered cubic platinum to form an extensive solid solution region. [2-5] It has also been established that atomic ordering occurs within this solid solution when the alloys are slowly cooled or annealed at temperatures below about 1200°C. [3-5] The present study confirms these conclusions. Atomic ordering has been observed in alloys containing from about 20 to 65 atomic percent Cr. This has been established by the observation of superstructure lines in our Debye-Scherrer x-ray diffraction patterns. At the stoichiometric composition, Pt_3Cr, the atomic ordering produces a $Cu_3Au(L1_2)$ type structure,[6,8] and complete atomic ordering may apparently exist. [8] At the composition PtCr, the atomic ordering produces a $CuAu(L1_0)$ type structure [8] but the degree of ordering has not yet been determined. For other compositions within the ordered region, there is apparently a continuous variation in site occupancies so that the structure changes progressively from the Cu_3Au type to the CuAu type with increasing chromium content. [8] The atomic ordering reaction takes place quite rapidly, particularly in alloys containing over 20 atomic percent Cr, for which it is usually not possible to retain the completely disordered condition in alloys which have been rapidly quenched from above the order-disorder transition temperature. The temperatures of the order-disorder transition have been reported for several alloys containing less than 50 atomic percent Cr and are plotted in Fig. 4. [4,6] The approximate locations of the order-disorder transition temperatures for alloys containing 18 and 20 atomic percent Cr were established by quenching sealed quartz tubes containing the alloy filings into cold water, and noting from the x-ray patterns whether or not the alloys were ordered. These points are also shown in Fig. 4. A smooth curve may be drawn through these points in order to roughly delineate the region of the ordered γ' phase, and it appears reasonable to extrapolate this curve until it intersects the solvus line. The solvus

line was established mainly by the use of electron probe micro-analysis of alloys quenched from various temperatures within the two-phase $\gamma + \beta$ or $\gamma' + \beta$ regions. A sharp change in the direction of the solvus line apparently exists at about 970°C, and this sharp change in solubility may well be associated with the order-disorder transition since it seems to occur approximately at the point where the extrapolated order-disorder transition temperature curve would intersect the solvus line. Further data is needed to verify this suggestion and such data could perhaps be obtained through high-temperature x-ray diffraction studies.

Attempts were made to determine the order-disorder transition temperatures by the use of high-temperature dilatometry methods. Dilatometric measurements were conducted on a cylindrical sample of $Cr_{20}Pt_{80}$, which had been previously given a homogenization annealing treatment. Filings from this alloy had yielded an x-ray diffraction pattern of a disordered face-centered cubic structure when these filings were quenched from 980°C. The cylindrical dilatometer sample was, therefore, heated to 1000°C in a high vacuum in hopes of seeing an inflection in the dilatometer curve somewhere between 900°C and 1000°C, which could be associated with the order-disorder transition. However, the data revealed a smooth curve from 300°C to 1000°C with no inflections. This data was kindly obtained for us by the Argonne National Laboratory.

A similar attempt was made to detect the order-disorder transition in a homogenized cylindrical sample of $Cr_{50}Pt_{50}$ which was heated and cooled in a high temperature vacuum dilatometer between 25°C and 1300°C.[9] Again, the data indicated a smooth curve with no inflections, either on heating or on cooling. The sensitivity of this dilatometer was believed to be sufficient to detect a volumetric change in this sample of less than 0.1%. This data was obtained by Mr. Joseph Valentich at the Westinghouse Research Laboratories.

Ordering reactions, such as that which is observed in the alloy $Cr_{50}Pt_{50}$, are usually accompanied by a change in crystal symmetry together with increases in hardness and flow stress as the alloy transforms from the disordered face-centered cubic to an ordered tetragonal CuAu type structure.[10] This reaction is accompanied by the accumulation of sizable internal strains arising from the lattice misfit between mutually coherent parent and product phases. The transforming system frequently attempts to relieve these strains through shear and twinning of the ordered phase. All of the previously known structures of the CuAu type are in fact tetragonal.[11] However, x-ray diffraction patterns from filings of the alloy $Cr_{50}Pt_{50}$ indicated that even though this alloy possesses the CuAu type structure, it is apparently still cubic. High angle diffraction lines show well-resolved K_α doublets but no detectable splitting. Nevertheless, one may observe profuse twinning in the microstructure of this alloy as shown in Fig. 5a. The factors responsible for this twinning are not known but it appears that it is not brought about by a change in crystal symmetry. Variations in lattice parameters are shown in Fig. 6.

5. Chromium Terminal Solid Solution - α

The body-centered cubic chromium solid solution can dissolve a maximum of about 10 atomic percent platinum at 1500°C. However, at lower temperatures there is a significant decrease in solubility so that near 800°C the maximum solubility is about one atomic percent platinum. Chromium-rich alloys, which have been annealed at low temperatures, frequently contain a fine precipitate of the β phase. This fine precipitate is responsible for our inability to obtain an electron probe microanalysis of the chromium-rich phase in alloys annealed at 900°C, since it was virtually impossible to focus the beam into a single-phase region. Precipitation effects are also visible in our x-ray diffraction patterns, where one observes some sharp lines of the β phase together with rather diffuse lines of the body-centered cubic

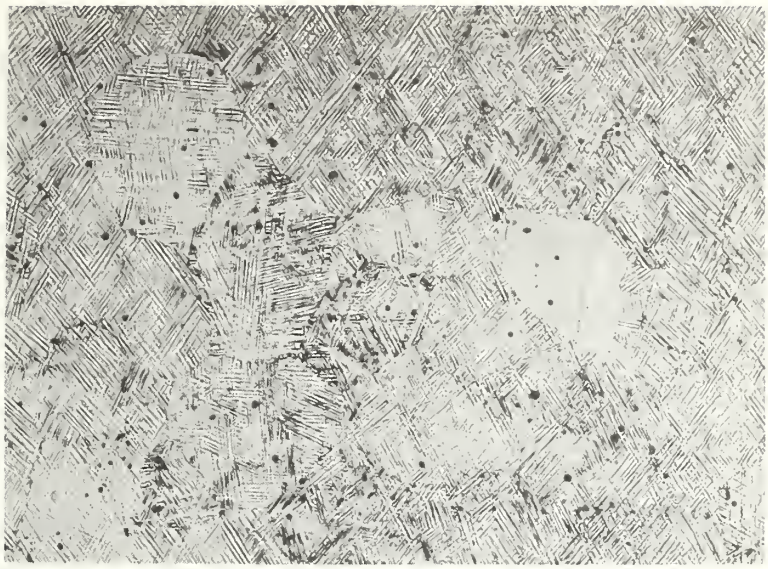

160X (a)

50 at. % Cr, 50 at. % Pt equilibrated at 800°C for two months. The appearance of microtwinning is difficult to explain since x-ray diffraction data indicates that this alloy possesses a cubic ordered structure of the CuAu type. There was no detectable evidence of tetragonality.

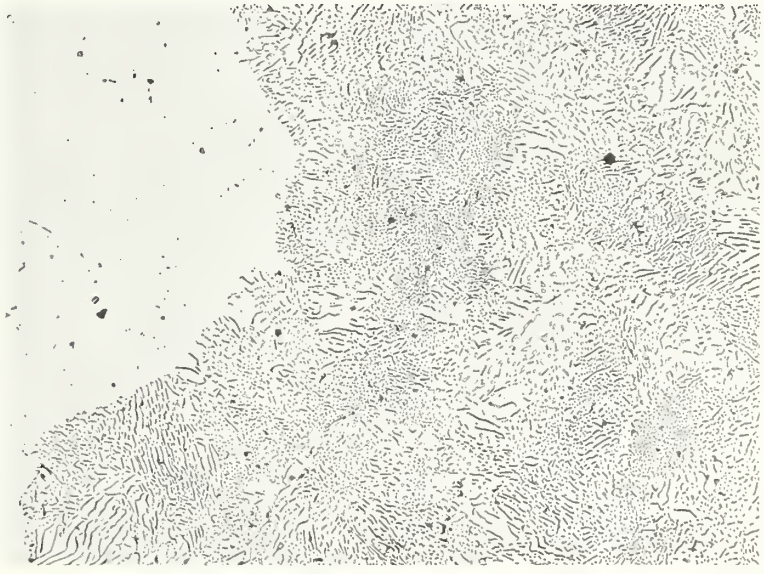

160X (b)

60 at. % Cr, 40 at. % Pt equilibrated at 800°C for two months. The fine structure consists of β phase particles in a matrix of γ'. The fine structure has nucleated at a prior grain boundary of γ phase and is now advancing toward the interior of the large γ phase grain.

Fig. 5 - Microstructures of chromium-platinum alloys.

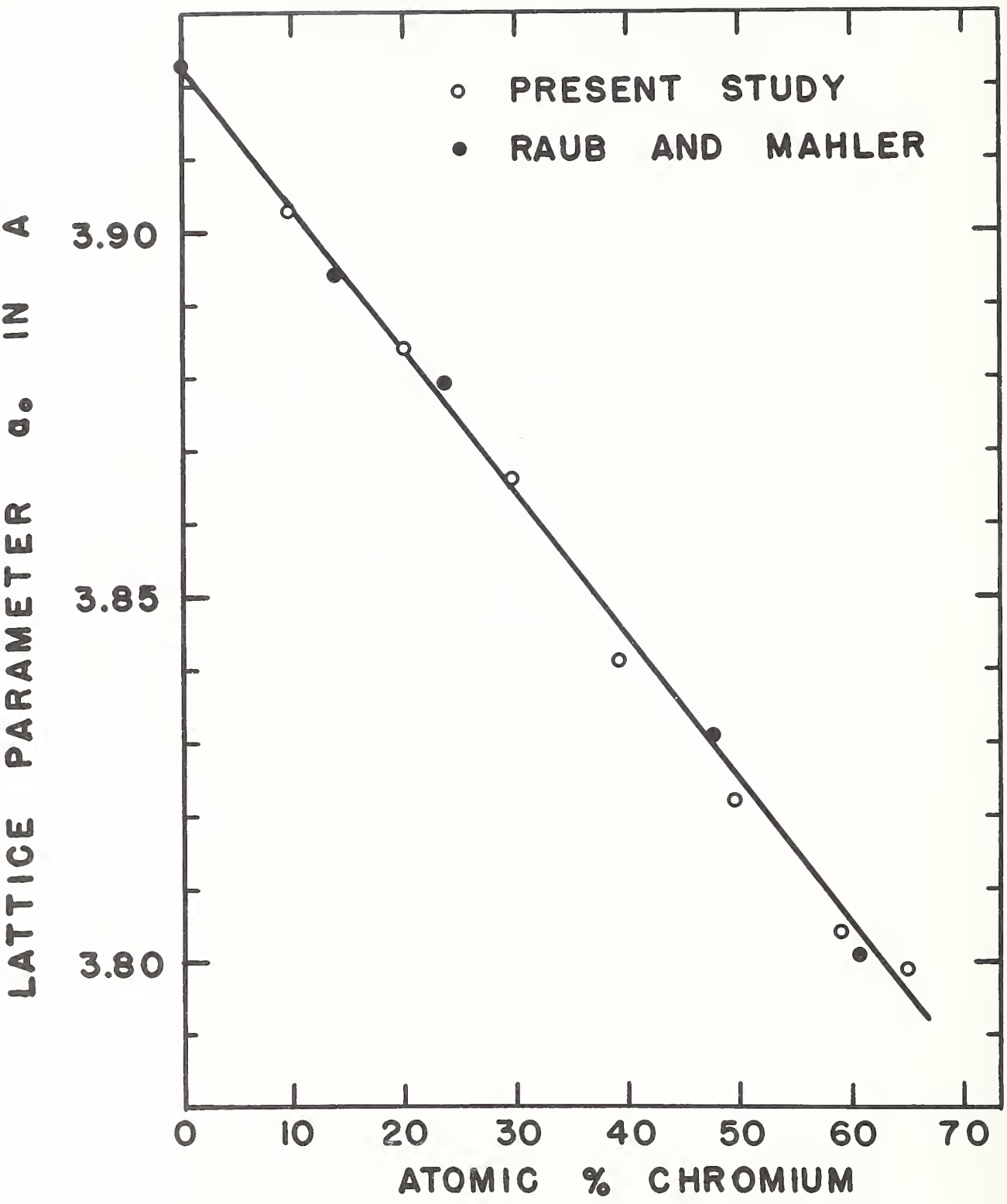

Fig. 6 - Variation in the lattice parameters of Cr-Pt alloys as a function of alloy composition. Comparison is made with the data of Raub and Mahler (Ref. 5).

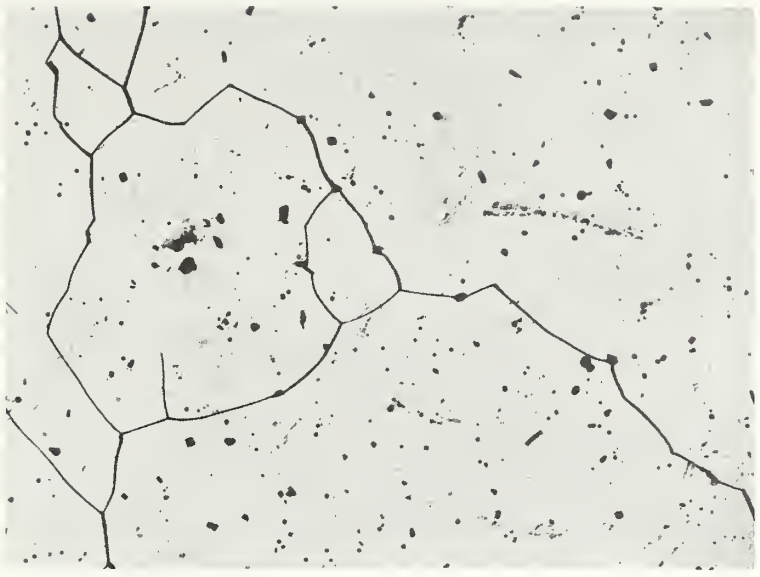

160X (a)

65 at. % Cr, 35 at. % Pt equilibrated at 980°C for 17 hrs. Large grains are γ phase containing etch pits and inclusions of Cr_2O_3. Grain boundaries are free of the β phase.

80X (b)

65 at. % Cr, 35 at. % Pt equilibrated at 950°C for 27 days. A small amount of $(\beta + \gamma')$ now appears at grain boundaries of the γ phase.

Fig. 7 - Microstructures of chromium-platinum alloys.

160X (a)

65 at. % Cr, 35 at. % Pt equilibrated at 900°C for 42 days. The fine structure consists of β phase particles in a matrix of γ′ and has entirely consumed the large prior grains of γ phase. Dark spots are oxide inclusions.

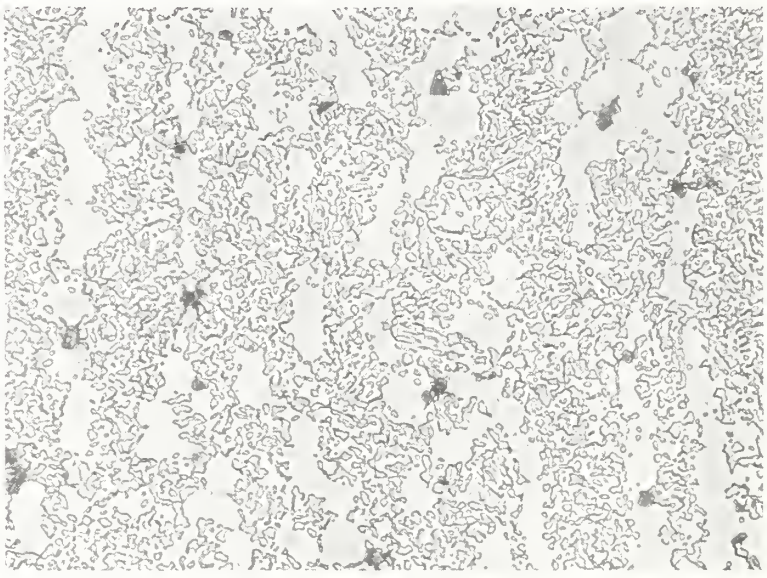

370X (b)

70 at. % Cr, 30 at. % Pt equilibrated at 800°C for four months. A prior structure consisted of β phase islands in a matrix of γ phase and was formed during annealing at 1300°C. The former γ phase has transformed to β + γ′. Clear areas are prior β phase islands.

Fig. 8 - Microstructures of chromium-platinum alloys.

160X (a)

75 at. % Cr, 25 at. % Pt equilibrated at 1400°C for 12 hrs. Islands of γ phase in a matrix of β phase.

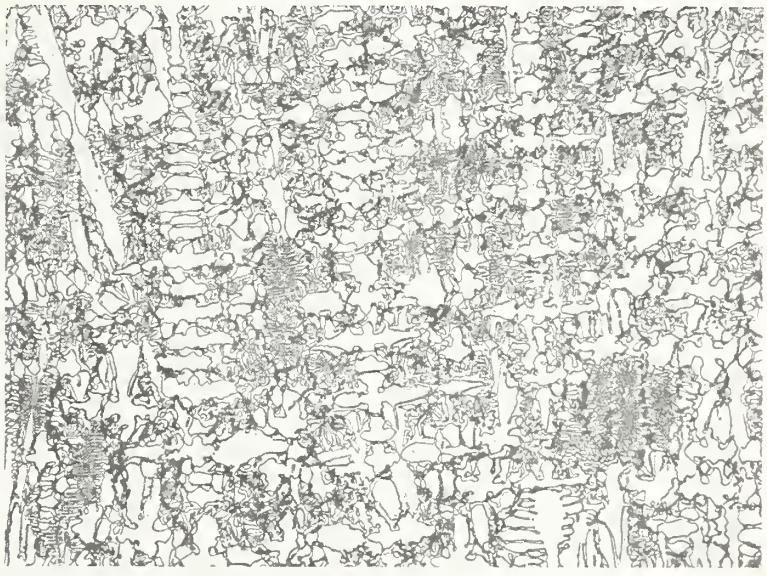

208X (b)

76 at. % Cr, 24 % Pt after arc-melting. Dendritic β phase and interdentritic (β + γ) eutectic structure.

Fig. 9 - Microstructures of chromium-platinum alloys.

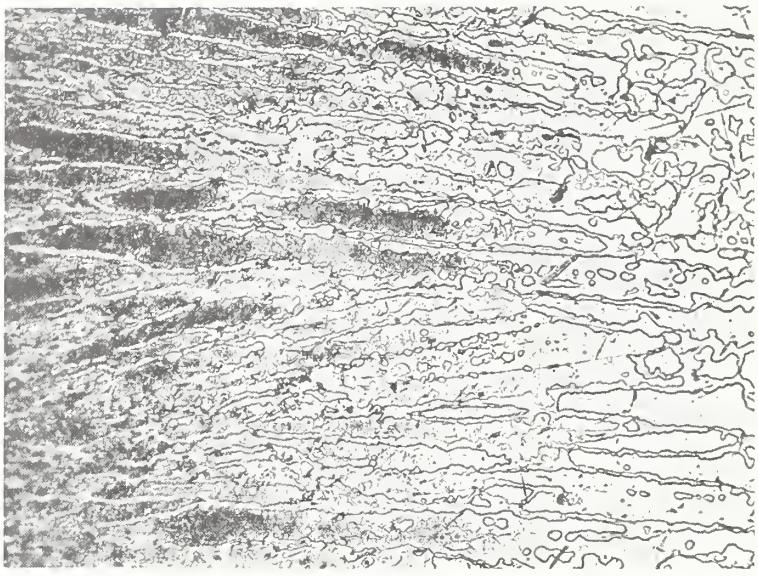

208X (a)

88 at. % Cr, 12 at. % Pt after arc-melting. Area on the left side was in close proximity to the cold copper crucible and the cooling rate is most rapid here. Dark islands in this region are an unresolved fine eutectic structure of ($\alpha + \beta$) which tends to form a coarser ($\alpha + \beta$) structure in those regions which have cooled more slowly. See Fig. 11b.

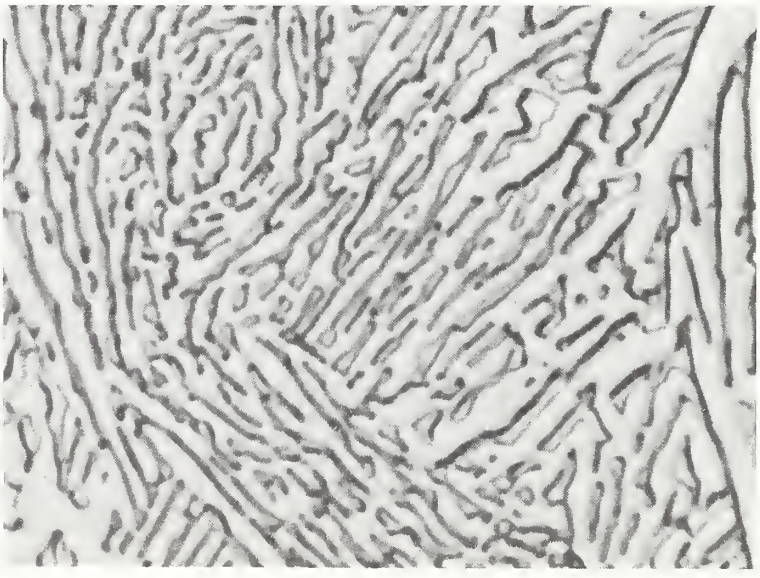

2500X (b)

The dark islands appearing in Figs. 10a and 11b are shown under high magnification. The structure is apparently that of a fine eutectic consisting of lamellar β phase in a matrix of α phase.

Fig. 10 - Microstructures of chromium-platinum alloys.

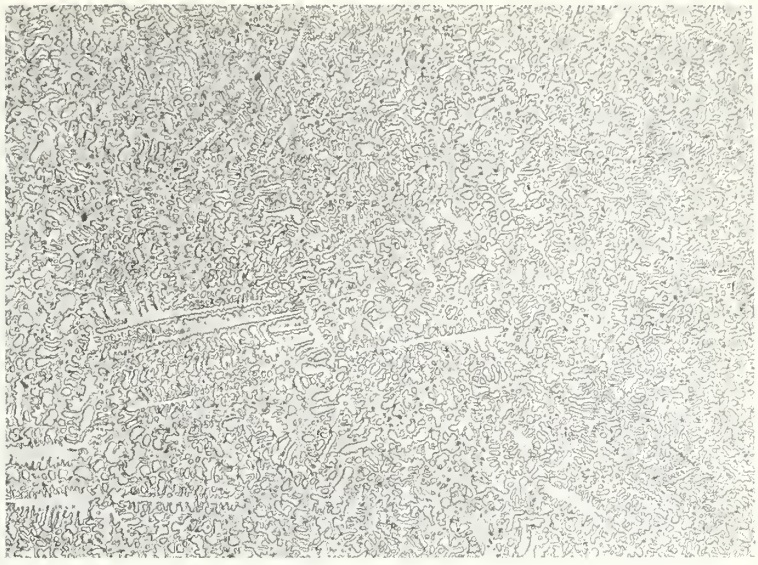

80X (a)

86 at. % Cr, 14 at. % Pt after arc-melting. This region has cooled at a slower rate than the region shown in Fig. 10b and contains dendritic β phase with interdendritic partially decomposed α phase.

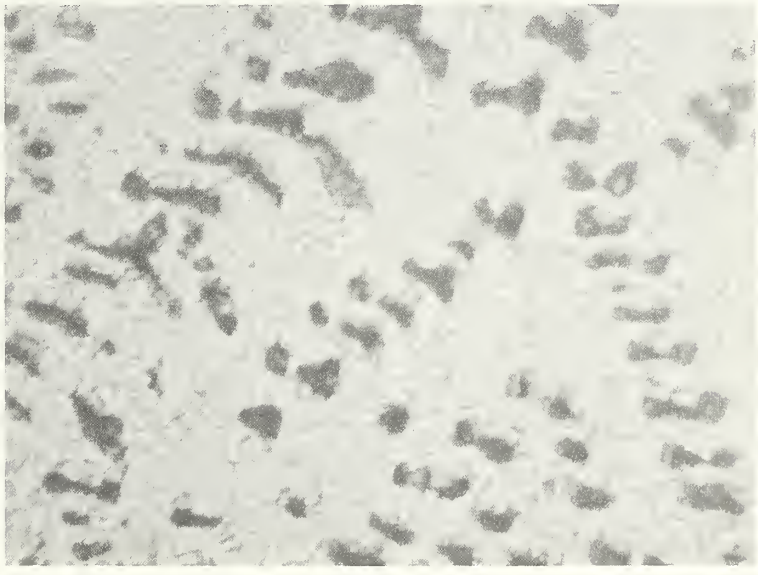

160X (b)

80 at. % Cr, 20 at. % Pt after arc-melting. Dendritic β phase (grey) with interdendritic regions containing two different eutectic structures. Dark islands are the Cr-rich eutectic of (α + β) shown in Fig. 10a. Lighter etching fine structure is the Pt-rich eutectic of (γ + β) shown in Fig. 9b. The x-ray pattern of this alloy contains mainly the lines of the β phase but also contains two distinct lines identified as the (111) of β phase and the (110) of α phase.

Fig. 11 - Microstructures of chromium-platinum alloys.

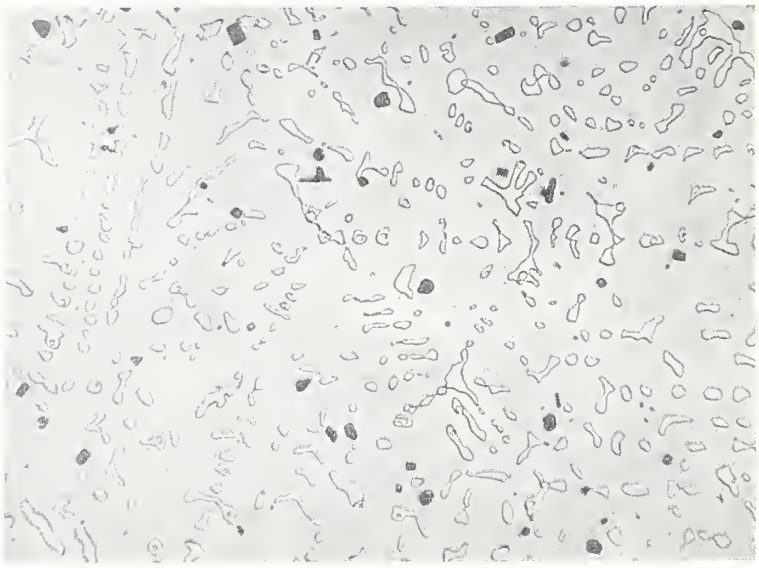

130X (a)

84 at. % Cr, 16 at. % Pt equilibrated at 1100°C for one month. Globular α phase in a matrix of β phase. Grey inclusions are Cr_2O_3.

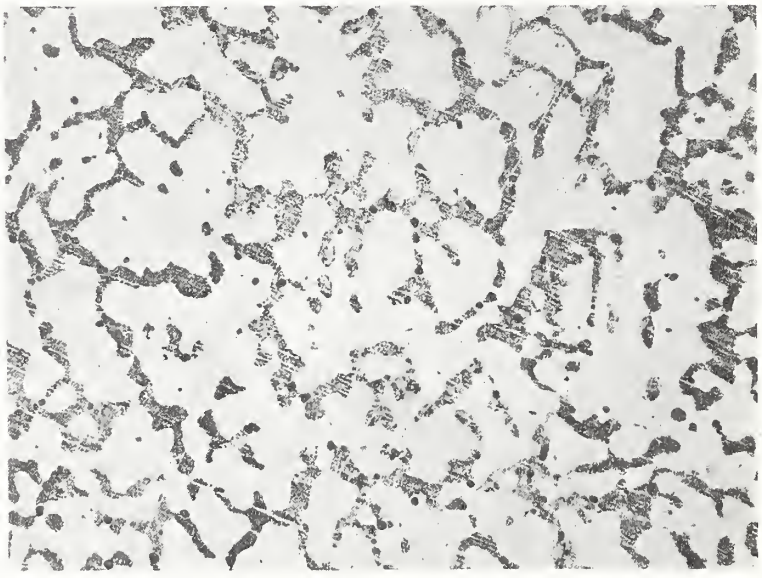

160X (b)

90 at. % Cr, 10 at. % Pt equilibrated at 1400°C for 12 hrs. Islands of α phase containing some precipitated β phase in a matrix of β. The cooling rate after quenching in this region was not sufficient to prevent precipitation in the supersaturated α phase.

Fig. 12 - Microstructures of chromium-platinum alloys.

structure in powders annealed at low temperatures or slowly cooled. Our cooling rates during quenching of the chromium-rich alloy powders were apparently always too slow to prevent some decomposition of the chromium solid solution which exists at high temperatures.

6. Intermediate Phase, β

Raub and Mahler[5] were the first investigators to report the existence of an intermediate phase having the A15 (β-W) crystal structure in the chromium-platinum system. They suggested that this phase possesses the stoichiometric composition $PtCr_3$, and that it could not have a composition range since its lattice parameter did not change with composition. We have observed that the lattice parameter of this phase does indeed show a composition dependence, and that it varies from $a_o = 4.684$ to $a_o = 4.708$ with increasing platinum content.[12] Quantitative electron-probe microanalyses of equilibrated two-phase alloys has confirmed a previous report that the composition range of this phase does not include the stoichiometric composition $PtCr_3$[13]. The maximum solubility range of this phase occurs at about 970°C, where it is stable from 76.5 atomic percent Cr to 83.0 atomic percent Cr.

7. Syntectic: $L_1 + L_2 \rightleftharpoons \beta$

Raub and Mahler[5] reported that eutectic formation occurs on both sides of the β phase, while the phase itself forms under a maximum in the melting curve. The present study is in agreement with these observations, but our data indicate that the β phase may, in fact, decompose at high temperatures via a syntectic reaction rather than by congruent melting as depicted in Fig. 321 of Hansen and Anderko's review.[7] We have arrived at this conclusion after a careful study of alloys in the "as-cast" condition which were prepared in 2% increments over the composition range from 76 to 86 atomic percent chromium.

These alloys were arc melted and then slowly solidified by gradually reducing the arc current. This procedure produces a large temperature gradient between the bottom of the alloy sample (which is in contact with the copper hearth) and the top of the alloy sample, which is the last portion to solidify. This large temperature gradient is apparently responsible for significant variations in the microstructure of each alloy parallel to the direction of the temperature gradient. Certain characteristic microstructures have been observed, however, which are identifiable as eutectic structures. The microstructural identification is confirmed, in most cases, by x-ray diffraction patterns obtained from powders of these "as-cast" alloys.

It appears to be quite significant that in none of our "as-cast" alloys were we able to obtain more than about 70% of the β phase. Thus, if a congruent melting point were to exist, then it might be expected that at least one of our alloy samples would be in close enough proximity to the composition of congruent melting that almost all of this sample would crystallize as the β phase. On the contrary, both x-ray diffraction and metallographic studies revealed the presence of appreciable amounts of either the Cr solid solution or the Pt solid solution, together with the β phase in all of the "as-cast" samples. For alloys in the vicinity of 80 atomic percent Cr, one observes both the Cr solid solution and the Pt solid solution present simultaneously, together with the β phase. This is rather remarkable, especially since the microstructure of "as-cast" $Cr_{80}Pt_{20}$ (Fig. 11b) contains two distinct eutectic structures coexisting in this alloy with the β phase. A photomicrograph of the dark-etching area in Fig. 11b is shown in Fig. 10b in order to verify that this area is in fact a eutectic structure. This dark-etching structure has been associated with a Cr-rich eutectic existing at about 85 atomic percent chromium, whereas the lighter etching eutectic is associated with a Pt-rich eutectic existing at about 76 atomic percent chromium. These relationships are supported by our metallographic and x-ray diffraction data. (See Figs. 9b, 10a, 10b).

It is difficult to explain the coexistence of two different eutectic structures in a binary "as-cast" alloy. The common eutectic or peritectic reactions do not produce such a structure. Our observation that the alloy $Cr_{82}Pt_{18}$ melts at about 1580°C seems to rule out a monotectic reaction. Therefore, we are led to conclude that only a syntectic reaction could produce the observed coexistence of both a Pt-rich and a Cr-rich eutectic structure in our "as-cast" alloys.

8. Eutectic: $L \rightleftharpoons \gamma + \beta$

Fig. 9b shows this eutectic structure in the "as-cast" alloy $Cr_{76}Pt_{24}$. X-ray diffraction patterns from powdered samples of this alloy indicate the presence of γ phase and β phase only. Melting point determinations indicated a eutectic temperature of about 1530°C. Decreasing amounts of this eutectic structure were obtained in alloys containing higher chromium contents.

9. Eutectic: $L \rightleftharpoons \alpha + \beta$

Fig. 10a shows the structure of this eutectic in an "as-cast" alloy, $Cr_{88}Pt_{12}$. The type of structure observed seems to depend rather strongly on the cooling rate since a wide variety of structures were observed in the "as-cast" alloy. X-ray diffraction patterns of the "as-cast" alloy indicated only α and β phases, while melting point studies suggested a eutectic temperature of about 1500°C. Decreasing amounts of this eutectic structure were observed in other "as-cast" alloys in the vicinity of this composition.

REFERENCES

1. Müller, L., Determination of the Melting Points of Platinum Alloys, Ann. Physik (5), 7, pp. 9-47, (1930).

2. Nemilow, W. A., The Alloys of Platinum with Chromium, Z. Anorg. Chem., 218, pp. 33-44, (1934).

3. Friederich, E. and Kussmann, A., The Ferromagnetism of Platinum-Chromium Alloys, Phys. Zeit., 36, pp. 185-192, (1935).

4. Gebhardt, E. and Köster, W., Study of the Constitution of the Platinum-Chromium System, Z. Met., 32, pp. 262-264, (1940).

5. Raub, E. and Mahler, W., The Alloys of Chromium with Platinum, Iridium, Rhodium and Ruthenium, Z. Met., 46, pp. 210-215, (1955).

6. Kussmann, A., Müller, K. and Raub, E., Thermomagnetic Measurements on Alloys of the Platinum Metals with Chromium, Z. Met., 59, pp. 859-863, (1968).

7. Hansen, M. and Anderko, K., "Constitution of Binary Alloys", McGraw-Hill, New York, (1958).

8. Pickart, S. J. and Nathans, R., Neutron Diffraction Investigation of Pt-Based Alloys of the First Transition Series, J. Appl. Phys., 34, pp. 1203-1204, (1963).

9. Valentich, J., Thermal Expansion Measurement, Instruments & Control Systems, 42 (Oct), pp. 91-94, (1969).

10. Arunachalam, V. S. and Cahn, R. W., Order-Hardening in CuAu, J. Mat. Science, 2, pp. 160-170, (1967).

11. Laves, F., Crystal Structure and Atomic Size – Table XXXI, p. 186, in: "Theory of Alloy Phases", Trans. ASM, 48A, American Society for Metals, Cleveland, Ohio, (1956).

12. Waterstrat, R. M. and van Reuth, E. C., Effects of Compositional Variations on the Atomic Ordering in A15 Phases, Proc. Third Bolton Landing Conf. on Ordered Alloys, Claitor's Publishing Division, Baton Rouge, La., (1970).

13. Waterstrat, R. M. and van Reuth, E. C., Nonstoichiometric A15-Type Phases in the Systems Cr-Pt and Cr-Os, Trans. Met. Soc. AIME, 236, pp. 1232-1233, (1966).

IV. VANADIUM-PLATINUM CONSTITUTION DIAGRAM

A. Previous Studies

There have apparently been no previous studies designed to elucidate the constitution diagram of the vanadium-platinum alloy system. However, there has been sufficient study of individual alloys to establish that various intermediate phases are formed and to determine their crystal structures.[1-3] Some of the phases which have been identified are apparently not in a state of stable equilibrium at room temperature.[3] Other phases seem to result from contamination of the alloy samples by oxygen or by nitrogen.[3] There is some evidence that a metastable phase can be obtained by cold-working the alloy powders.[4] An investigation of the constitution diagram is, therefore, essential in order to identify which of these structures belong to equilibrium phases, and perhaps also to suggest some reasons for the existence of the various structures which have been observed.

B. Materials

The vanadium metal used in this investigation was obtained from the U. S. Bureau of Mines, Boulder City Metallurgy Research Laboratory through the courtesy of Mr. T. A. Sullivan. The metal was in the form of electrolytic dendrites having a nominal purity of about 99.95%. A typical analysis of this metal is shown in Table 1.

The platinum metal was in the form of 1/32-inch sheet and was from a stock supply whose original source was unknown. Spectrographic analysis, shown in Table 5, revealed that this metal had a nominal purity of about 99.9% with the principal impurity being palladium which was present to the extent of between 100 and 1000 ppm.

Table 5

Typical Analyses of the Materials Used in Preparing the Experimental Alloys †

Impurity	Vanadium	Platinum
	U.S. Bureau of Mines	Stock Supply
Ag	ND	<10
C	80	--
Cr	60	ND
Cu	32	<100
Fe	135	<10
H	10	--
Mg	ND	<100
N	35	--
O	220	--
Pd	ND	<1000
Ru	ND	<100
Si	ND	<100

† Values are given in ppm.

ND Not detected spectrographically.

No other elements were detected spectrographically.

C. Alloy Preparation

The experimental alloys were prepared by weighing the desired amount of each constituent metal and then melting these metals in an arc furnace under an inert atmosphere.

1. Weighing

The components of each alloy were weighed to an accuracy of ± 0.01 gram, and each sample had a total weight of about 20 grams. The weights were checked after each melting in order to establish that no excessive weight changes had occurred. In most cases, there was very little weight change, and in all cases weight changes were less than 1%.

2. Melting

All samples were arc melted on a water-cooled copper hearth using a non-consumable tungsten electrode and a furnace atmosphere of special high purity helium and argon in equal proportions by volume. The purity of these gasses is given in Section III, Table 2. Techniques of melting were similar to those which are described in Section III, C-2. Alloys rich in vanadium were melted using cylinders of compressed vanadium dendrites which were prepared by placing the appropriate quantity of vanadium in a 1/2-inch diameter hardened-steel die and compressing this in a hydraulic press until a firm, compact cylinder was obtained. In some cases, the platinum sheet was wrapped around these cylinders prior to melting the alloys.

Special care was taken with brittle alloys to insure that no losses of metal occurred when these alloys shattered under the impact of arc initiation. Such losses could usually be prevented by breaking up the alloy before melting. In cases where such shattering still occurred, we exercised scrupulous care in collecting all scattered fragments for remelting.

D. Composition Determination of the Melts

Since weight changes during alloy preparation were always quite small, it appeared safe to assume that the actual compositions of the alloy samples were quite close to the nominal

intended compositions. This assumption was verified throughout the investigation by the results of electron probe microanalyses. Our sample, $V_{50}Pt_{50}$ (nominal), was submitted to a chemical analysis which indicated that its composition was indeed 50.0 atomic percent V and 50.0 atomic percent Pt. A portion of this same sample, together with samples of pure platinum and pure vanadium, were then used for calibrating the electron probe data on a quantitative basis.

Lattice parameter measurements were of little value in determining alloy compositions since they were rather insensitive to composition apparently due to the close similarity in the atomic diameters of vanadium and platinum.

E. Temperature Measurement

A platinum versus platinum-10% rhodium thermocouple was used in measuring temperatures up to 1500°C. Temperatures above 1500°C were measured with a tungsten versus tungsten-26% rhenium thermocouple. These thermocouples were periodically calibrated against a standard platinum-6% rhodium versus platinum-30% rhodium thermocouple which had been calibrated at the National Bureau of Standards up to 1600°C. The thermocouples were also calibrated at secondary fixed points, such as the melting points of nickel or platinum, using the methods described in connection with our solidus determinations.

F. Thermal Treatments

1. Homogenization

All samples were homogenized by heating to within about 200°C of the solidus temperature for a length of time which could be considered sufficient to establish chemical equilibrium at that temperature. Thus, the samples could be considered

as being equilibrated at the homogenization temperature since all precautions normally used in an equilibration treatment were observed.

The samples were suspended in a tantalum bucket within the hot zone of our tantalum-strip resistance furnace, operating at a pressure of between 5×10^{-6} and 5×10^{-7} mm Hg. Any reaction with the tantalum bucket was apparently insignificant, and was not detected by the electron probe. The electron probe also indicated that our samples had been adequately homogenized since no composition gradients were detected. This was further verified by metallographic and x-ray diffraction studies.

2. Equilibration

Most of our annealing treatments at temperatures up to 1100°C were done by sealing the samples in quartz tubes which had been baked-out, evacuated, and filled with a partial pressure of high purity argon. However, alloys containing between 33 and 60 atomic percent vanadium were found to be seriously contaminated at 1100°C, apparently by a reaction with the quartz tubes. An attempt was made to prevent this reaction by wrapping the samples in tantalum foil, but this was unsuccessful. Many small crystals were observed on the interior walls of the tubes. These were collected and submitted to x-ray diffraction and electron probe analysis. The crystals were found to contain vanadium, tantalum, and silicon. X-ray precession pictures indicated that the crystals were tetragonal with possible space groups I4cm, $I\bar{4}c2$, or I4/mcm. The latter space group is that of the compound V_5Si_3. The lattice constants of our crystals ($a_o = 6.46$, $c_o = 12.08$), however, resemble those of Nb_5Si_3 ($a_o = 6.57$, $c_o = 11.88$). We concluded that a Vanadium-Tantalum Silicide had been formed.

In order to prevent this contamination, we decided to seal our samples in pure platinum tubes, which were then evacuated and filled with an appropriate partial pressure of pure argon before closing the tubes by compressing the ends. This method seemed to be quite satisfactory in preventing contamination of the alloy samples. It was essential that the tubes contain the correct amount of argon gas so that they would not collapse when heated to the annealing temperature. A platinum tube, which collapses on the samples, will often rupture in the vicinity of any sharp edges on the samples.

All samples were suspended in a vertical platinum-wound resistance furnace using either nichrome or platinum wire to hold the tubes. Some of these samples were also annealed in our tantalum-strip resistance furnace in a high vacuum, and no contamination was detected under these conditions. The tantalum-strip resistance furnace was also used for all annealing treatments above 1100°C. Pressures of between 5×10^{-5} and 5×10^{-7} mm Hg were obtained during the annealing treatments and temperatures were controlled to within ± 10°C.

All samples were rapidly cooled from the annealing temperature by turning off the furnace power. The cooling rate was sufficiently rapid to permit identification of the prior structures existing at the annealing temperature, either by metallographic or x-ray diffraction studies. Samples annealed in quartz tubes were quenched in cold water. A summary of the equilibration treatments for the vanadium-platinum alloys is given in Table 6.

G. Methods for Determination of Phase Boundaries

1. Solidus Temperatures

The procedures used in determining the solidus temperatures were similar to those used in our study of the

chromium-platinum system. (See Section III, G-1.) Although there is no problem of high vapor pressures, as was the case with the chromium alloys, there is nevertheless a problem in preventing chemical reactions between vanadium and some refractory materials at high temperatures. In most cases, this was solved by using thoria crucibles in our solidus measurements, but high purity alumina crucibles were satisfactory for the platinum-rich alloys.

Our success in determining solidus temperatures by direct observations of melting for the chromium-platinum alloys encouraged us to use similar methods for the vanadium-platinum alloys. The method appeared to be equally satisfactory in this case, partly because a congruent melting maximum exists in both the Cr-Pt and V-Pt systems, and this gives rise to sharply defined melting points. The method is described in Section III, G-1, and illustrated in Section III, Fig. 2. No special modifications were required for the vanadium-platinum alloys other than the use of thoria crucibles for alloys containing more than 30% vanadium. Solidus temperatures, as much as 50° lower, were obtained in some cases when alumina crucibles were used with these alloys. The thoria crucibles appeared to be quite resistant to any reaction with vanadium, and for this reason we feel that our solidus temperatures are fairly reliable.

2. Liquidus Temperatures

In most cases, we did not attempt to determine the liquidus temperatures, but in the region of the β phase, we were able to observe an appreciable temperature interval between the first observation of melting and the temperature at which the sample became completely molten. In these cases, we have presented the temperatures of complete melting as points on the liquidus curve. These points should only be regarded as

approximate, however, and would require verification by more accurate methods.

3. Invariant Reactions

The existence of invariant reactions and the temperatures at which these reactions occur were established mainly by comparing metallographic and x-ray diffraction data from alloys annealed above and below the transformation temperatures. The phases existing above the transformation temperatures could be retained to room temperature by rapid quenching in each case, except for the alloy $V_{50}Pt_{50}$. In this case, high temperature dilatometry was employed to locate the transformation temperature.

Although the comparative method may appear to be excessively tedious, it has several significant advantages. Perhaps the most important advantage is the fact that one can anneal the sample for as long as is necessary to insure that an equilibrium structure has been formed at the annealing temperature. This avoids the uncertainty of possible metastable conditions developing, as may occur when using methods employing slow cooling. In addition, the comparative method in many cases offers clear, unequivocal evidence as to whether or not the sample was above or below the transformation temperature, when with other methods the evidence may be ambiguous. Finally, the comparative method permits one to begin with any arbitrary annealing temperatures. Once it is established whether this temperature is above or below the transition point, it is only necessary to select some other annealing temperature on the opposite side of this transition point. When the transition temperature has been bracketed in this manner, it is not very difficult to locate the exact transition temperature since the data converge rapidly. In most cases, less than six annealing treatments were needed to establish the transition temperatures within the accuracy of the temperature measurement itself.

Eutectic temperatures are readily obtained by direct visual observations of melting using the methods described in Section IV, G-1 for the determination of solidus temperatures. Metallographic examination of the melted alloys can reveal evidence regarding the proximity of the eutectic composition. Thus, metallographic examination of a few melted alloys usually enables one to locate the eutectic composition.

4. Other Phase Boundaries

The solvus lines and the phase boundaries of intermediate phases were obtained by electron probe microanalysis whenever this method was feasible. The procedures are described in the Appendix. Unfortunately, the alloys in this system were frequently unsuited to this method due to the presence of unresolvable fine structures in the alloy samples. These structures usually resulted from the eutectoid decomposition of phases occurring at high temperatures. At least three separate eutectoid transformations occur in this system, and we were therefore forced to rely on metallographic studies to locate many of these phase boundaries. The metallographic studies require more effort and time than the electron probe measurements, but the results seem to be sufficiently reliable to establish the location of the phase boundaries to the desired accuracy. Electron probe microanalysis was effective mainly in establishing the boundaries of the β phase region in this alloy system.

H. Experimental Results

1. General

The proposed constitution diagram for the vanadium-platinum system is presented in Fig. 13. Discussions of various phase regions are given below. All alloys were examined either metallographically or by means of x-ray powder

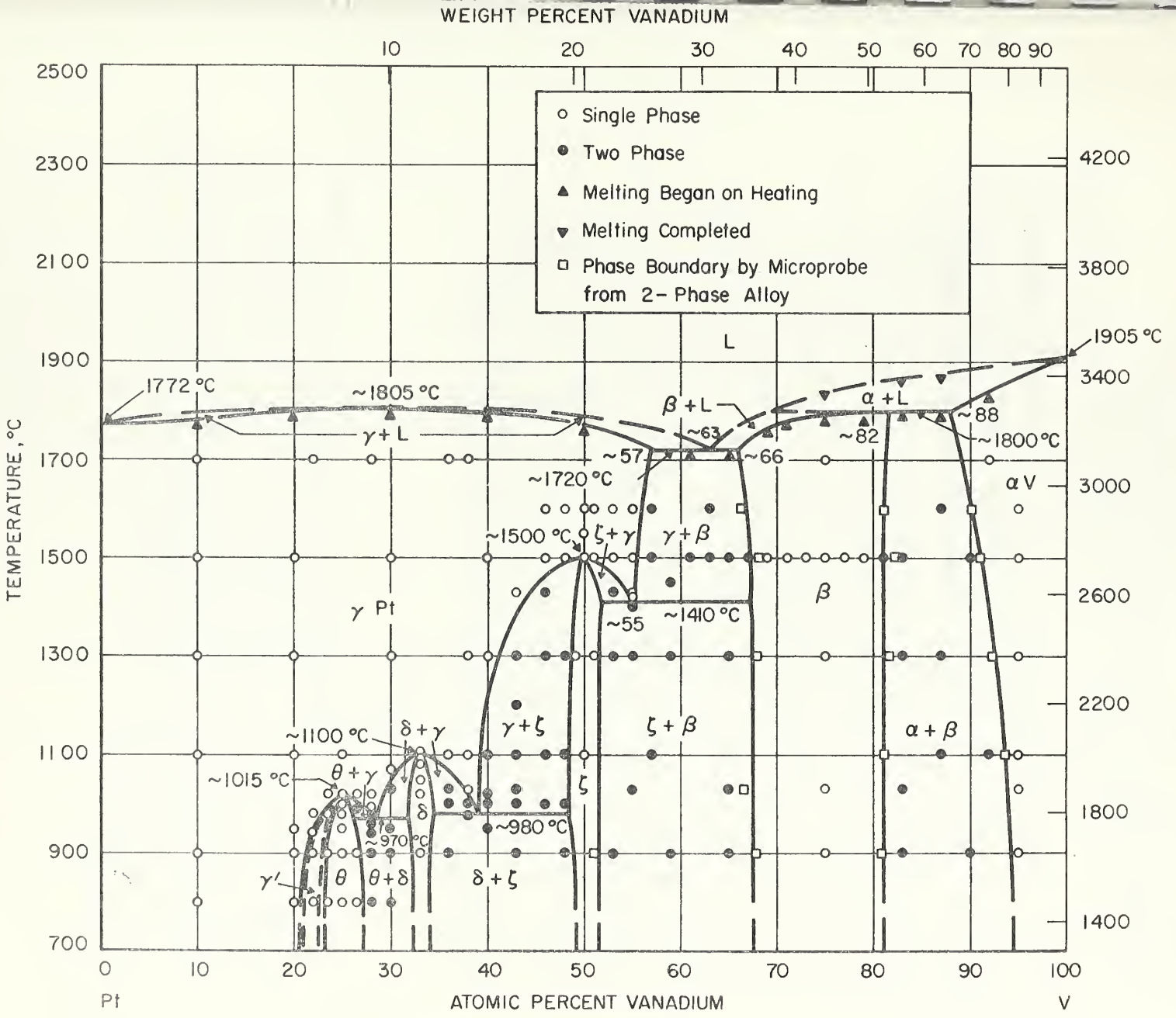

Fig. 13 - The vanadium-platinum constitution diagram.

patterns, or both. There was generally good agreement among the metallographic, x-ray, and electron probe data.

2. Solidus

The solidus was determined mainly by the technique of direct observation of melting as described in Section III, G-1. Melting generally occurred quite rapidly at a definite temperature except for alloys containing over 70 atomic percent vanadium which melted over a significant temperature range. Each solidus measurement was accompanied by a simultaneous calibration using high purity platinum wire as a melting point standard. The calibration was accomplished using the same experimental conditions as was used in determining the solidus temperature of the alloy sample. It was possible to detect fairly small temperature differences between the melting point of the standard wire and the temperature at which the alloy sample began to melt since the thermocouple had a sensitivity of about ± 1°C. It was necessary to use thoria crucibles for all alloys containing more than 30% vanadium, since vanadium apparently reacts with alumina crucibles at these high temperatures.

3. Liquidus

In most cases, we did not attempt to determine liquidus temperatures, but in the case of the alloys $V_{75}Pt_{25}$, $V_{83}Pt_{17}$, and $V_{87}Pt_{13}$, which melt over an appreciable temperature range, we assumed that the temperatures at which melting appeared to be completed (e.g., the sample abruptly collapsed and dropped into the crucible) were in fact the approximate liquidus temperatures as shown in Fig. 13.

4. Equilibration

Each sample was first homogenized by annealing in a high vacuum at a temperature within 200°C below the solidus temperature for various periods of time. Electron microprobe data indicated that single-phase samples were homogeneous and that our two-phase alloys contained homogeneous phases. A summary of the equilibration treatments is given in Table 6.

Table 6

Summary of Equilibration Treatments for Vanadium-Platinum Alloys

Temperatures (°C)	Time	Alloys (atomic % V)
1700°	2 hrs.	10,22,28,36,38,75,92
1600°	4 hrs.	46,49,50,51,53,55,57,63,87,95
1550°	2 hrs.	50
1500°	24 hrs.	10,20,30,40,46,49,50,51,53,55,57, 61,63,65,67,69,71,73,75,77,79,81, 83,90,95
1450°	5 hrs.	59
1430°	4 hrs.	55
1430°	26 hrs.	43,46,53
1420°	4 hrs.	55
1400°	4 hrs.	55
1300°	3 days	10,20,30,38,40,43,46,48,49,51,53, 55,59,65,75,83,87,95
1200°	1/2-hr.	43
1110°	1 hr.	33
1100°	2 hrs.	33,48
1100°	18 days	10,20,25,33,36,38,40,43,46,48,50, 57,87,92,95
1090°	2 hrs.	33
1080°	2 hrs.	33
1070°	2 hrs.	30
1050°	2 hrs.	33
1030°	3 wks.	30,36,38,43,55,65,75,83,95
1020°	2 hrs.	23.5,25,26.5,28,33,40
1010°	2 hrs.	25
1000°	2 hrs.	25,36,38,40,43,46,48
995°	2 hrs.	28
990°	2 hrs.	26.5
980°	2 hrs.	22,23.5,25,28
975°	2 hrs.	38
960°	2 hrs.	28
950°	2 hrs.	20,25,30,40
940°	2 hrs.	22,28
900°	6 wks.	10,20,22,23.5,25,26.5,28,30,33, 36,43,48,53,59,65,75,83,90,95
800°	7 days	10,20,22,23.5,25,26.5,28,30

5. Platinum Terminal Solid Solution - γ

It was found that vanadium will dissolve in face-centered cubic platinum to form an extensive solid solution at temperatures above 1500°C, but at lower temperatures there are at least three different order-disorder type transformations. These transformations occur at the stoichiometric compositions $V Pt_3$, $V Pt_2$, and V Pt. Each of these three order-disorder transformations is accompanied by a change in crystal symmetry. Consequently, as the ordered phase forms in the disordered matrix, there is an accumulation of internal strains which presumably gives rise to the microscopical observations of shear and twinning in the ordered phases.

In addition to these three order-disorder reactions, we have also observed atomic ordering in our alloy, $V_{22}Pt_{78}$. In this case, there is no change in crystal symmetry since the ordered structure is a $Cu_3Au(L1_2)$ type cubic structure. However, the fact that this ordered structure is not observed at the ideal (AB_3) stoichiometric composition, and is only found in a region where one would expect to observe two other phases ($\gamma + \theta$), raises some doubts as to whether it is in fact an equilibrium phase in this binary system. Maldonado and Shubert[3] have reported the formation of a Cu_3Au type structure in their alloy, $V Pt_3$, but our alloy $V Pt_3$ did not produce this structure, even after a similar heat treatment (5 minutes at 1000°C). Our alloy $V_{23.5}Pt_{76.5}$, however, did exhibit the Cu_3Au type structure after annealing for two hours at 980°C, but this same alloy showed only the $TiAl_3$ type structure of the θ phase when annealed at 900°C and at 800°C. We have, therefore, designated the Cu_3Au type phase as γ' in our constitution diagram (Fig. 13), and its approximate stability range is delineated with a dashed line. Further work is needed to establish its mode of formation and whether it is actually a binary equilibrium phase.

Lattice parameters were obtained for alloys within the region of the disordered platinum solid solution, γ, whenever it was possible to retain this structure by quenching the x-ray diffraction powders from high temperatures. This data is shown in Table 7, and indicates that increasing amounts of vanadium in the face-centered cubic γ solid solution produce a gradual decrease in the lattice parameter. It was not possible to retain the high temperature face-centered cubic structure by rapid cooling of alloy powders containing more than about 40 atomic percent vanadium. We attempted to retain the high temperature structures by rapid cooling of the bulk samples, but this method was found to be unreliable since it is still necessary to remove the x-ray powders from such samples by some process whereby the powder particles are severely deformed. There is evidence that such deformation can produce a structure change in V Pt [4] and we have observed similar behavior in V Pt_3 and V Pt_2 alloys. If one attempts to relieve the strains in these powders by reannealing them at the original annealing temperatures, then one is again faced with the problem of obtaining sufficiently rapid cooling of the powders. We were, therefore, unable to obtain direct evidence of a face-centered cubic structure in alloys containing over 40 atomic percent vanadium, but the continuity of the platinum solid solution in this region is inferred from metallographic examination of these alloys and by other evidence which will be considered in the subsequent discussion.

6. Vanadium Terminal Solid Solution - α

The extent of the vanadium terminal solid solution was determined mainly by electron probe microanalysis of two-phase alloys annealed and quenched from various temperatures within the $\alpha + \beta$ region of the diagram (Fig.13). Lattice parameter measurements were attempted, but the alloy powders apparently undergo either a slight contamination or a precipitation

Table 7

Lattice Parameters of γ Phase
V-Pt Alloys

Composition (atomic % V)	Lattice Parameter - a_o (Å)
0	3.924
10	3.900
20	3.887
25	3.879
28	3.875
30	3.872
36	3.864
40	3.861

of the β phase, which produces line-broadening effects and consequent inaccuracies in locating the positions of the diffraction lines.

Our data indicate that platinum will dissolve in body-centered cubic vanadium to form a solid solution which extends to about 12 atomic percent platinum at 1800°C, but this solubility decreases at lower temperatures. Metallographic studies indicated that no precipitation occurs in the alloy $V_{92}Pt_8$ if it is rapidly cooled from 1700°C, but some precipitation was observed when this alloy was reannealed at lower temperatures. The "as-cast" alloy $V_{92}Pt_8$ appeared to possess a greater resistance to tarnishing in air than a similar sample of pure vanadium.

7. Intermediate Phase θ

Dwight, Downey and Conner[6] have identified the crystal structure of $V Pt_3$ as being isotypic with $TiAl_3$, and this has been confirmed by Maldonado and Schubert.[3] The unit cell of this structure is tetragonal and belongs to the space group I4/mmm. The lattice constants for $V Pt_3$ obtained in our study were $a_o = 3.839$ Å, $c_o = 7.796$ Å, and we have noted that these values are smaller than the values reported by Dwight, Downey and Conner.[6] The experimental uncertainty in our measurements, however, is at least ± 0.01 Å, and therefore the significance of this discrepancy may be questionable. Our use of very high purity vanadium may also account for some discrepancies with the previous data.

We have observed that the lattice constants of the θ phase exhibit a significant composition dependence. This suggests that it is stable over a composition range of several percent. We obtained the values $a_o = 3.860$, $c_o = 7.819$ for the θ phase alloy, $V_{23.5}Pt_{76.5}$, while the θ phase alloy, $V_{26.5}Pt_{73.5}$ yielded the values $a_o = 3.847$, $c_o = 7.796$. We have, therefore, estimated that the composition range of the θ phase extends from 23 to 27 atomic percent vanadium at 800 to 900° C, with an uncertainty of ± 1 atomic percent.

The θ phase apparently forms from the face-centered cubic terminal solid solution of platinum via an order-disorder reaction which occurs at 1015 ± 5°C. If the alloy $V Pt_3$ is annealed at a temperature above this transformation temperature, and then quenched in cold water, one may retain the face-centered cubic structure to room temperature. One may also produce the face-centered cubic structure by subjecting θ phase filings to severe plastic deformation at room temperature. Subsequent annealing of these severely deformed powders will apparently induce recovery and recrystallization, and one ultimately

obtains the equilibrium structure which exists at the annealing temperature. Incomplete annealing of cold-worked θ phase filings may produce metastable structures, and this might perhaps explain why Maldonado and Schubert[3] observed a Cu_3Au type structure in their alloy $V Pt_3$. However, we have never observed a Cu_3Au type structure in our alloy $V Pt_3$ for any of the various annealing treatments used in this study, nor even for the annealing treatment used by Maldonado and Schubert (5 minutes at 1000°C).[3]

As mentioned previously, however, we did observe a Cu_3Au type structure when we reannealed some filings of a θ phase alloy, $V_{23.5}Pt_{76.5}$, for two hours at 980°C. We are not certain whether this structure represents that of a binary equilibrium phase in this system, or whether it is stabilized by some impurity. It is interesting, however, that one can obtain either a $TiAl_3$ type ordered structure, a Cu_3Au type ordered structure, or a disordered face-centered cubic structure in this alloy simply by annealing the alloy filings at the appropriate temperature. The relationship of the $TiAl_3$ type structure to the Cu_3Au type structure has been discussed by H. J. Beattie,[7] and is illustrated in Figure 4 of his paper. We have reproduced this illustration in our Fig. 14. Both of these ordered structures are based on a face-centered cubic arrangement of the atoms. The type of atomic ordering which occurs will determine whether one obtains a cubic Cu_3Au type unit cell of approximately the same size as that of the disordered face-centered cubic structure, or whether the atomic ordering will essentially double this unit cell to produce a tetragonal $TiAl_3$ type structure. It may be noteworthy that a change in crystal symmetry occurs only in the case of the tetragonal $TiAl_3$ type structure, and thus there will be an accumulation of internal strains during a transformation to this structure. These strains are relieved by shear or twinning which is apparently responsible for the striations which are seen in Fig. 15.

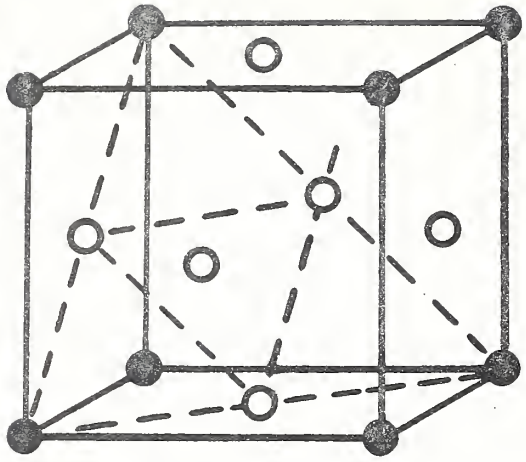

Cu_3Au - type

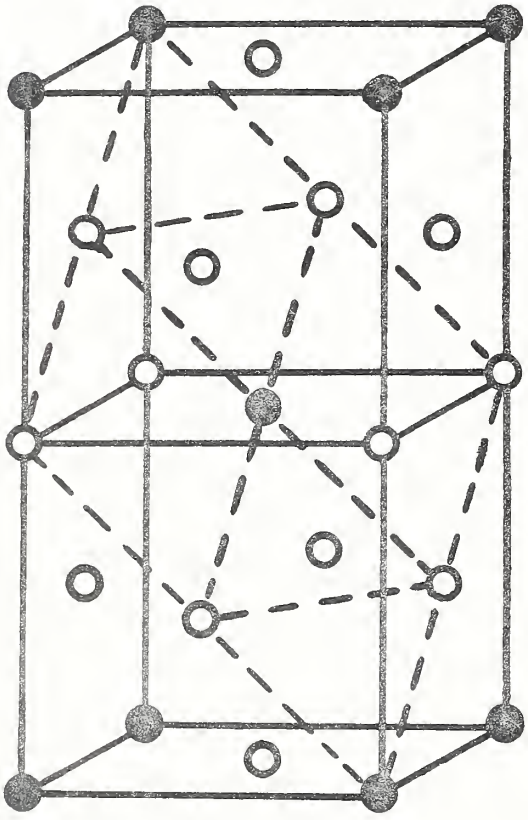

Al_3Ti - type

Fig. 14 - Relationship of the Al_3Ti-type and Cu_3Au-type structures.

Table 8

X-ray Diffraction Pattern of θ Phase $V Pt_3$

Tetragonal $TiAl_3$-type Structure

$a_o = 3.839$ Å, $c_o = 7.796$ Å

$d_{(obs)}$ (Å)	Relative Intensity		hkl
	Observed	Calculated †	
3.881	vw	6	002
3.589	vw	17	101
3.438 *	vvw		
3.283 *	vw		
2.716	w	5	110
2.208	vs	100	112
--	--	5	103
1.950	m	16	004
1.922	ms	31	200
1.726	mw	2	202
1.698	vw	4	211
1.662 *	vw		
1.586	mw	2	114
1.469	vvw	3	105, 213
1.370	ms	18	204
1.361	m	9	220
--	--	<1	006
1.247	w	1	222
1.235	vw	1	301
1.217	w	1	310
1.175	ms	10	116
1.163	s	21	312, 215
--	--	1	303
1.118	ms	9	224
1.079	vw	1	206, 107
1.050	vvw	1	321
1.034	mw	1	314

(Table 8 Continued)

Table 8 (Continued)

0.9993	vw	1	305, 323
0.9771	m	2	008
0.9641	ms	3	400
0.9416	vvw	<1	226
0.9360	vvw	1	217, 402
--	--	1	411
0.9207	vvw	<1	118
0.9035	vvw	<1	330
0.8907	s	12	316
0.8853	ms	6	332
--	--	1	325, 413
0.8722	ms	6	208
0.8648	ms	6	404
0.8624	ms	6	420
--	--	1	109, 307
0.8422	w	1	422
0.8245	w	<1	334
--	--	1	415
0.7949	s	10	228
0.7894	vs	23	424
--	--	<1	0·0·10
0.7755	m	3	219, 406
	m	4	327

* These very weak lines are attributed to the presence of some unidentified impurity.

† Relative intensities were calculated assuming complete ordering of the vanadium and platinum atoms on the available lattice sites; two vanadium atoms in positions 000, $^1/_2\ ^1/_2\ ^1/_2$, and six platinum atoms at $00^1/_2$, $^1/_2\ ^1/_2\ 0$, $0\ ^1/_2\ ^1/_4$, $0\ ^1/_2\ ^3/_4$, $^1/_2\ 0\ ^1/_4$, $^1/_2\ 0\ ^3/_4$. The calculated intensities do not include an absorption correction and the absorption is appreciable in our sample. The observed relative intensities therefore are suitable for comparison only among lines whose Bragg angles (or d-values) are not greatly different.

80X (a)

25 at. % V, 75 at. % Pt equilibrated at 900°C. Large grains of θ phase with microtwinning.

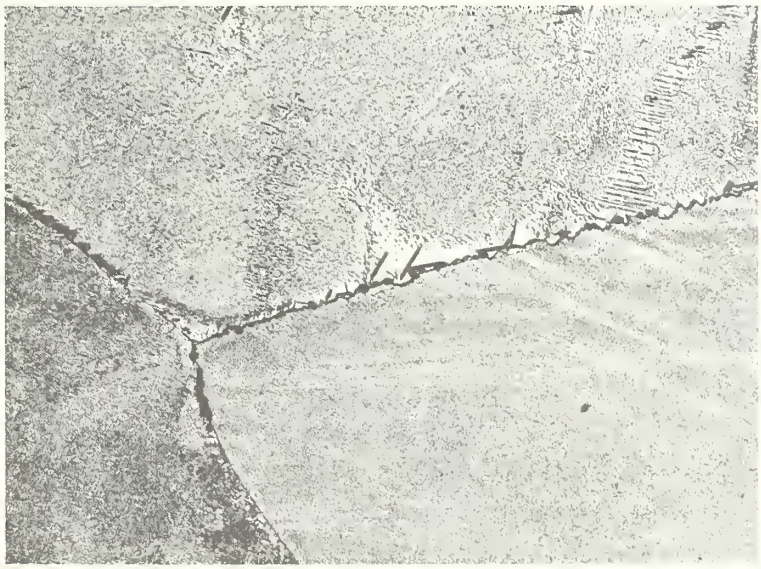

160X (b)

28 at. % V, 72 at. % Pt equilibrated at 950°C for 27 days. Fine structure is presumably due to the eutectoid decomposition of γ to form θ phase + δ phase.

Fig. 15 - Microstructures of vanadium-platinum alloys.

A similar transformation occurs in the V-Ni system and is associated with age-hardening effects.[8,9] An x-ray diffraction pattern of θ phase $V Pt_3$ is presented in Table 8.

8. Intermediate phase δ

The crystal structure of the phase $V Pt_2$ has been identified as an $MoPt_2$ type structure by Schubert et al.[2,3] Their identification was confirmed in a subsequent study by Giessen and Grant,[10] who reported a more accurate determination of the lattice parameters. The structure is orthorhombic and belongs to the space group Immm. The vanadium and platinum atoms are ordered in the two crystallographic positions. The lattice parameters obtained in this study were $a_o = 2.724$ Å, $b_o = 8.302$ Å, and $c_o = 3.786$ Å, all ± 0.01 Å. The values obtained were not significantly affected by changes in the alloy composition, which suggests that this phase is stable only within a rather narrow composition range. Metallographic studies suggested that the composition range of this phase extends from about 32.5 to 34.0 atomic percent vanadium at 900°C, with an uncertainty of ± 1 atomic percent.

The δ phase forms from the face-centered cubic platinum solid solution through an order-disorder reaction which occurs at 1105 ± 5°C. If the alloy $V Pt_2$ is quenched from a temperature above this transition temperature, one may retain the face-centered cubic structure to room temperature. It is also possible to produce the face-centered cubic structure by severe plastic deformation of δ phase alloy filings. These filings may be subsequently annealed to produce an equilibrium structure, and this occurs in a manner quite similar in behavior to that which has been described for the θ phase alloys. In both cases, it is possible that the structure transformation is produced by the destruction of long-range ordering resulting from severe cold-working of the alloy powders. It is also possible that incomplete

Table 9

X-ray Diffraction Pattern of δ Phase V Pt_2

Orthorhombic $MoPt_2$-type Structure

a_o = 2.724 Å, b_o = 8.302 Å, c_o = 3.786 Å

$d_{(obs)}$ (Å)	Relative Intensity		hkl
	Observed	Calculated +	
4.107	w	16	020
3.429	m	44	011
2.575	mw	20	110
2.230	vs	100	031
2.209	vs	99	101
2.073	w	9	040
1.950	w	8	121
1.932	ms	63	130
1.893	m	30	002
1.723	w	3	022
1.530	mw	8	112
1.511	m	12	141
1.399	w	5	042
1.382	m	9	060
1.363	m	9	200
1.356	s	35	132
1.292	vw	1	220
1.267	w	4	211
1.252	vw	2	013
1.172	ms	19	161
1.162	ms	20	231
1.149	m	19	033, 103
1.139	vw	3	240, 152
1.133	w	3	071
1.118	m	8	062
1.107	m	10	202, 123

(Table 9 Continued)

Table 9 (Continued)

1.089	w	3	170
1.069	w	1	222
--	--	0	080
1.014	vw	<1	251
1.005	mw	3	053, 143
0.9770	w	3	242
0.9718	m	6	260
0.9505	w	3	004
0.9449	mw	4	172
--	--	<1	181
0.9222	w	2	024, 213
--	--	0	082
0.9043	vw	1	310
0.8980	m	5	091
0.8875	vw	2	114
0.8844	ms	17	301, 163
0.8799	m	12	233
0.8751	w	9	190, 271
0.8651	s	32	073, 262, 321, 330, 044
0.8541	ms	13	134
0.8312	w	2	0·10·0
--	--	0	280
0.8161	mw	2	312
0.8140	mw	4	341
--	--	<1	253
0.7952	ms	17	350, 192
0.7894	mw	1	154
0.7867	s	24	332
0.7799	m	13	064
0.7780	m	16	204
0.7770	m	15	1·10·1

† Relative intensities were calculated assuming complete ordering of the vanadium and platinum atoms on the available lattice sites; two vanadium atoms in positions 2(a) (000) ($^1/_2$ $^1/_2$ $^1/_2$) and four platinum atoms at positions 4(g) (0y0) ($^1/_2$,$^1/_2$ + y, $^1/_2$) (0, - y, 0) ($^1/_2$, $^1/_2$ - y, $^1/_2$) where y = 0.341. The calculated intensities do not include an absorption correction and this may be appreciable in our sample. The observed relative intensities are therefore suitable for comparing only those lines whose Bragg angles (or d-values) are not very different.

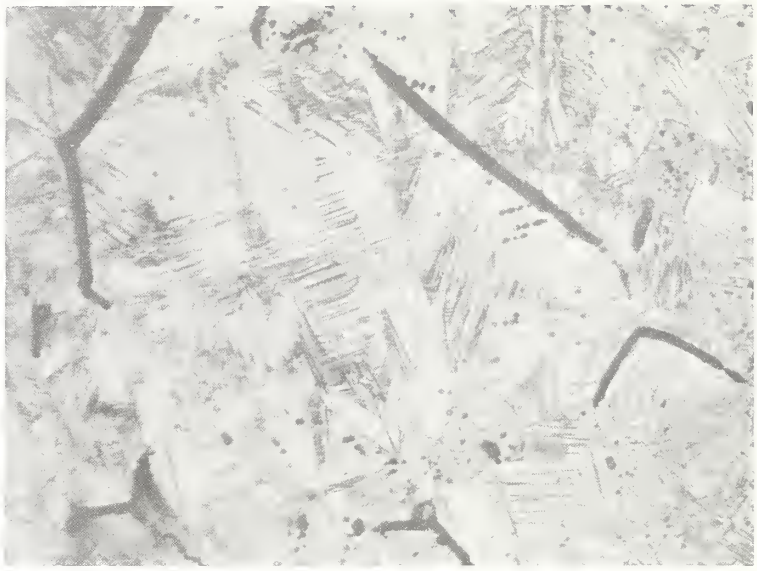

160X (a)

33 at. % V, 67 at. % Pt equilibrated at 900°C. Large grains of δ phase heavily etched to reveal microtwinning.

400X (b)

40 at. % V, 60 at. % Pt equilibrated at 1300°C for 3 days. Alloy is composed of the γ solid solution with no evidence of any second phase.

Fig. 16 - Microstructures of vanadium-platinum alloys.

annealing of the cold-worked powders would produce a metastable phase, and this may account for the observation of a CuAu type structure in certain V-Pt alloys.[3]

The formation of the ordered phase V Pt_2 from the face-centered cubic solid solution involves a change in crystal symmetry, as in the case of V Pt_3, and consequently, one observes similar evidence of the existence of internal strains. This can be seen in the form of striations within each grain as shown in Fig. 16a. One may also expect to observe age-hardening effects in these alloys. An x-ray diffraction pattern of the δ phase V Pt_2 is presented in Table 9.

9. Intermediate Phase ζ

Schubert et al.[2,3] were the first to report the existence of a phase V Pt having the AuCd-type structure. We have confirmed this identification, but we were unable to confirm their identification of a CuAu type structure at this same composition, except for alloy filings which had been severely deformed by cold-working. The severely deformed alloy powders produce x-ray diffraction patterns having rather broad lines which did not permit careful indexing, but nevertheless, these lines did appear to be those of a CuAu type ordered phase.[4] If these deformed powders were reannealed at various temperatures, however, they would invariably transform to the AuCd type structure. Thus, it appeared that the CuAu type structure was a metastable phase, and that the true equilibrium structure of the phase V Pt is the AuCd type structure.

Metallographic examination of the alloy V Pt, however, revealed profuse twinning (see Fig. 20b) and this at first suggested to us that the AuCd type structure may have been formed by a martensitic transformation. If such were the case, then it would be likely that some unidentified structure existed at

high temperatures which had probably not been retained to room temperature, even by rapid cooling. On the other hand, it also appeared possible that the AuCd type structure, which is highly ordered, may have been formed by an order-disorder transformation from an extension of the face-centered cubic platinum solid solution in a manner similar to the mode of formation of $V Pt_3$ and $V Pt_2$.

An attempt was therefore made to detect evidence of any structure transformations which may occur in this alloy from room temperature up to within about 100°C of its melting point. This was done by using a high temperature vacuum dilatometer to detect small changes in specimen length during several heating and cooling cycles. This dilatometer had been designed and constructed by Mr. Joseph Valentich at the Westinghouse Research Laboratories,[11] who kindly conducted the measurements on our sample. The sample was prepared by carefully grinding a portion of an arc melted button to obtain a cylindrical sample of about 1/4-inch diameter by 1-1/4-inches long. The alloy is quite brittle, and we are indebted to Mr. John Kumpula of the National Bureau of Standards for his skillful and patient effort in preparing this sample without any visible cracks. The cylindrical sample was then homogenized and stress-relieved by annealing it in a tantalum V-block holder at a temperature of 1600°C, followed by slow cooling to room temperature.

Subsequent heating and cooling cycles in the high temperature dilatometer from 25°C to 1650°C to 25°C revealed evidence of only one transformation occurring at about 1500 ± 10°C. Data for a typical heating and cooling cycle are shown in Fig. 17. The arrest was fairly sharp and occurred at nearly the same temperature during heating and during cooling. A volume change of about 0.6% is suggested by this data with the low temperature phase apparently having a smaller specific volume (i.e., greater density). The dilatometer is capable of

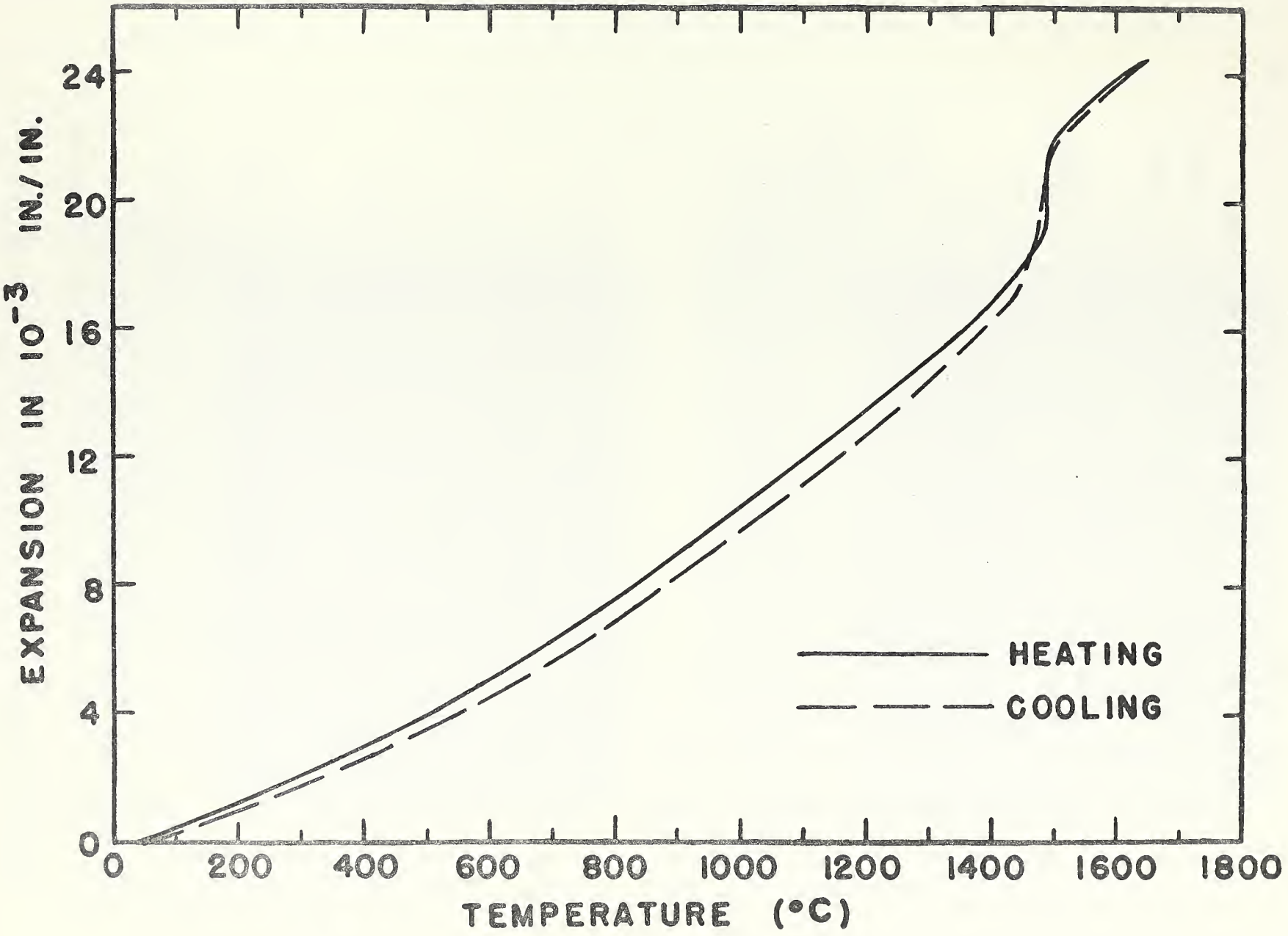

Fig. 17 - Thermal expansion of VPt as a function of temperature.

detecting volumetric changes of less than 0.1% and we have, therefore, concluded that the AuCd type structure which we have observed in our V-Pt alloys is probably stable from room temperature up to 1500°C, where it apparently transforms to another structure which is stable only above 1500°C, and probably up to the melting point of this alloy (~1770°C). Metallographic studies of alloys in the equiatomic composition region suggest that the high temperature phase is, in fact, a continuation of the face-centered cubic platinum solid solution from which the ζ phase forms by an order-disorder reaction at about 1500°C. The onset of ordering apparently produces a distortion of the face-centered cubic structure resulting in the orthorhombic AuCd type structure. It is interesting to observe that the AuCd type structure has been considered to be a distortion of a close-packed hexagonal structure,[12] a distortion of a body-centered cubic structure,[13] and, as in the present case, a distortion of a face-centered cubic structure.[4,13]

It appears that the ζ phase coexists with the β phase on the V-rich side of the equiatomic stoichiometry as a result of a eutectoid decomposition of the high temperature γ phase. On the Pt-rich side, however, the ζ phase coexists with the face-centered cubic γ phase, and apparently this gives rise to the unusual microstructure shown in Fig. 18b. This structure consists of parallel ribbons of the ζ phase apparently having a strong epitaxial relationship with the matrix γ phase, since this structure is stable even after annealing for three days at 1300°C. The ribbons are not simply due to twinning of the γ phase since, first, they have a different crystal structure which is revealed strongly by polarized light, and secondly, they have a different composition (richer in vanadium) than the matrix phase as revealed by an electron beam target current scanning image shown in Fig. 19a. The formation of ribbons of the ζ phase, which are strongly coherent with the face-centered

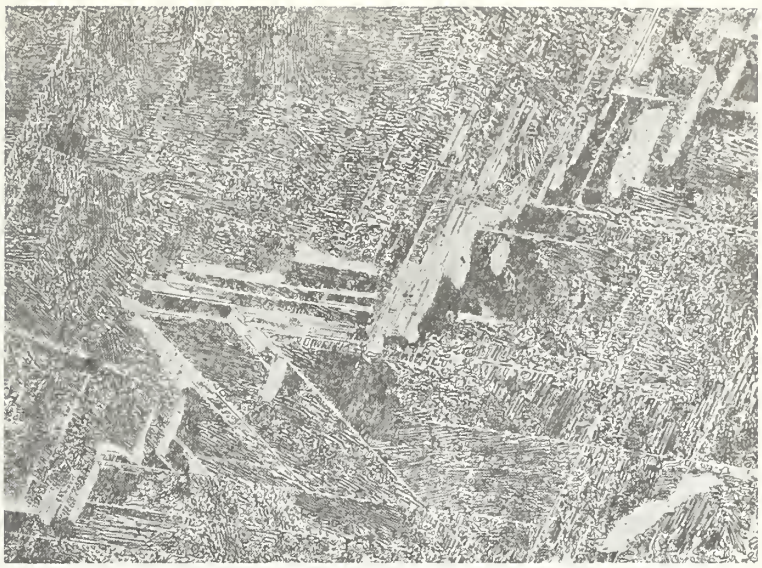

208X (a)

43 at. % V, 57 at. % Pt equilibrated at 900°C for 6 weeks. Prior γ phase regions have decomposed eutectoidally to form δ phase + ζ phase.

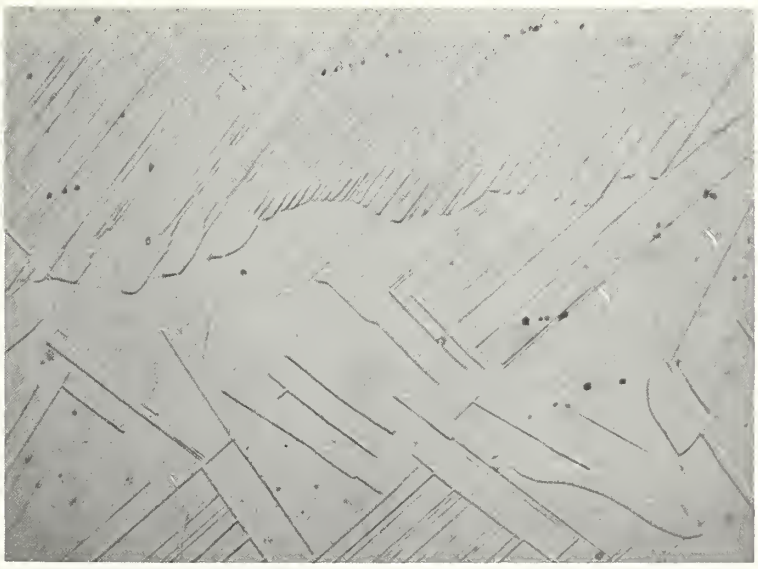

500X (b)

43 at. % V, 57 at. % Pt equilibrated at 1300°C for 3 days. Ribbons of ζ phase in a matrix of γ phase. See Fig. 19a.

Fig. 18 - Microstructures of vanadium-platinum alloys.

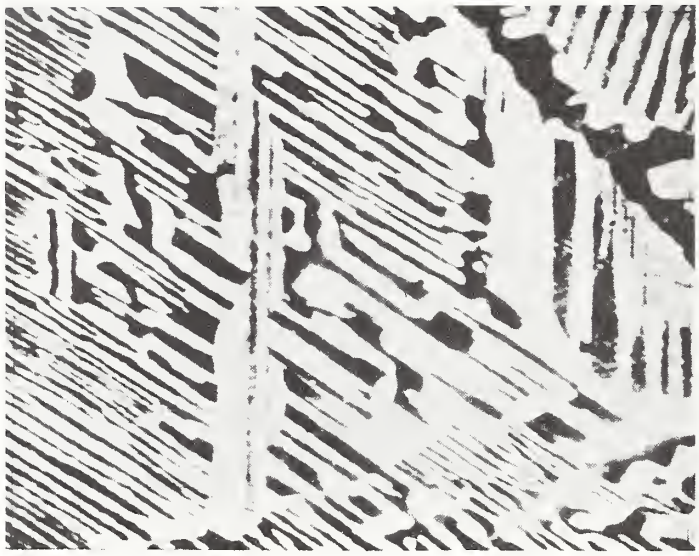

1000X (a)

43 at. % V, 57 at. % Pt equilibrated at 1300°C for 3 days. This is an electron beam target-current scanning image of the structure shown in Fig. 18b. It reveals that V-rich ribbons (dark) co-exist with a Pt-rich matrix (light).

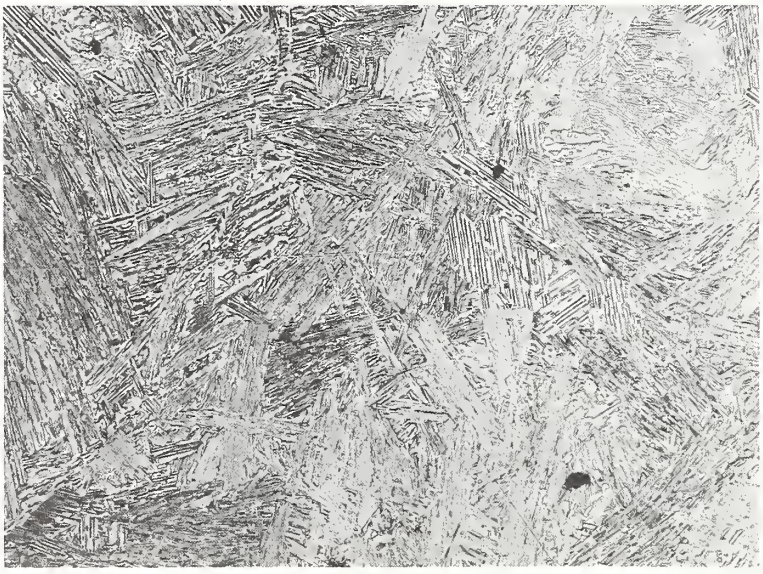

80X (b)

46 at. % V, 54 at. % Pt equilibrated at 1300°C for 3 days. Bands of VPt in a matrix of γ phase.

Fig. 19 - Microstructures of vanadium-platinum alloys.

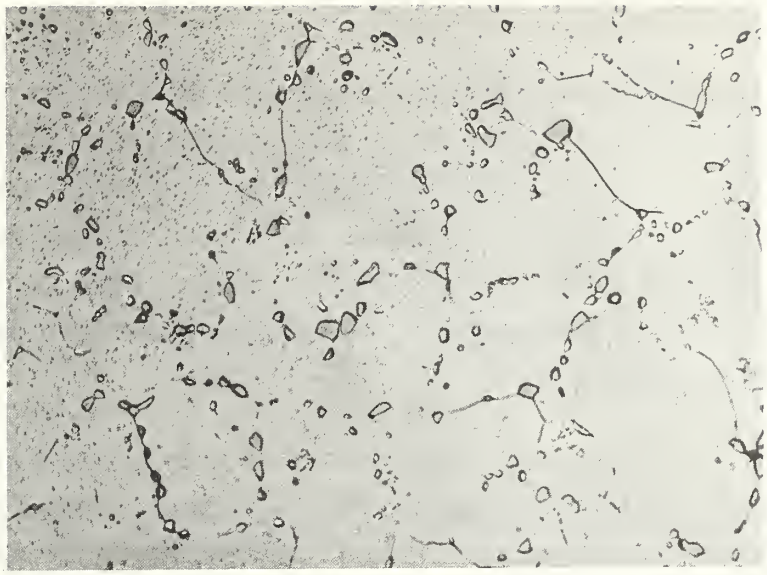

400X (a)

48 at. % V, 52 at. % Pt equilibrated at 1300°C for 3 days. Small globules of γ phase at grain boundaries of the ζ phase.

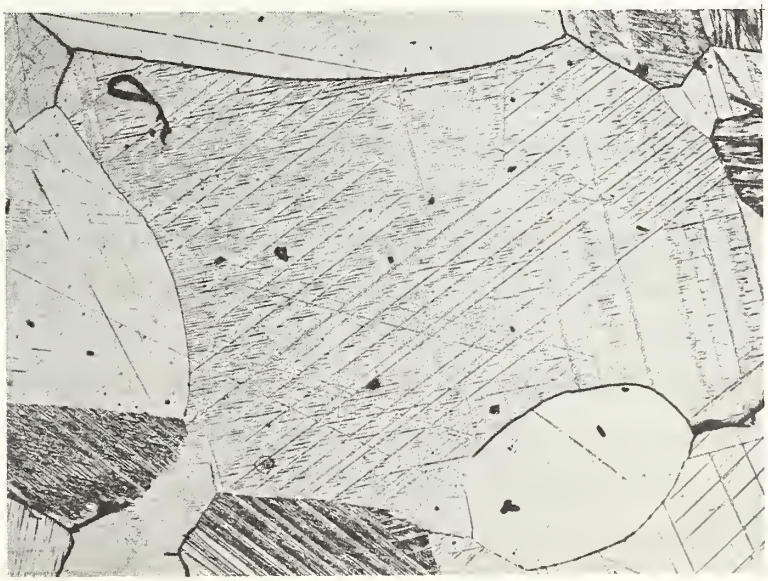

52X (b)

50 at. % V, 50 at. % Pt equilibrated at 1500°C. ζ phase grains showing microtwinning.

Fig. 20 - Microstructures of vanadium-platinum alloys.

cubic γ phase, suggests interesting possibilities of fibre reinforcement to obtain superior mechanical properties. Unfortunately, alloys in this composition range seem to suffer from some form of intergranular embrittlement, and it may therefore be necessary to first grow single crystals of the γ phase in order to take full advantage of the reinforcement provided by the ζ phase ribbons.

The AuCd type structure is orthorhombic and belongs to the space group Pmma. We have indexed all the lines in the powder pattern of the ζ phase, and have also calculated the relative line intensities. This is shown in Table 10. The intensity agreement is satisfactory for all lines except (200). The intensity of the (200) line appears to be significantly stronger than the calculations would indicate, and the reason for this discrepancy has not yet been discovered. Attempts to improve the intensity agreement by assuming variations in the degree of long-range atomic ordering, or by variations in the atomic position parameters z_e or z_f, were unsuccessful. The final lattice parameters obtained for our alloy V Pt were $a_o = 4.413$ Å, $b_o = 2.693$ Å, $c_o = 4.767$ Å $\pm$ 0.005 Å. There was apparently some change in line positions produced by composition variations, but these were rather small and we did not attempt to determine the variation in lattice parameters. It appears, however, that the ζ phase does possess a significant compositional range of stability which we have estimated from metallographic observations as being from 49.0 to 51.5 atomic percent vanadium $\pm$ 1 atomic percent.

It was observed that vanadium-platinum alloys having compositions in the equiatomic region are quite susceptible to contamination, particularly when the alloy lumps or powders are heated in quartz tubes. In such cases, one usually sees many extra lines in the x-ray diffraction patterns, but

Table 10

X-ray Diffraction Pattern of ζ Phase V Pt

Orthorhombic AuCd-type Structure

a_o = 4.413 Å, b_o = 2.693 Å, c_o = 4.767 Å

d(obs) (Å)	d(calc) (Å)	Relative Intensity		hkl
		Observed	Calculated +	
4.741	4.766	w	13	001
3.218	3.238	m+	61	101
2.674	2.693	mw	22	010
2.528		vvw		
2.370	2.383	mw-	17	002
2.332	2.345	mw-	18	011
2.195	2.206	m+	38	200
2.089	2.097	m	42	102
2.062	2.071	s	100	111
	2.002	--	3	201
1.777	1.785	w	7	012
1.699	1.707	m+	12	210
1.650	1.655	m	12	112
1.611	1.619	mw	10	202
1.600	1.607	mw	11	211
1.582	1.589	vw	5	003
	1.495	--	1	103
1.401	1.405	mw	6	301
1.384	1.388	mw-	6	212
1.364	1.368	m	16	013
1.342	1.347	mw	8	020
	1.307	--	1	113
	1.296	--	1	021
1.287	1.289	w	5	203
1.249	1.252	w	8	302

(Table 10 Continued)

Table 10 (Continued)

1.244	1.246	vs	19	213
	1.243	vs	8	121
	1.192	--	<1	004
1.1669	1.1723	vw	4	022
1.1605	1.1629	s	19	213
	1.1504	ms	8	104
1.1471	1.1494	ms	10	220
	1.1351	ms	4	312
1.1309	1.1330	ms	12	122
	1.1173	--	1	221
1.1013	1.1032	mw	4	400
	1.0897	--	<1	014
	1.0794	--	<1	303
	1.0747	--	<1	401
1.0566	1.0579	mw	7	114
	1.0485	--	1	204
1.0336	1.0353	mw	6	222
1.0265	1.0272	vw	3	023
1.0190	1.0208	w	3	410
	1.0019	--	<1	313
0.9995	1.0011	mw	3	402
	1.0005	mw	1	123
	0.9982	mw	3	411
	0.9770	--	<1	214
0.9702	0.9723	mw	5	321
	0.9533	--	1	005
	0.9384	--	3	412
	0.9318	--	1	105
0.9305	0.9312	mw	5	223
0.9252	0.9259	mw	7	304
0.9158	0.9168	m^+	10	322
0.9058	0.9062	w	3	403

(Table 10 Continued)

Table 10 (Continued)

	0.8987	m^-	4	015
0.8976	0.8977	m^-	2	030
	0.8924	--	1	024
	0.8822	--	2	031
0.8807	0.8806	m	7	115
	0.8756	s	7	314
	0.8751	s	3	205
0.8744	0.8747	s	15	124
	0.8678	--	3	501
0.8641	0.8650	m	13	131
0.8588	0.8588	m^+	16	413
0.8530	0.8533	mw	9	420
	0.8422	--	<1	323
	0.8401	--	1	032
0.8394	0.8400	vw	2	421
	0.8323	m	10	215
0.8319	0.8315	m	4	230
	0.8276	w	7	502
	0.8273	--	2	224
0.8255	0.8260	s	17	511
	0.8252	s	5	132
0.8191	0.8191	vw	5	231
	0.8095	--	1	404
0.8033	0.8034	mw	10	422
	0.8000	--	1	305
0.7943	0.7944	vw	6	006
0.7911	0.7911	vw	7	512
	0.7851	vw	8	232
	0.7819	--	3	106
0.7814	0.7816	ms	22	033
		w	10	025
		--	<1	414
		--		503

(Table 10 Continued)

Table 10 (Continued)

† Relative intensities are calculated assuming complete ordering of the vanadium and platinum atoms; two platinum atoms are in positions 2(e) at $\frac{1}{4}, 0, z_e$; $\frac{3}{4}, 0, 1-z_e$; and two vanadium atoms are in positions 2(f) at $\frac{1}{4}, \frac{1}{2}, z_f$; $\frac{3}{4}, \frac{1}{2}, 1-z_f$. The best intensity agreement was obtained for $z_e = 0.180 \pm 0.005$, $z_f = 0.660 \pm 0.005$ (standard deviations are estimated). Variations in the degree of ordering and increments of 0.01 in the z parameters were considered but in each case they produced a less satisfactory agreement between observed and calculated intensities than shown above. The observed and calculated intensities are not corrected for absorption which is appreciable in the sample. Comparison of relative intensities was therefore primarily confined to lines whose Bragg angles (or d-values) were not greatly different.

these lines are not seen after an equivalent heat treatment in our tantalum-strip high vacuum annealing furnace, or when the alloys are sealed in pure platinum tubes under a partial pressure of pure argon. For example, when proper precautions are taken during annealing of the alloy V Pt, we have observed an x-ray pattern showing only the lines of a AuCd type structure, but when the same alloy is annealed in a quartz tube which was either evacuated to 10^{-6} mm Hg or filled with a partial pressure of pure argon, then one obtains many extra lines, presumably due to a contamination of the sample by silicon. Further details are given in Section IV, F-2.

10. Intermediate Phase β

Greenfield and Beck[1] were apparently the first investigators to report the existence of an intermediate phase having the A15 (β-W) crystal structure in the vanadium-platinum alloy system. They did not attempt to determine its range of homogeneity, however. We have observed a broad homogeneity range for this phase extending from 67.5 to 81.0 atomic percent vanadium ± 1.0 atomic percent. The extent of this composition range was established mainly by electron probe microanalyses of two-phase alloys annealed at various temperatures and rapidly cooled. These results were in good agreement with data obtained by means of x-ray diffraction and metallographic examinations. The lattice parameters of this cubic structure varied with composition from a_o = 4.813 Å (V-rich) to a_o = 4.831 Å (Pt-rich), and it was further established by density measurements that the large deviations from the "ideal" (A_3B) composition were not due to atom vacancy formation on the lattice sites.[14] An A15 type phase having a similarly broad composition range has been reported for the vanadium-iridium alloy system.[15] An x-ray diffraction pattern for the β phase V_3Pt is presented in Table 11.

Table II

X-ray Diffraction Pattern of β Phase V_3Pt

Cubic Cr_3Si-type Structure

$a_o = 4.817$ Å

$d_{(obs)}$ (Å)	Relative Intensity		hkl
	Observed	Calculated †	
3.403	s	67	110
2.405	ms	45	200
2.152	m	25	210
1.965	vs	100	211
1.701	mw	10	220 22
1.528	m	15	310
--	--	3	222
1.339	w	5	320
1.290	s	51	321
1.206	m	10	400
1.137	m	9	411, 330
1.079	m †	16	420
1.052	mw	5	421
1.028	m †	15	332
0.9848	mw	5	422
0.9456	m †	18	510, 431
0.8954	mw	7	520, 432
0.8801	ms	31	521
0.8521	m	17	440
0.8266	m	15	530, 433
0.8029	ms	33	600, 442
0.7922	w	5	610
0.7817	vs	134	611, 532

† Relative intensities were calculated assuming complete ordering of the vanadium and platinum atoms on the available lattice sties; two platinum atoms in positions 2(a) 000, $^1/_2\ ^1/_2\ ^1/_2$ and six vanadium atoms in positions 6(c) $(0\ ^1/_4\ ^1/_4\ ^1/_2)\ (0, ^3/_4, ^1/_2)\ (^1/_2\ 0\ ^1/_4)\ (^1/_4\ ^1/_2\ 0)\ (^3/_4\ ^1/_2\ 0)$. The

calculated intensities do include an absorption correction and the absorption is appreciable in our sample. The observed relative intensities are therefore suitable for comparison only among lines whose Bragg angle (or d-values) are not greatly different.

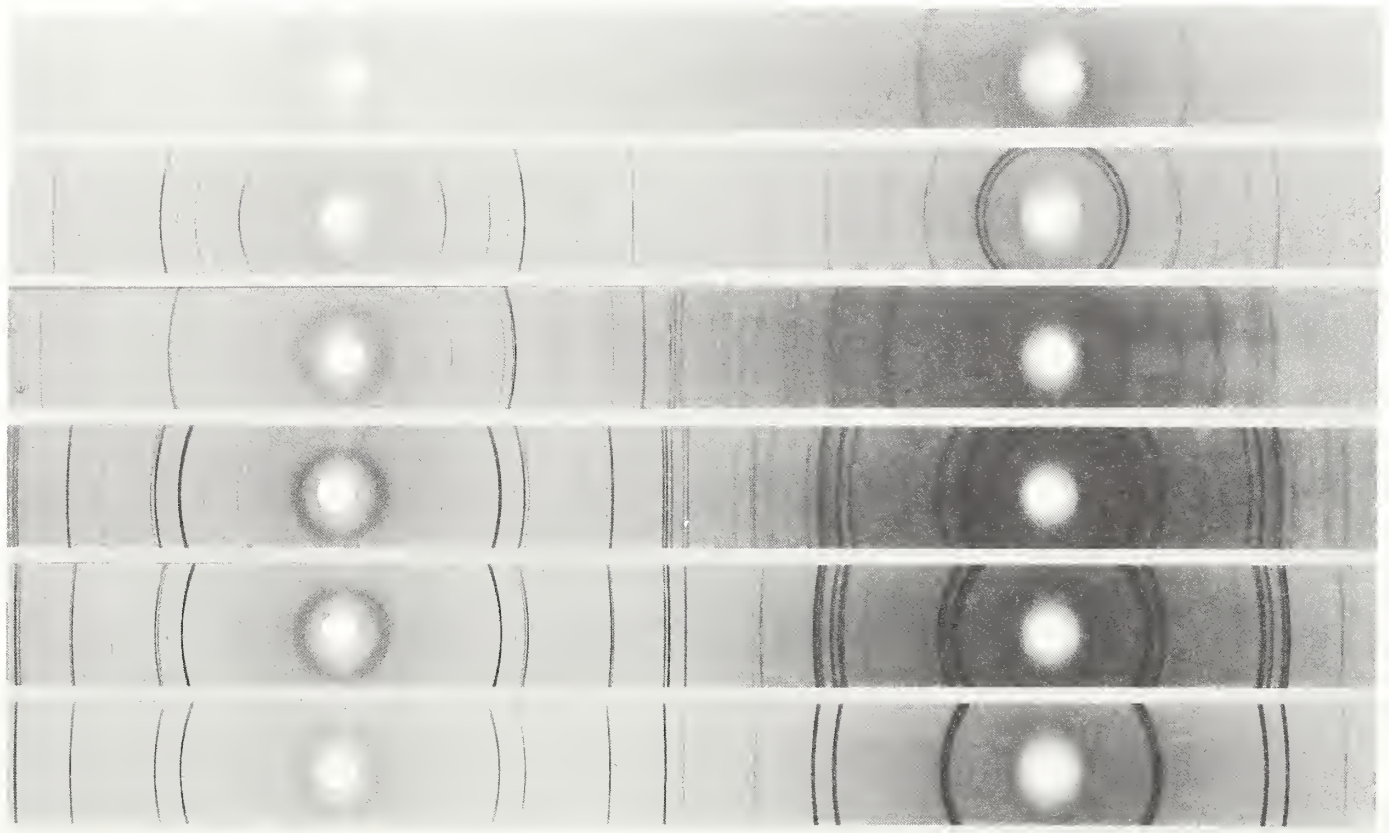

Fig. 21 - Powder X-ray diffraction patterns of single phase V-Pt alloys obtained with nickel-filtered copper radiation (Reduced 53% for reproduction.).

11. Eutectoid: $\gamma \rightleftharpoons \theta + \delta$

The existence of this eutectoid transformation was established by x-ray diffraction studies on alloy powders annealed in evacuated quartz tubes and quenched from various temperatures. The eutectoid transformation temperature was located at 970° ± 10°C, and the eutectoid composition at 28.5 ± 1 atomic percent vanadium.

12. Eutectoid: $\gamma \rightleftharpoons \delta + \zeta$

This eutectoid transformation was established by both x-ray diffraction and metallographic studies on alloys quenched from various temperatures. A typical eutectoid microstructure is shown in Fig. 18a. The eutectoid temperature was found to be 980° ± 10°C, and the eutectoid composition was established at 39.0 ± 1 atomic percent vanadium.

13. Eutectoid: $\gamma \rightleftharpoons \zeta + \beta$

The existence of this eutectoid reaction was established entirely by metallographic studies on alloys which were annealed at various temperatures followed by rapid cooling in our tantalum-strip resistance furnace. The alloys were cooled by turning off the furnace power. The alloy $V_{55}Pt_{45}$ was particularly helpful for establishing the eutectoid reaction temperature, since this alloy was composed entirely of a finely decomposed structure having a feathery appearance when cooled from above the eutectoid temperature as shown in Fig. 22b. When this alloy was annealed below the eutectoid reaction temperature, however, and rapidly cooled, we observed the spheroidized structure shown in Fig. 23a. In this manner, it was possible to bracket the eutectoid temperature by a series of annealing treatments and the eutectoid reaction temperature was thereby located at 1410 ± 10°C. The eutectoid composition was located by means of metallographic observations at 55.0 ± 1 atomic percent vanadium.

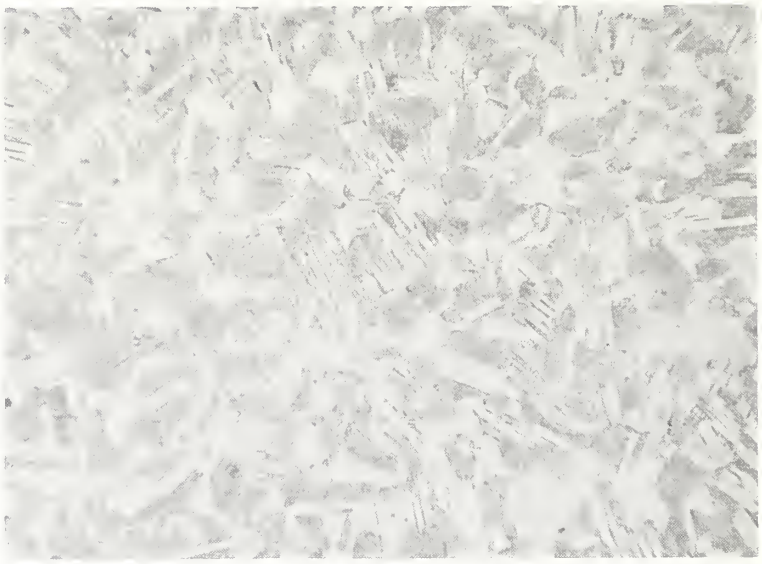

130X (a)

53 at. % V, 47 at. % Pt equilibrated at 1430°C. Alternating bands of ζ phase (light) and former γ phase eutectoidally decomposed (dark).

80X (b)

55 at. % V, 45 at. % Pt equilibrated at 1430°C and cooled rapidly. Dark feathery structure is eutectoidally decomposed γ phase.

The light area is a small amount of retained primary γ phase.

Fig. 22 - Microstructures of vanadium-platinum alloys.

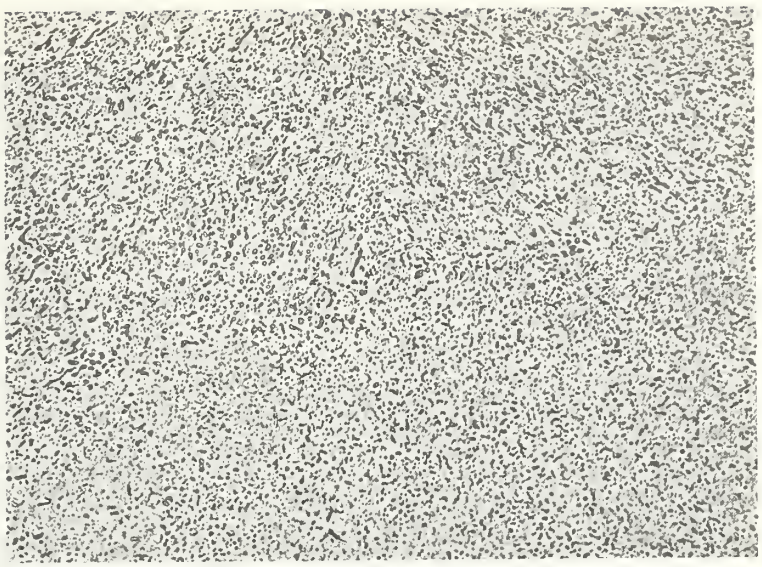

208X (a)

55 at. % V, 45 at. % Pt equilibrated at 1400°C. Spheroidized particles of β phase in a matrix of ζ phase.

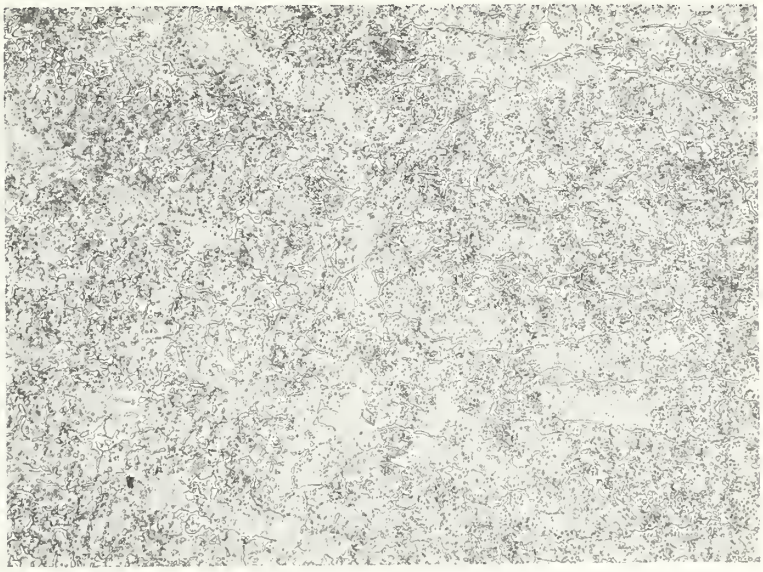

80X (b)

57 at. % V, 43 at. % Pt equilibrated at 1600°C. Particles of β phase in a matrix of prior γ phase which has undergone a eutectoid decomposition during cooling.

Fig. 23 - Microstructures of vanadium-platinum alloys.

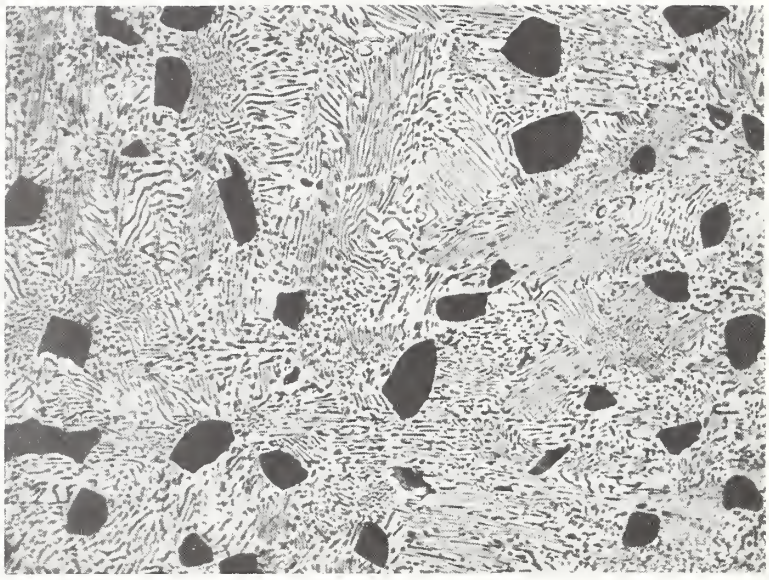

1000X (a)

57 at. % V, 43 at. % Pt equilibrated at 1500°C. Particles of β phase in a matrix of eutectoidally decomposed prior γ phase.

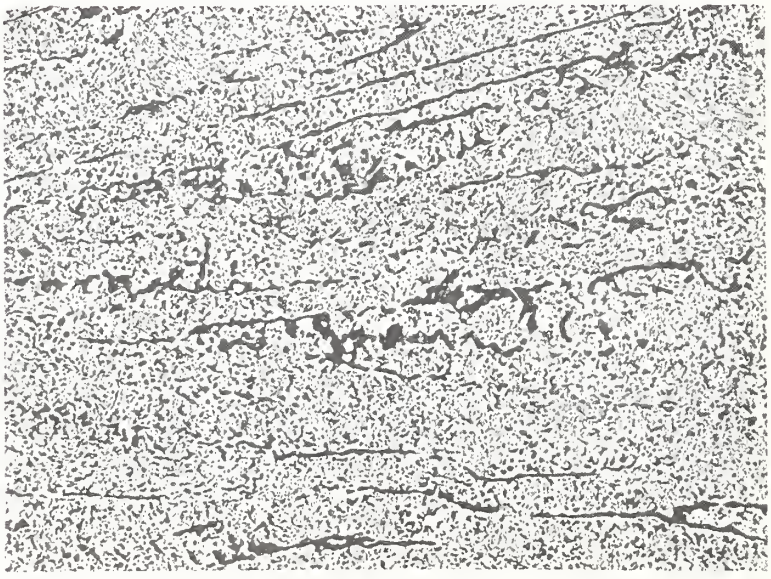

208X (b)

57 at. % V, 43 at. % Pt equilibrated at 1100°C. Dark areas are β phase. Light areas are ζ phase.

Fig. 24 - Microstructures of vanadium-platinum alloys.

14. Eutectic: $L \rightleftharpoons \gamma + \beta$

This eutectic reaction was located at 1720 ± 10°C by melting point measurements.

The eutectic composition was estimated at 63.0 ± 1 atomic percent vanadium by examining the microstructure of specimens which had been used in the melting point determinations. A typical eutectic structure is shown in Fig. 25a.

15. Peritectic: $L + \alpha \rightleftharpoons \beta$

The existence of this peritectic reaction was established mainly by melting point determinations. Alloys containing 70 to 90 atomic percent vanadium melted rather sluggishly, and it was possible to determine the temperature at which melting was first observed and also the temperature at which melting was essentially completed. All melting point measurements on these vanadium-rich alloys were conducted using high purity thoria crucibles. Metallographic evidence for the peritectic composition was difficult to obtain, but it appears that it is located at 81.5 ± 1 atomic percent vanadium.

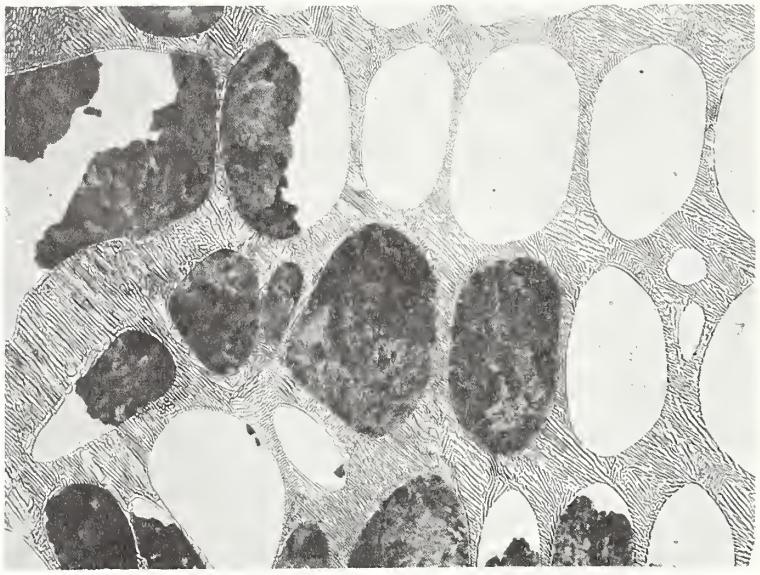

400X (a)

59 at. % V, 41 at. % Pt "as-cast" condition. Primary γ grains have partially transformed via a eutectoid reaction. Eutectic structure surrounding the primary grains is $\gamma + \beta$.

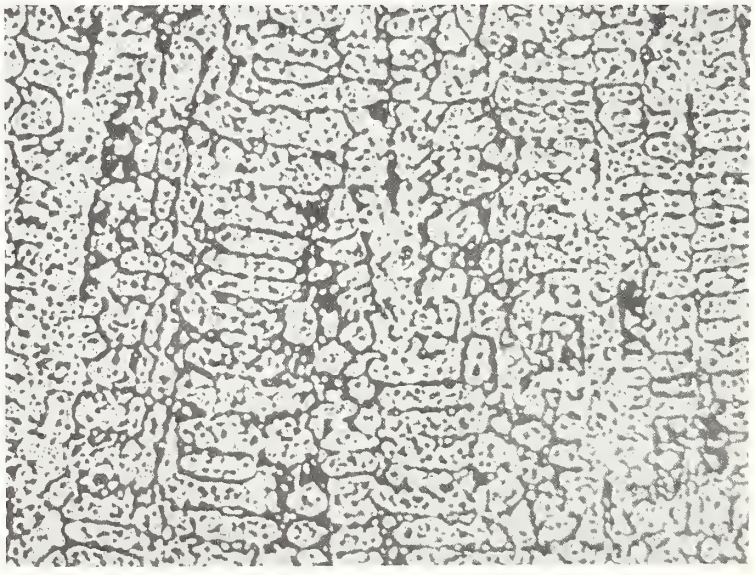

160X (b)

59 at. % V, 41 at. % Pt equilibrated at 1300°C. Dark areas are β phase. Light areas are ζ phase.

Fig. 25 - Microstructures of vanadium-platinum alloys.

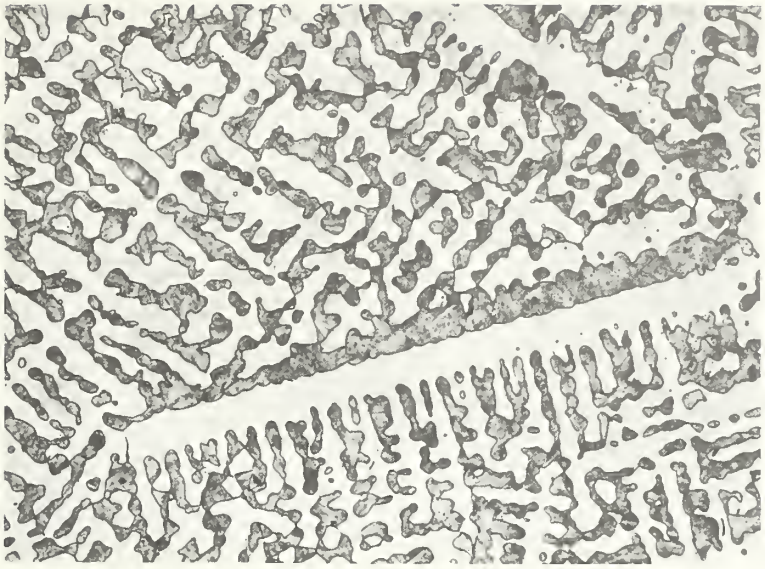

150X (a)

63 at. % V, 37 at. % Pt equilibrated at 1500°C. Islands of eutectoidally decomposed γ phase (dark) in a matrix of β phase (light).

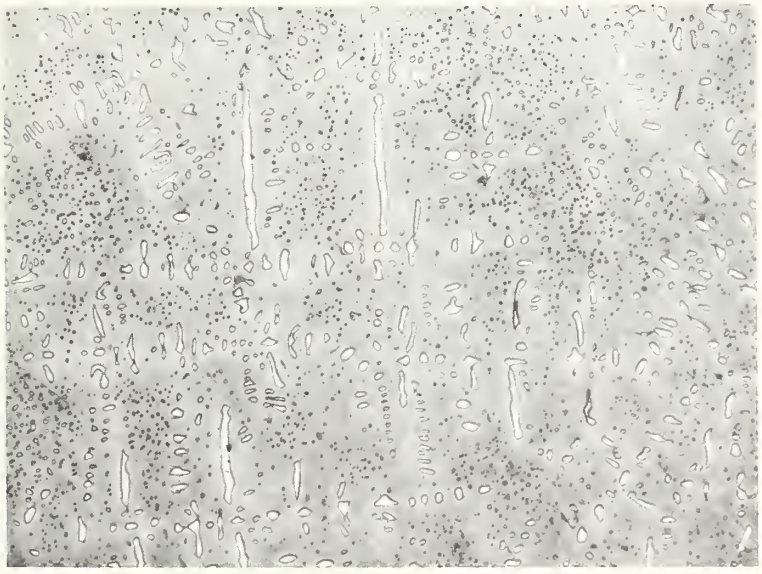

160X (b)

83 at. % V, 17 at. % Pt equilibrated at 1030°C. Spheroidal particles of αV in a matrix of β phase.

Fig. 26 - Microstructures of vanadium-platinum alloys.

80X (a)

87 at. % V, 13 at. % Pt equilibrated at 1300°C. The two phases are β phase and αV.

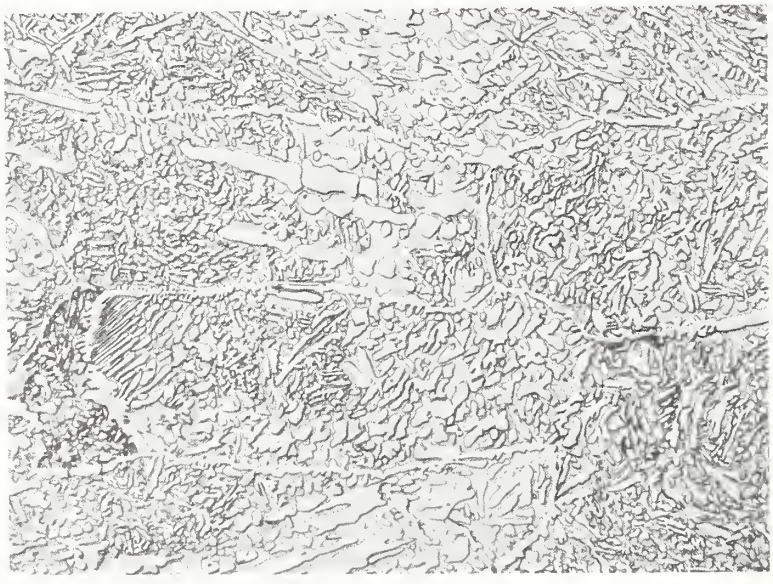

160X (b)

87 at. % V, 13 at. % Pt equilibrated at 1100°C. The two phases are β phase and αV.

Fig. 27 - Microstructures of vanadium-platinum alloys.

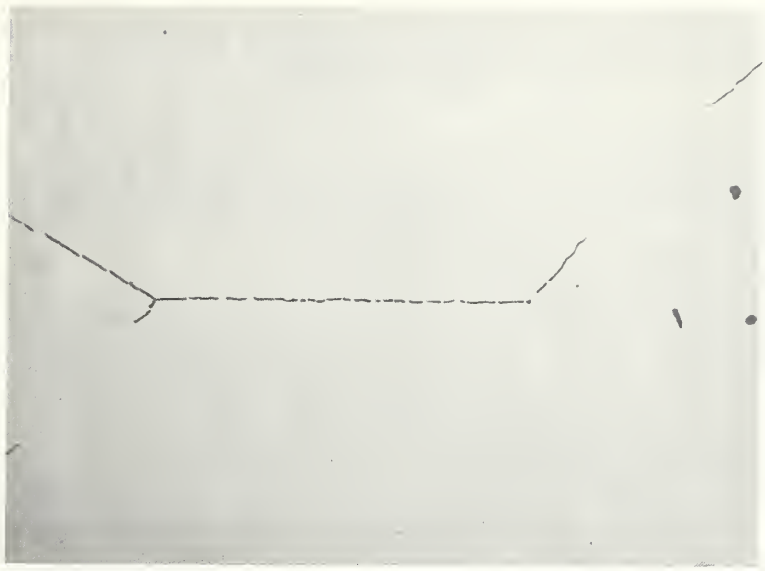

40X (a)

92 at. % V, 8 at. % Pt equilibrated at 1100°C. Large grains of αV with a small amount of β phase precipitated at grain boundaries.

Fig. 28 - Microstructures of vanadium-platinum alloys.

REFERENCES

1. Greenfield, P. and Beck, P. A., Intermediate Phases in Binary Systems of Certain Transition Elements, Trans. AIME, 206, pp. 265-276, (1956).

2. Schubert, K., Frank, K., Gohle, R., Maldonado, A., Meissner, H. G., Raman, A. and Rossteutscher, W., Some Structure Data for Metallic Phases, Naturwissenschaften, 50, p. 41, (1963).

3. Maldonado, A. and Schubert, K., Structure Investigations in some of the T^5-T^{10} Homologous and Quashihomologous Alloy Systems, Z. Met., 55, pp. 619-626, (1964).

4. Waterstrat, R. M., Crystal Structure Transformations in V Pt Produced by Plastic Deformation at Room Temperature, Trans. Met. Soc. AIME, 245, pp. 1360-1361, (1969).

5. Sullivan, T. A., Electrorefining Vanadium, J. of Metals, 17, pp. 45-48, (1965).

6. Dwight, A. E., Downey, J. W. and Conner, R. A., Some AB_3 Compounds of the Transition Metals, Acta Cryst., 14, pp. 75-76, (1961).

7. Beattie, H. J., Close-Packed Structures, in: "Intermetallic Compounds", pp. 144-165, John Wiley and Sons, Inc., New York, (1967).

8. Peters, E. T., Ryan, J. J., Vilks, I. and Tanner, L. E., Mechanical Behavior of Intermetallic Compounds, ASD TDR, Part III, pp. 62-1087, (1964).

9. Tanner, L. E., The Ordering of Ni_3V, Phys. Stat. Sol., 30, pp. 685-701, (1968).

10. Giessen, B. C. and Grant, N. J., The Crystal Structures of VNi_2, VPd_2, VPt_2 and Related AB_2 Phases, J. Less Common Metals, 8, pp. 114-119, (1965).

11. Valentich, J., Thermal Expansion, Measurement Instruments & Control Systems, 42 (Oct), pp. 91-94, (1969).

12. Steeple, H., The Crystal Structure of the Cadmium-Magnesium Alloy, CdMg, Acta Cryst., 5, pp. 247-249, (1952).

13. Ölander, A., The Crystal Structure of AuCd, Z. Krist., 83, pp. 145-148, (1932).

14. Waterstrat, R. M. and van Reuth, E. C., Effects of Compositional Variations on the Atomic Ordering in A15 Phases, Proc. Third Bolton Landing Conf. on Ordered Alloys, pp. 95-110, published by Claitor's Publishing Division, Baton Rouge, La., (1970).

15. Giessen, B. C., Dangel, P. N. and Grant, N. J., New Phases in the Vanadium-Iridium System and a Tentative Constitution Diagram, J. Less Common Metals, 13, pp. 62-70, (1967).

V. CHROMIUM-IRIDIUM CONSTITUTION DIAGRAM

A. Previous Studies

In 1955, Raub and Mahler [1] published the results of their investigation of ten different alloys spanning the entire composition range in the chromium-iridium alloy system. The existence of two intermediate phases was established. One of these phases was identified as having a close-packed hexagonal crystal structure and was stable over a wide composition range. The other intermediate phase was identified as possessing an A15 (β-W) type crystal structure and was stable over a more restricted range of composition. A subsequent study of five different chromium-iridium alloys by Knapton [2] essentially confirmed the findings of Raub and Mahler, but the observed lattice parameters were not in good agreement with those of the previous study. Knapton also reported the existence of an unidentified phase in an alloy containing 25 atomic percent iridium after it had been annealed at 1200°C.

The information obtained in these two investigations was very limited in nature, and was therefore insufficient to permit the establishment of a constitution diagram. No further work on the chromium-iridium system has since been reported.

B. Materials

The chromium metal used in this study had a nominal purity of 99.999% with respect to nongaseous impurities, but it contained approximately two atomic percent oxygen. The presence of oxygen in our experimental alloys was manifested by the appearance of oxide inclusions (presumably Cr_2O_3), and it seems probable that most of the oxygen in these alloys exists in this form. It would be possible to remove most of the oxygen from the alloys by heat-treating either the alloys or the chromium metal used to prepare the alloys in an atmosphere of dry hydrogen. However, no deoxidation treatment was employed in this study since it seemed unlikely that the presence of this amount of oxygen would shift the location of the

binary phase boundaries to any significant extent. This conclusion was supported by our previous experience in determining phase boundaries in the Cr-Pt system.

The iridium metal used was in the form of powder having a nominal purity of 99.95%. This powder was compressed into 1/2-inch diameter pellets before melting them together with the chromium metal droplets. Spectrographic and chemical analyses of both of our starting materials are listed in Table 12.

C. Alloy Preparation

All experimental alloys were prepared by arc-melting the appropriate quantities of each pure element under an inert atmosphere of 50% argon and 50% helium. Considerable weight losses occurred during melting, particularly for alloys having high iridium contents. This is presumably due to the high vapor pressure of chromium at the temperatures needed to melt these alloys. Losses were minimized to some extent by placing the iridium pellets on top of the chromium droplets so that the iridium would receive the initial impact of the electric arc. Nevertheless, metal losses during melting were usually about 2% and occasionally as high as 4%.

An alloy having a nominal starting composition of $Cr_{50}Ir_{50}$ was submitted to a chemical analysis after melting in order to determine whether the weight losses were caused by vaporization of both elements or primarily by the loss of only one component. This alloy had a weight loss of 2.6% during melting, and the chemical analysis revealed that this entire loss could be attributed to vaporization of Cr. All of our alloy compositions were therefore determined by measuring the total weight loss during melting and attributing the loss entirely to a depletion of the chromium content.

Each sample was melted at least four times and was inverted in the hearth after each melt. The melting chamber was

Table 12

Chemical and Spectrographic Analyses of the Material Used in Preparing the Experimental Alloys †

	Chromium	Iridium
Impurity	Leico Metals, Inc.	Engelhard Industries, Inc.
Ca	<10	<1
Fe	<10	<1
Mg	<10	<1
Ni	<10	ND
Pb	<10	ND
Pt	ND	<10
Rh	ND	<10
Si	<10	<10
C	16	
H*	295	
O*	6540	
N*	6	

† Values are given in ppm.

ND Not detected spectrographically

* Values obtained by vacuum fusion analysis

No other elements were detected spectrographically.

evacuated to a pressure of 10^{-3} mm or less between each melting, and was flushed several times with the high purity argon-helium gas mixture. Special precautions were taken with brittle alloys to insure that no fragments of the alloy were lost if the sample shattered under the arc.

D. Composition Determination of the Melts

Alloy compositions were determined by chemical analysis, electron probe microanalysis, or by monitoring weight losses during melting. The chemical analysis of our alloy $Cr_{50}Ir_{50}$ had established that weight losses during melting for this alloy could be attributed entirely to the vaporization of chromium. We have therefore calculated all of our alloy compositions by assuming that the observed weight losses were due entirely to a loss of chromium. This procedure yielded alloy compositions which were quite compatible with compositions determined by electron probe microanalyses. Calibration of the electron probe was accomplished by using samples of pure chromium and pure iridium together with a portion of our sample $Cr_{50}Ir_{50}$ which had been chemically analyzed. Compositions are therefore considered to be reliable within an experimental uncertainty of ± 1 atomic percent.

E. Temperature Measurement

A platinum versus platinum-10% rhodium thermocouple was used to measure temperatures up to 1500°C. Temperatures above 1500°C were measured with a tungsten versus tungsten-26% rhenium thermocouple. These thermocouples were periodically calibrated against a standard platinum-6% rhodium versus platinum-30% rhodium thermocouple at temperatures up to 1600°C. The standard thermocouple had been calibrated at the National Bureau of Standards. In addition, calibration against secondary standards was accomplished using the melting points of pure nickel, platinum, rhodium, and iridium as described in Section III-G. A calibration of temperature versus furnace current was also helpful in establishing temperatures within the hot zone of the furnace during the various annealing treatments.

F. Thermal Treatments

1. Homogenization

All samples used in this study were initially homogenized by heating to within 300°C of their solidus temperatures for several hours. The homogenization treatment was conducted with all the precautions normally used in the equilibration treatments so that the samples could be considered as being equilibrated at the homogenization temperature. Equilibrations at lower temperatures were conducted consecutively in order of decreasing temperature.

The samples were contained in tantalum buckets suspended by tantalum wire within the tantalum-strip resistance furnace during the annealing treatments. For annealing treatments above 1500°C, the tantalum buckets were lined with tungsten strips to prevent any reaction between the samples and their containers. This was necessary since Ir and Ta form a low melting eutectic. The furnace operated at pressures between 5×10^{-6} and 5×10^{-7} mm Hg. There was no significant visible contamination of the samples by tantalum and this was later verified by electron-probe microanalysis.

All samples appeared to be well homogenized. This was checked by electron probe and metallographic examinations together with observations of the sharpness of x-ray powder patterns obtained from filings which had received brief "strain-anneal" heat-treatments.

It was at first anticipated that alloy samples containing high contents of iridium might undergo serious depletion of their chromium contents when annealed in a high vacuum at temperatures as high as 2000°C. These temperatures were necessary both from the standpoint of adequate homogenization, and also to establish the phase relationships at these high temperatures.

Chromium losses at these temperatures, however, were not excessive during the relatively brief periods of time needed

for equilibration and, in addition, it was found that such losses were confined mainly to a thin layer at the surfaces of the samples. This layer was either removed or avoided during subsequent studies.

2. Equilibration

Samples to be equilibrated at temperatures up to 1100°C were sealed in quartz tubes (previously baked out and evacuated) under a partial pressure of pure argon. These tubes were placed in a platinum-wound furnace capable of being controlled within a temperature range of ± 1°C. Alloys to be annealed at 1350°C were wrapped in tantalum foil and placed in platinum tubes. The platinum tubes were then evacuated and filled with a partial pressure of argon sufficient to keep the tubes from collapsing at the annealing temperature. The platinum tubes were then sealed by crimping the end of each tube in a special device capable of exerting sufficient pressure to cold weld the end of the tube. This method permitted annealing the samples for prolonged periods of time at 1350°C in a platinum-wound furnace in air. Equilibration at temperatures above 1350°C was accomplished using a tantalum-strip resistance furnace operating at a pressure of 5×10^{-6} to 5×10^{-7} mm Hg. The samples were suspended in tantalum buckets but electron probe analysis indicated no contamination of the samples by tantalum. Temperatures in this furnace were controlled usually to within ± 10°C, but more accurate control is possible over shorter periods of time.

Samples annealed in the tantalum-strip furnace were cooled rapidly from the annealing temperature by turning off the power to the heating elements. Samples annealed in quartz tubes were quenched in cold water. The cooling rates in all cases were apparently sufficient to permit retention of the phases existing at the annealing temperature. However, atomic ordering in the Ir solid solution could not be suppressed by rapid cooling and it was not possible to retain the disordered face-centered cubic structure for alloys containing between 23 and 32 atomic percent Cr.

A summary of the equilibration treatments used for all alloy samples is given in Table 13.

G. Methods for Determination of Phase Boundaries

1. Solidus Temperatures

The experimental difficulties associated with solidus determinations in the chromium-iridium alloy system were formidable. The alloys melt at temperatures up to about 2400°C and at such high temperatures the chromium vaporizes readily. Chromium losses during a solidus determination may therefore be quite large and would introduce serious errors in composition determination, particularly when conventional techniques such as thermal analysis are employed. Furthermore, the alloys and their vapors will react with many refractory materials. Thermocouples are rapidly contaminated by chromium vapor even when they are enclosed in protective refractory tubes.

In order to prevent excessive losses of chromium, it is essential that the method used for solidus determination should minimize the length of time during which the alloys are exposed to high temperatures, particularly when they are partially or completely molten. Conventional thermal analysis techniques are therefore ruled out since such techniques require that alloys in the molten condition be heated or cooled slowly in order to obtain reliable thermal arrest data. The use of microscopic methods to detect incipient melting, however, are attractive since it is required only that the sample be heated long enough to obtain a uniform temperature, and this temperature need not produce complete melting. The amount of molten material present in the sample can be only a few percent and will still be detectable by this method.

We have, therefore, adopted a relatively crude but effective method for solidus determination which involves heating the sample to temperatures in the vicinity of the anticipated solidus temperature until evidence of partial melting is seen in the alloy microstructure after rapid cooling. The sample is exposed to the

Table 13

Summary of Equilibration Treatments
for Chromium - Iridium Alloys

Temperatures (°C)	Time	Alloys (atomic % Cr)
2160°	1/2 hr.	16
2120°	1/2 hr.	23
2020°	1/2 hr.	36
2000°	24 hrs.	4, 16, 23, 28
2000°	2 hrs.	29, 31, 33.5
1800°	10 hrs.	16, 23, 28, 29, 31, 33.5
1800°	2 hrs.	36, 48.5, 58
1700°	1 hr.	70
1600°	24 hrs.	4, 16, 23, 28, 29, 31, 33.5, 36, 48.4, 58, 63
1550°	2 hrs.	70, 78, 85, 90, 95
1400°	24 hrs	70, 72, 74, 76, 78, 83, 85
1400°	13 hrs.	90, 95
1350°	2 weeks	4, 16, 23, 28, 29, 31, 33.5, 36, 48.4, 58, 63
1100°	1 month	4, 16, 23, 28, 29, 31, 33.5, 36, 48.4, 58, 63, 70, 78, 85, 90, 95

desired temperature for only about one minute and usually only a small fraction of the sample is ultimately melted. The method has been described in detail in Section III, G-1.

The refractory crucibles used to support the sample during a solidus determination were made of pure thoria. This material is stable at the high temperatures employed but there was some evidence that a slight reaction had occurred between the sample and the thoria crucibles. A violet color was noted at the surface of the thoria where it had been in contact with the alloy sample, but very little erosion of the crucible had occurred, and it is felt that contamination of the sample was insignificant. Metallographic studies showed no difference in structure between the surface and the interior of the alloy samples. The nature of the reaction was not identified.

Contamination of the tungsten versus tungsten-26% rhenium thermocouple was apparently not very significant since only a slight change in emf was noted after the sample had been exposed at a given temperature during the solidus determinations. This is noteworthy since chromium vapor readily penetrates most refractory tubes used in protecting the thermocouple. Our thermocouples, however, were protected not only by a refractory tube of BeO, but also by an outer sheath of pure tantalum. This outer sheath is apparently less permeable by chromium vapor than the ceramic refractories. Although the tantalum may react to some extent with chromium vapor (no visible reaction was detected), it appears to be an effective barrier which acts to prevent contamination of the thermocouple. The tip of the thermocouple is not exposed to the direct impingement of chromium vapor since it is inserted in a small hole drilled into the tantalum holder. (See Fig. 2, Section III.) The use of this sheathed thermocouple for temperature measurement was apparently rather successful and suggests further application of such methods in cases where metallic vapors are present at high temperatures. Our temperature measurements were also checked by simultaneous monitoring of furnace current. The furnace current

had previously been calibrated against temperature using a standard thermocouple up to 1500°C and secondary melting point standards from 1500°C to 2447°C (melting point of pure Ir). The temperature indicated by the tungsten versus tungsten-26% rhenium thermocouples was usually in good agreement with temperatures deduced by reference to a plot of furnace current versus temperature provided that care was taken to insure that furnace operating conditions remained constant. In this connection, it is important to maintain a uniform temperature and flow of water coolant to the furnace. It is also important to reproduce the geometrical arrangement of the holder and thermocouple for each run as well as their exact location within the hot zone of the furnace so that the experimental conditions correspond closely to those which existed during the calibration.

2. Liquidus Temperatures

We were unable to devise a suitable method for determining the liquidus temperatures of the Cr-Ir alloys and consequently the locations of the liquidus lines are simply estimated from the general form of the solidus and the location of the invariant reactions. The results of our metallographic examination of the solidus samples was also taken into consideration in estimating the location of the liquidus through application of the lever rule.

3. Other Phase Boundaries

The boundaries of intermediate phases were determined by metallographic studies and by electron probe micro-analyses whenever it was possible to use this method. The boundaries of the two-phase region $\gamma + \epsilon$ could not be determined by either of these two methods, however, and it was therefore necessary to rely on x-ray diffraction techniques for such alloys. Alloy powders were obtained from the bulk samples by grinding them with a dental diamond wheel and sieving out the course diamond particles from the residue. The alloy powders so obtained were given

a strain-relief anneal for a few minutes in a high vacuum at the same temperature used for annealing the original bulk sample. Such procedures were apparently quite satisfactory since the x-ray patterns so obtained contained sharp lines with well resolved K_α doublets. Variations of the lattice parameters as a function of alloy composition were relatively small and it was therefore not possible to determine phase boundaries by this method.

A sufficient number of alloys were prepared in or near the two-phase $\gamma + \epsilon$ region to insure that the phase boundaries were reliably established. The compositions of the alloys were determined mainly by attributing the weight losses during melting entirely to depletion of the Cr contents of the alloys. This method appeared to be quite reliable. In some cases, the alloy compositions determined by this method were verified by electron probe microanalysis of certain single phase alloys. (See Table 14.)

Table 14

Comparison of Alloy Compositions Determined by Weight Loss and by Electron Probe Microanalysis

Nominal Starting Composition	Atomic % Cr by Weight Loss	Atomic % Cr by Microprobe Analysis
$Cr_{30}Ir_{70}$	28.0 At. % Cr	28.3 At. % Cr
$Cr_{50}Ir_{50}$	48.0 At. % Cr	48.4 At. % Cr
$Cr_{60}Ir_{40}$	57.7 At. % Cr	58.1 At. % Cr

H. Experimental Results

1. General

The proposed constitution diagram for the chromium-iridium system is shown in Fig. 29. All alloys were examined either metallographically or by x-ray diffraction methods or both. The data obtained by these methods was in good agreement with the results of the electron microprobe analyses.

2. Solidus and Liquidus

For both chromium-rich and iridium-rich alloys, it was usually possible to detect the first signs of melting by direct visual observations particularly on sharp edges or corners of the sample. In some cases, melting was indicated by the appearance of small molten beads which formed on the surface of the sample. Whenever the first signs of melting were detected the furnace power was immediately turned off. This permitted the sample to cool rapidly. The sample was then removed from the furnace and subjected to metallographic examination. By observing the relative amounts of unmelted solid and chilled liquid it was possible to estimate the approximate location of solidus and liquidus boundaries.

In the case of the iridium-rich alloys, there were visible signs of melting when only about 5% of the sample was liquid as established by subsequent metallographic examination. The chilled liquid was usually observed at prior grain boundaries and produced a rounded appearance in each grain as shown in Fig. 30a. Losses of chromium during a solidus determination were minimized by an initial rapid heating of the sample to within about 100°C of the expected solidus temperature and then raising the temperature in 10° increments allowing about one minute for thermal equilibration following each increment. Thermocouple readings established whether the temperature had in fact reached a nearly stable level. In most cases the entire run did not last more than 15 minutes and it appears that this may explain why the chromium losses were not very great.

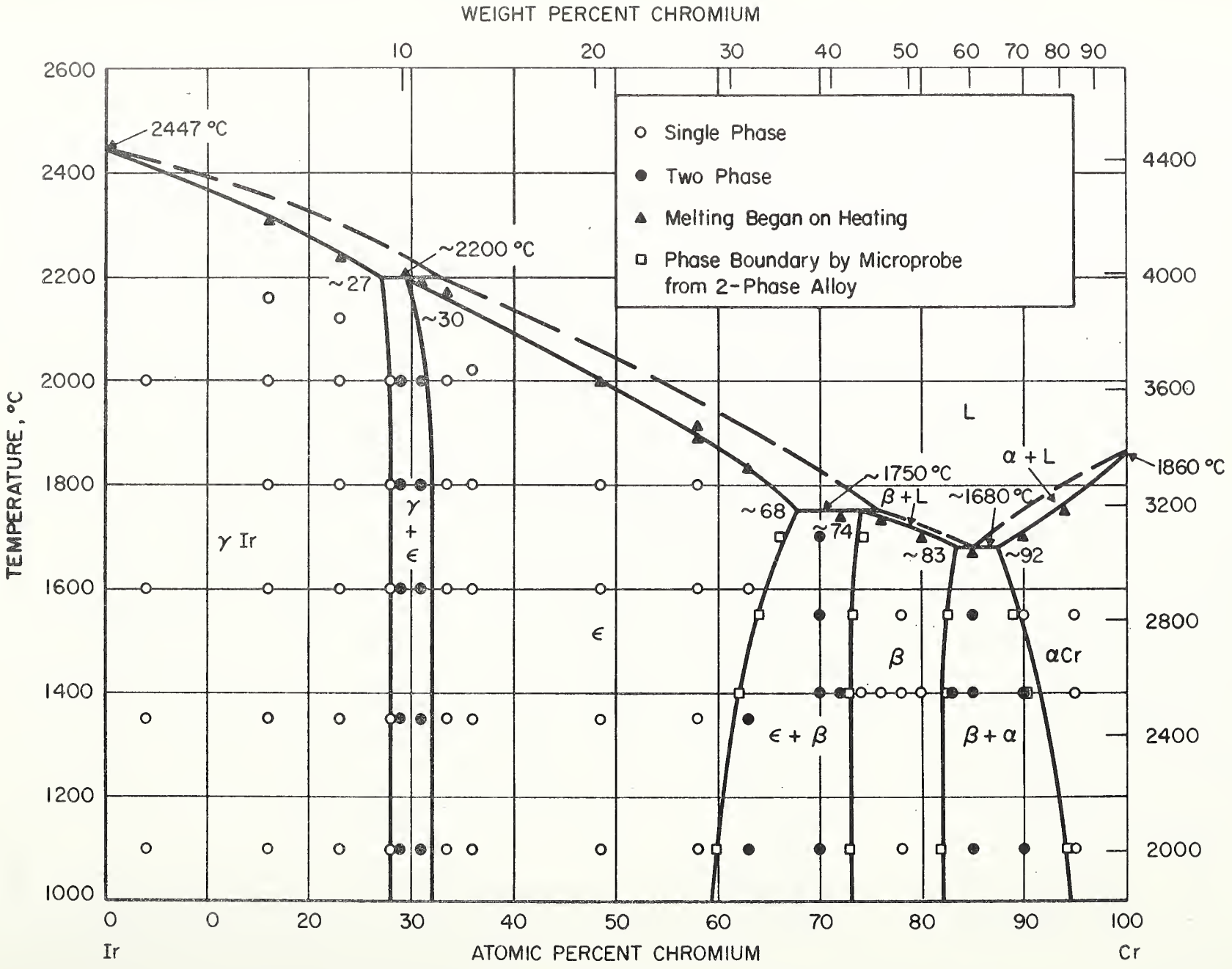

Fig. 29 - The chromium-iridium constitution diagram.

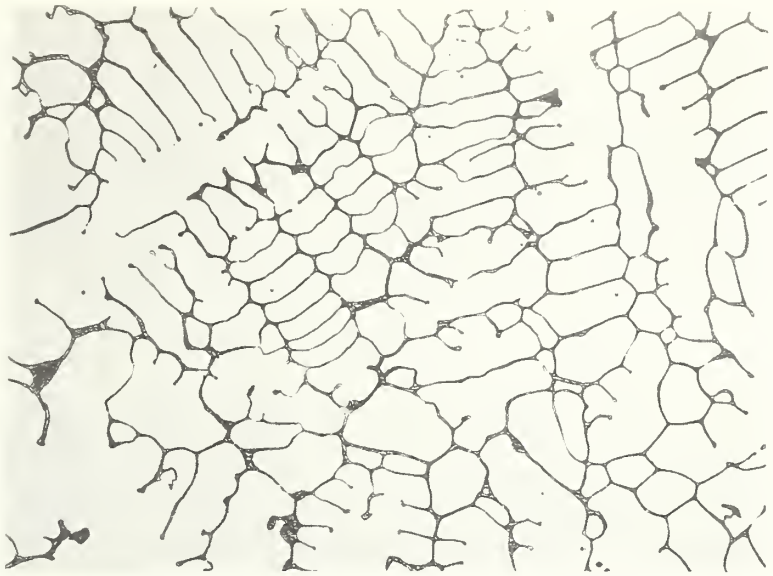

160X (a)

16 at. % Cr, 84 at. % Ir heated to 2250°. Melting has occurred at the grain boundaries.

80X (b)

28 at. % Cr, 72 at. % Ir equilibrated at 2000°C. Large grains of γ Ir showing twinning. Small dark pits are believed to be artifacts produced by polishing and etching.

Fig. 30 - Microstructures of chromium-iridium alloys.

In view of the considerable experimental problems in conducting these studies it is felt that the solidus determinations were reasonably accurate but it is difficult to estimate the probable error. At best the error would be ± 10°C and it seems likely that the maximum error would be no more than ± 50°C.

3. Iridium Terminal Solid Solution - γ and γ'

The solubility of chromium in face-centered cubic iridium extends to 28 atomic percent chromium and is essentially temperature-independent. It has been previously established that atomic ordering occurs in the vicinity of 25 atomic percent Cr[1] and that the ordered alloys are ferromagnetic.[1, 3] The critical temperatures of the order-disorder transformation have not yet been established but they appear to be strongly composition-dependent. It was found that rapid cooling after arc-melting did not suppress the ordering reaction in alloys containing 23 to 28 atomic percent Cr but that in the alloy containing 16 atomic percent Cr atomic ordering could be produced only by annealing the alloy powder for several days at temperatures between 600° and 700°C.

The ordered phase (γ') possesses a $Cu_3Au(L1_2)$ type structure and it appears that the order-disorder transition temperatures could perhaps be obtained by high-temperature x-ray diffraction studies.

4. Chromium Terminal Solid Solution - α

The maximum solubility of iridium in body-centered cubic chromium is about 13 atomic percent Ir at the eutectic temperature (1670°C). The solvus line shows a pronounced temperature-dependence and there is evidence of precipitation of a second phase in alloys containing more than 5% Ir even after rapid cooling. X-ray diffraction patterns obtained from powders of these alloys show diffuse or broadened lines of the disordered

body-centered cubic α solid solution. The line broadening was not eliminated by a "strain-anneal" type heat treatment.

The presence of the precipitate in our alloys accounts for a slight discrepancy between the location of the solvus boundary as determined by metallographic studies and the boundary determined by electron microprobe analysis. In this case, the metallographic data is more reliable since the electron beam measures a small percentage of the precipitated phase and thus yields composition values for the α solid solution which are slightly too high in Ir content. In alloys annealed at 1100°C, however, both the metallographic and electron probe data indicate a solubility of about 6% Ir in the chromium terminal solid solution.

5. Intermediate Phase ϵ

Raub and Mahler [1] were the first investigators to report the existence of an intermediate phase having a disordered hexagonal close-packed structure in the Cr-Ir system. They reported that this phase was stable over a broad composition range and the present study essentially confirms these findings.

The iridium-rich boundary of this phase lies at about 32 atomic percent Cr and is nearly temperature-independent. It is perhaps noteworthy that alloys in this region are neither ordered nor ferromagnetic whereas the face-centered cubic γ phase alloys at 28 atomic percent Cr are strongly ordered and also ferromagnetic. Crystal structure therefore seems to play an important role in permitting the occurrence of ordering and ferromagnetism in the Cr-Ir alloy system.

The chromium-rich boundary of the ϵ phase extends to a maximum chromium content of about 68 atomic percent Cr at 1750°C but the solubility is temperature-dependent and decreases to 60 atomic percent Cr at 1100°C. Variations in the lattice parameters of the ϵ phase as a function of composition are illustrated in Fig. 31.

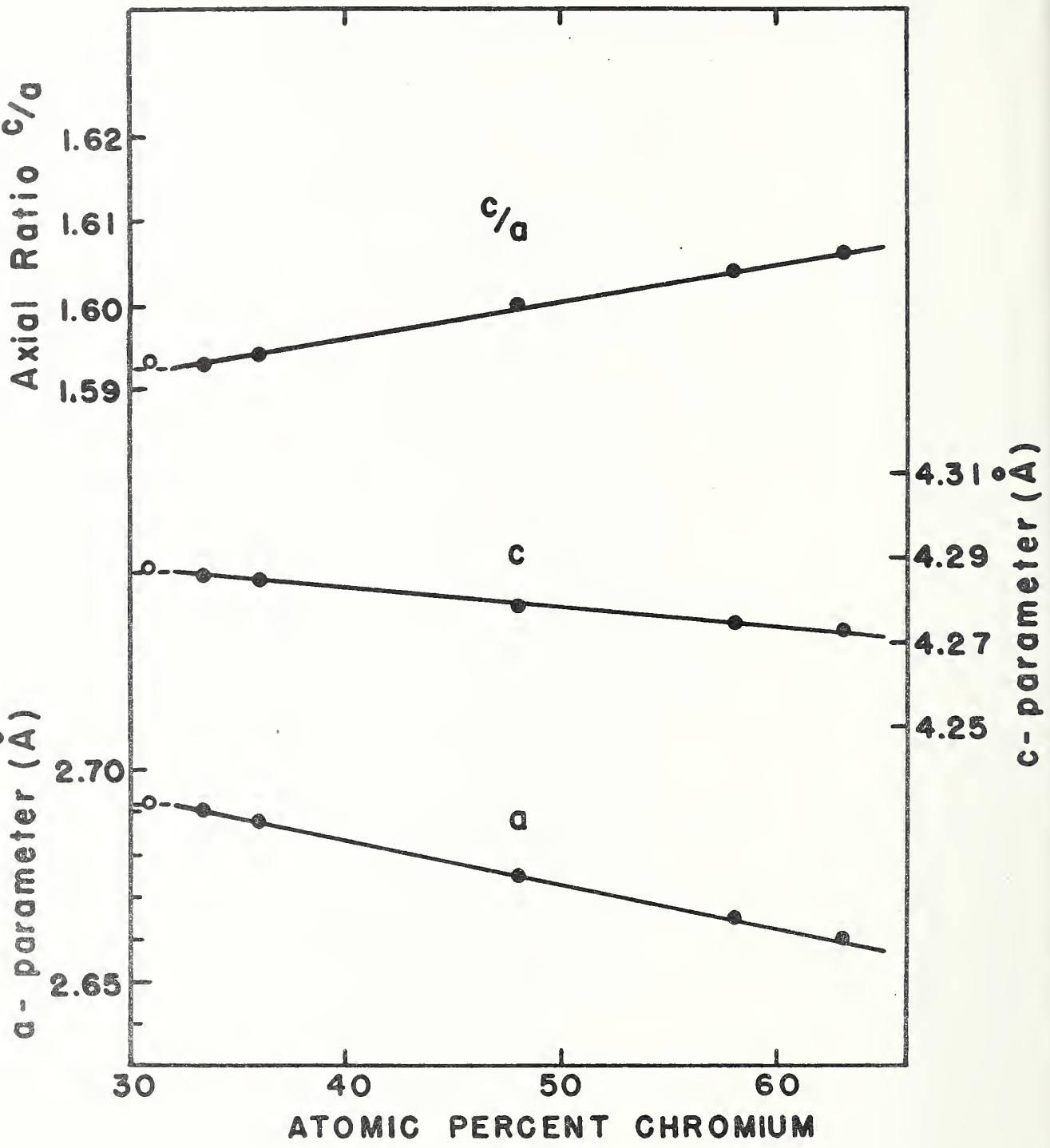

Fig. 31 - Lattice parameters of ∈ phase Cr-Ir alloys.

6. Intermediate Phase β

Raub and Mahler[1] first reported the existence of a phase having the A15 (β-W) crystal structure in the chromium-iridium alloy system and they reported that it exists under a melting point maximum. We did not observe a melting point maximum. On the ∈-phase side we observed a peritectic reaction. A eutectic reaction was observed only on the ∝-phase side rather than on both sides as reported by Raub and Mahler.[1] It is perhaps noteworthy that Raub and Mahler stated that the eutectic structure which they observed on the ∈-phase side was "less distinct" than the eutectic structure which they observed on the ∝-chromium side. Since they presented no photomicrographs for their Cr-Ir alloys one might therefore question whether the structure which they had reported was indeed a eutectic structure.

The composition range of the β phase was determined by electron probe microanalyses of two-phase alloys quenched from 1550°, 1400° and 1100°C. At 1400°C the composition range of the β phase extends from 73 atomic percent Cr to 82 atomic percent Cr and the lattice parameters vary from $a_o = 4.689$ to $a_o = 4.659$ with increasing chromium content.[4] For alloys annealed at lower temperatures Raub and Mahler[1] report a composition range for this phase extending from 72.5 to 78.5 atomic percent Cr with a similar variation in lattice parameters. The two investigations are therefore essentially in agreement except for the location of the Cr-rich boundary of the β phase and the questionable melting point maximum for this phase.

We found no evidence of the unidentified phase observed by Knapton[2] in his alloy containing 25 atomic percent Ir which had been annealed at 1200°C. Our alloy $Cr_{78}Ir_{22}$ yielded an x-ray diffraction pattern containing only the lines of the β phase after annealing at 1100°C for one month. Our alloy $Cr_{70}Ir_{30}$ yielded a pattern showing that the major constituent phase is the β phase with a relatively minor amount of the ∈ phase. No other lines were observed for this alloy annealed at 1100°C for one month.

80X (a)

29 at. % Cr, 71 at. % Ir equilibrated at 1800°C. Alloy contains γ Ir (twinned) plus a small amount of ϵ phase.

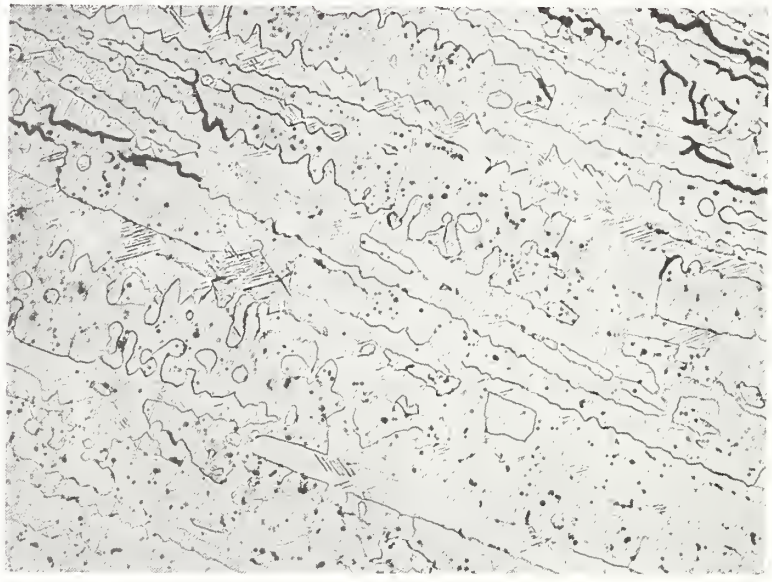

160X (b)

31 at. % Cr, 69 at. % Ir equilibrated at 1800°C. The columnar grains showing twinning are presumably γ Ir. Untwinned grains are ϵ phase.

Fig. 32 - Microstructures of chromium-iridium alloys.

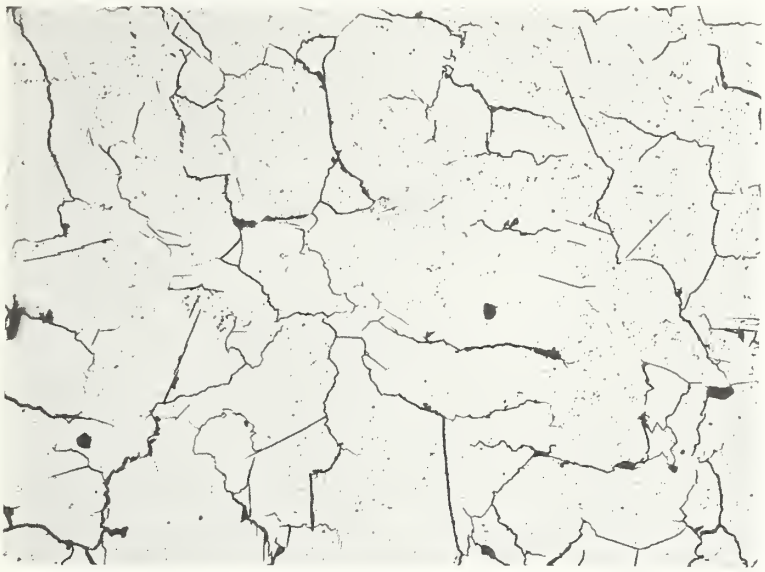

50X (a)

36 at. % Cr, 64 at. % Ir equilibrated at 2000°C. Large grains of ϵ phase.

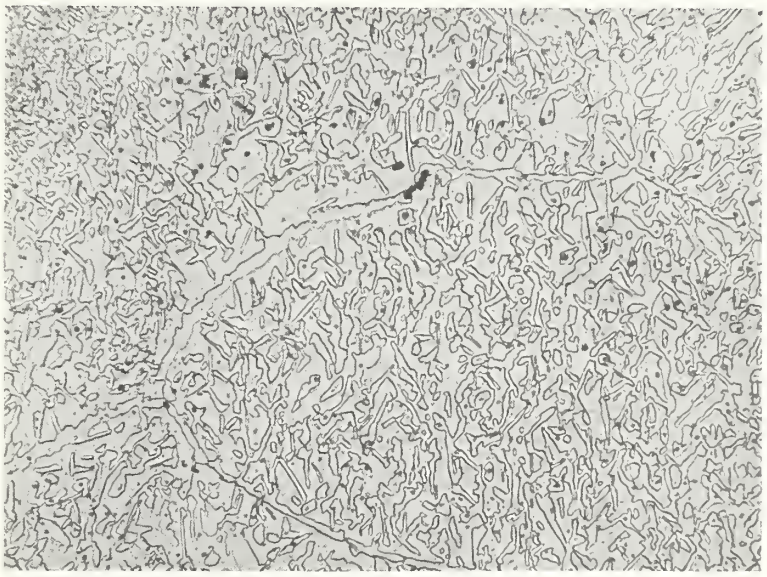

130X (b)

63 at. % Cr, 37 at. % Ir equilibrated at 1100°C. The matrix is ϵ phase. Particles of β phase have precipitated at prior grain boundaries and within the grains.

Fig. 33 - Microstructures of chromium-iridium alloys.

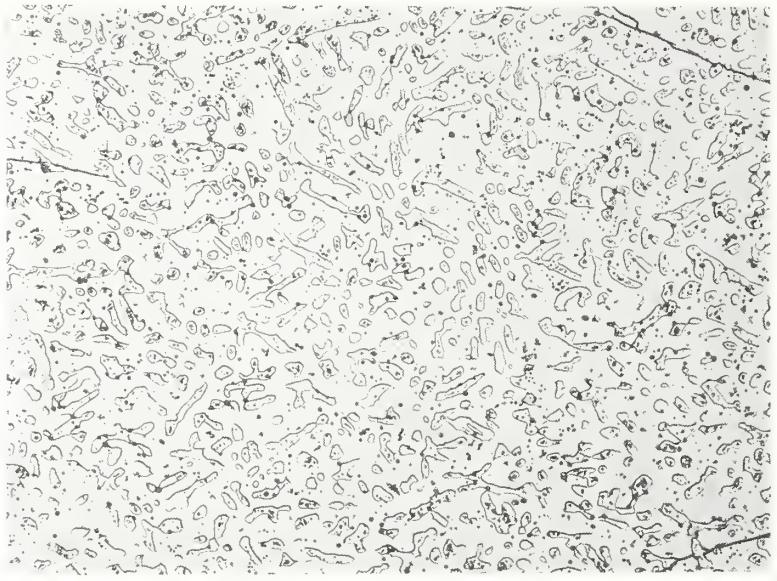

160X (a)

70 at. % Cr, 30 at. % Ir equilibrated at 1100°C. The matrix is β phase containing large grains of ∈ phase. Small dark spots are etch pits and oxide inclusions.

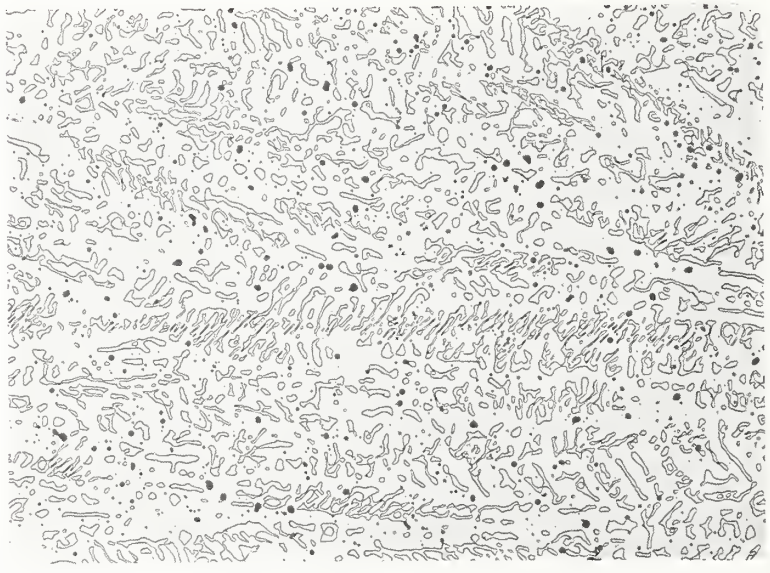

100X (b)

85 at. % Cr, 15 at. % Ir equilibrated at 1100°C. Matrix is β phase containing second phase particles of αCr. The distribution of αCr suggests that a prior eutectic structure may have existed.

Dark spots are oxide inclusions.

Fig. 34 - Microstructures of chromium-iridium alloys.

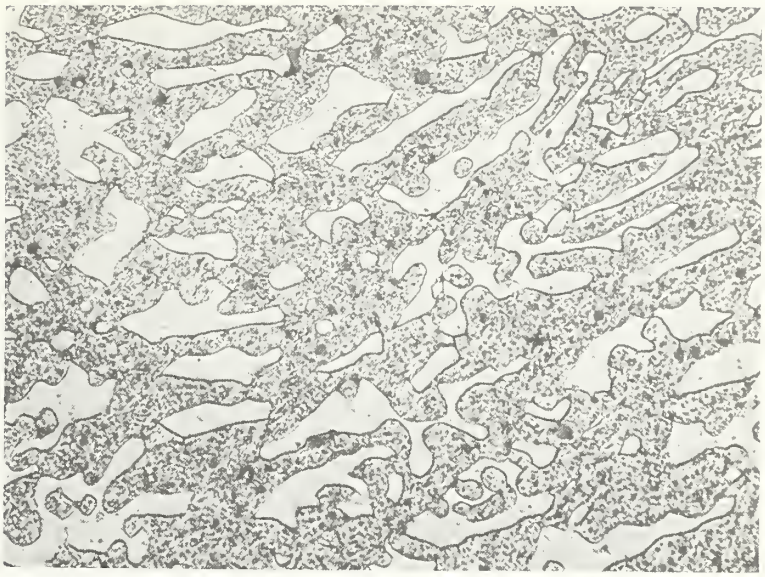

200X (a)

85 at. % Cr, 15 at. % Ir equilibrated at 1550°C. Matrix is αCr in which precipitation of β phase has occurred during rapid cooling. Large white areas are β phase.

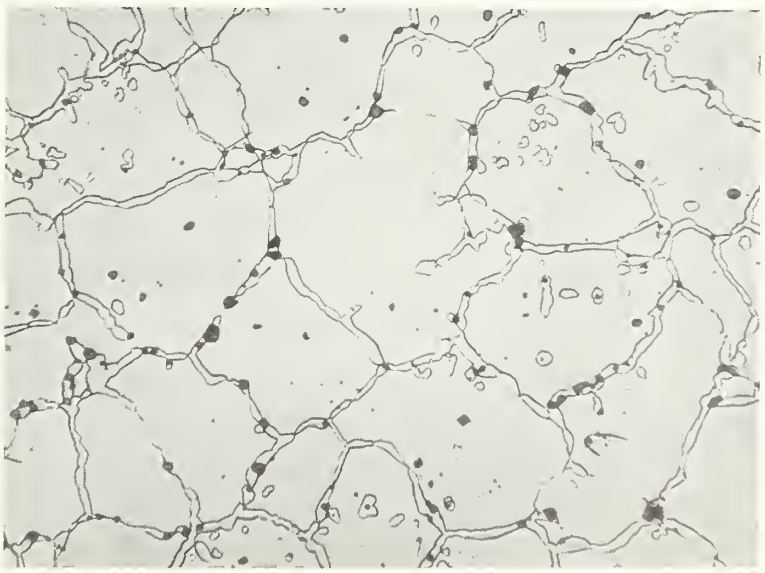

130X (b)

90 at. % Cr, 10 at. % Ir equilibrated at 1400°C. Large grains of αCr with a grain boundary network of β phase. Dark particles are oxide inclusions.

Fig. 35 - Microstructures of chromium-iridium alloys.

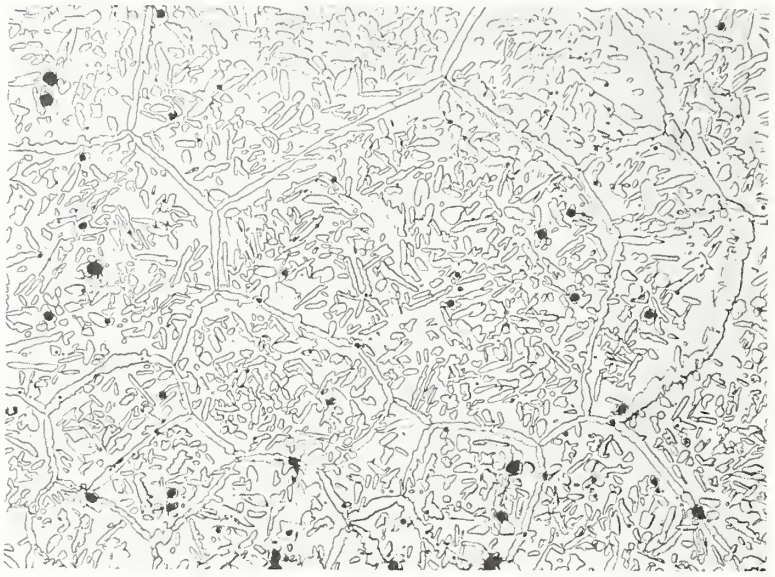

160X (a)

90 at % Cr, 10 at. % Ir equilibrated at 1100°C. β phase formed within grains of αCr and as a network at prior grain boundaries. Dark particles are oxide inclusions.

Fig. 36 - Microstructures of chromium-iridium alloys.

7. Peritectic: $\gamma + L \rightleftharpoons \epsilon$

The existence of this peritectic reaction was established mainly through measurements of solidus temperatures particularly for the alloy $Cr_{31}Ir_{69}$ which lies close to the peritectic horizontal at 2200° ± 20°C. Alloys annealed within the two-phase ($\gamma + \epsilon$) region below the peritectic horizontal had a twinned appearance (Fig. 32) but there was no clear distinction between γ and ϵ phase regions. X-ray diffraction patterns were obtained from powders of these alloys and were given a "strain-anneal" treatment at the temperature of the original equilibration. The patterns clearly revealed sharp, well-resolved lines of both a face-centered cubic phase and a hexagonal close-packed phase coexisting.

8. Peritectic: $\epsilon + L \rightleftharpoons \beta$

This peritectic reaction was also established mainly by solidus measurements. The results from the alloy $Cr_{70}Ir_{30}$ were most helpful in establishing the location of the peritectic horizontal at 1750° ± 10°C.

9. Eutectic: $L \rightleftharpoons \alpha + \beta$

The location of this eutectic reaction was established by extrapolation of both solidus and solvus lines in this composition region. Metallographic examination of the alloy $Cr_{85}Ir_{15}$ in the "as-cast" condition failed to reveal a typical lammelar eutectic structure but this may be due to decomposition of the eutectic structure during cooling. The direction of adjacent solidus boundaries definitely suggests the existence of a eutectic reaction.

REFERENCES

1. Raub, E. and Mahler, W., The Alloys of Chromium with Platinum, Iridium, Rhodium and Ruthenium, Z. Met., 46, 210-215 (1955).

2. Knapton, A. G., An X-ray Survey of Transition-Metal Systems for Sigma Phases, J. Inst. Metals, 87, 28-32, (1958-1959).

3. Friederich, E., About Ferromagnetic Platinum-Chromium and Platinum-Iridium Alloys, Z. Tech. Physik, 13, 59, (1932).

4. Waterstrat, R. M. and van Reuth, E. C., Effects of Compositional Variations on the Atomic Ordering in A15 Phases, Proc. Third Bolton Lauding Conf. on Ordered Alloys, Claitor's Publishing Division, Baton Rouge, La., (1970).

VI. CHROMIUM-RHODIUM CONSTITUTION DIAGRAM

A. Previous Studies

There have been only two previous studies devoted to the constitution of chromium-rhodium alloys. Both of these studies were very limited. Raub and Mahler[1] studied ten alloys spanning the entire composition range in increments of approximately 10 atomic percent. They mentioned the existence of only one intermediate phase having a hexagonal close-packed crystal structure. Greenfield and Beck[2] studied six Cr-Rh alloys and reported the existence of two intermediate phases; one having a hexagonal close-packed structure and the other having a β-W type structure. These two investigations were not in complete agreement in regard to the location of certain phase boundaries. The amount of information available from both investigations, however, was quite insufficient to establish a constitution diagram.

B. Materials

Both the chromium metal and the rhodium metal used in this study had nominal purities of 99.999% with respect to non-gaseous impurities. However, the chromium metal was found to contain about two atomic percent oxygen. Metallographic examination of an arc-melted sample of this "pure" chromium revealed the presence of a small amount of oxide inclusions (presumably Cr_2O_3) but the surface of the sample was remarkably bright and clean with no visible external evidence of the oxygen contamination. Nevertheless, when chromium-rhodium alloys were prepared using this chromium there was a visible green surface film on the top of each alloy sample. The presence of this green film on the top of the alloy ingots was initially attributed to the presence of additional oxygen which had been dissolved in the rhodium. Accordingly, we attempted to deoxidize the rhodium by annealing the compressed powder pellets at a high temperature in

dry hydrogen and then in a high vacuum. Surprisingly, the green film persisted. It was finally discovered that the formation of these visible green films on our Cr-Rh alloys could be prevented by annealing the chromium in dry hydrogen for four hours at 1700°C prior to melting the alloys. Thus, it appears that the green film was due to oxygen dissolved in the chromium rather than in the rhodium. We are unable to explain why the film did not appear on arc-melted samples of the untreated "pure" chromium which had not been deoxidized. The arc-melting was done under identical conditions in both cases using the same high purity inert gas atmosphere.

As a consequence of the above findings it was decided to deoxidize all of the alloys which we had already prepared and to prepare all future alloys using chromium which had been deoxidized by annealing in dry hydrogen. Several of our alloys were therefore deoxidized by heating them to 1400°C for three days in an atmosphere of dry hydrogen (see Table 15). All subsequent heat-treatments were then carried out in a high vacuum.

The nominal purities of our starting materials are given in Table 15.

C. Alloy Preparation

All alloys were prepared by arc-melting the appropriate amounts of each pure metal under an inert atmosphere of high purity containing 50% argon and 50% helium. The weight losses during melting were always less than one percent and were usually about 0.5%. We have therefore assumed that all of our alloys have compositions which correspond to their nominal starting compositions within the experimental error of our measurements (± one atomic percent). This assumption was supported by quantitative data obtained by electron microprobe analyses.

Each sample was melted at least four times and was inverted in the hearth after each melt. The melting chamber was

Table 15

Chemical and Spectrographic Analyses of the Materials Used in Preparing the Experimental Alloys †

	Chromium	Rhodium
Impurity	Leico Metals, Inc.	United Mineral and Chemical Corp.
Ag	ND	<1
Al	ND	1
Ca	<10	<1
Cu	ND	1
Fe	<10	4
Mg	<10	<1
Ni	<10	ND
Pb	<10	ND
Si	<10	2
C	16	-
H*	295	-
O*	6540	-
N*	6	-

† Values are given in ppm.

ND Not detected spectrographically.

* Values obtained by vacuum fusion analysis.

No other elements were detected spectrographically.

evacuated to a pressure of 10^{-3} mm or less between each melting and was flushed several times with the high purity argon-helium gas mixture.

D. Composition Determination of the Melts

Alloy compositions were determined mainly by electron probe microanalyses and this method was also used to establish

that our alloy compositions were substantially the same as their respective nominal starting compositions. For example, our alloy which was nominally $Cr_{50}Rh_{50}$ was found to contain 52.1 atomic percent Cr and 47.1 atomic percent Rh according to electron probe analyses. In this case pure Cr and pure Rh were used as standard reference materials for calibration of the microprobe. In all subsequent calibrations of the electron probe we used the samples of pure chromium, $Cr_{50}Rh_{50}$, and pure rhodium as standard reference materials and interpolated the data so obtained in order to establish the compositions of our other chromium-rhodium alloys. The alloys were also checked for the presence of impurities which might have been picked up during arc-melting or annealing, particularly such elements as copper, tungsten, and tantalum. No contaminants were detected. Compositions are therefore considered to be reliable within an experimental uncertainty of ± one atomic percent.

E. Temperature Measurement

A platinum versus platinum-10% rhodium thermocouple was used to measure temperatures up to 1500°C. Temperatures above 1500°C were measured with a tungsten versus tungsten-26% rhenium thermocouple. These thermocouples were periodically calibrated against a standard platinum-6% rhodium versus platinum-30% rhodium thermocouple at temperatures up to 1600°C. The standard thermocouple had been calibrated at the National Bureau of Standards. In addition, calibration against secondary standards was accomplished using the melting points of pure nickel, platinum, rhodium, and iridium as described in Section III-G. A calibration of temperature versus furnace current was also helpful in establishing temperatures within the hot zone of the furnace during the various thermal treatments.

F. Thermal Treatments

1. Homogenization

Alloys containing up to 35 atomic percent Cr were homogenized by annealing them at 1600°C for one hour in a high vacuum. Alloys containing more than 35 atomic percent Cr were homogenized at 1400°C for three days in an atmosphere of pure dry hydrogen which had been passed through a palladium alloy purifier before being introduced into the furnace.

The homogenization treatments were carried out using all the precautions normally taken during an equilibration treatment and the samples were therefore considered as being equilibrated at the homogenization temperature. Equilibration annealing treatments subsequent to the initial homogenization were carried out consecutively at progressively decreasing temperatures.

The annealing treatments were performed in our tantalum-strip resistance furnace operating at pressures of between 5×10^{-6} and 5×10^{-7} mm Hg. The samples were suspended in tantalum buckets suspended by tantalum wire in the hot zone of the furnace. However, for annealing treatments above 1500°C the tantalum buckets were lined with tungsten strips in order to prevent any reaction between the sample and its container. This was necessary since Rh and Ta react to form a low-melting eutectic. Electron probe studies showed that the samples were adequately homogenized and essentially uncontaminated. This was also verified by metallographic examination of the alloy samples and by the sharpness of x-ray powder patterns obtained from alloy filings which had been given a brief "strain-anneal" heat treatment.

Loss of Cr by evaporation from the alloy samples was not a serious problem. Losses of weight during annealing were quite small (less than 0.5% in most cases) and it appears that such losses were confined mainly to a thin layer at the surfaces of the samples. This layer was either removed or avoided in all subsequent studies.

2. Equilibration

Samples to be equilibrated at temperatures up to 1200°C were sealed in quartz tubes (previously baked out and evacuated) under a partial pressure of pure argon. These tubes were suspended with nichrome wire in a vertical platinum wound furnace capable of being controlled within a temperature range of ± 1°C. Equilibration at temperatures above 1200°C was done in a tantalum strip furnace operating at pressures between 5×10^{-6} and 5×10^{-7} mm Hg. Temperatures in this furnace were normally controlled to within ± 10°C but in some cases it appears that temperature fluctuations were within ± 5°C especially for those treatments involving relatively short periods of time.

Samples annealed in the tantalum-strip vacuum furnace were rapidly cooled from the annealing temperature by turning off the power to the heating elements. Samples annealed in quartz tubes were quenched in cold water. The cooling rates were usually sufficient to permit retention of the phases existing at the annealing temperature. However, alloys containing the α-chromium solid solution did show evidence of a decomposition during cooling. These alloys showed metallographic evidence of a Widmanstatten-type precipitate within the α-chromium phase regions but prior structures existing at the equilibration temperature appeared to be readily identifiable. A more detailed description of this behavior is given in our discussion of the experimental results.

A summary of the equilibration treatments used for all of the alloy samples is given in Table 16.

G. Methods for Determination of Phase Boundaries

1. Solidus Temperatures

The solidus temperatures of our alloys were determined by observations of incipient melting in alloys annealed at various temperatures above and below the solidus temperature.

Table 16

Summary of Equilibration Treatments
for Chromium-Rhodium Alloys

Temperature (°C)	Time	Alloys (atomic % Cr)
1600°	1 hr.	5, 10, 15, 20, 25, 30, 35
1550°	1/2 hr.	90, 95
1400°	24 hrs.	5, 10, 15, 20
1400° *	3 days	15, 30, 60, 70, 82.5, 85
1400°	6 hrs.	40, 50, 78, 90, 95
1300°	4 hrs.	70, 78, 82.5
1275°	6 hrs.	78
1250°	6 hrs.	78
1200°	66 hrs.	70, 75, 78, 82.5
1100°	3 wks.	5, 10, 15, 20, 30
1100°	2 wks.	25, 35, 40, 50
1100°	10 days	60, 70, 75, 78, 82.5, 85, 90, 95
900°	4 months	5, 10, 15, 20, 30, 40, 50
900°	2 months	60, 70, 75, 78, 82.5, 85, 90, 95

* This annealing treatment was conducted in atmosphere of pure dry hydrogen.

Metallographic examination was used to detect evidence of melting for some of the experimental alloys while in other cases it was possible to locate the solidus temperature with reasonable accuracy by direct observation of the sample during heating. This latter method has been described in detail in Section III, G-1 and is a rather effective technique when working in the vicinity of the eutectic compositions or when the solidus and liquidus are separated only by a small temperature interval as is the case for most of the Cr-Rh alloys. In most of our alloys, a sharp melting was observed at a fairly discrete temperature and the solidus temperature is therefore thought to be located with reasonable accuracy as indicated on the diagram of Fig. 37.

Losses of chromium during a solidus determination were not excessive. This may be partly due to the fact that the solidus temperatures were below the melting point of pure chromium and the time needed for a determination was rather short. The samples were supported in high-purity alumina (ΔRR grade) crucibles during the solidus determinations and there was no appreciable reaction between the metal samples and the crucibles at the temperatures involved. Nevertheless a slight violet color was noted on the surface of the crucibles particularly for alloys rich in chromium. This violet coloration was similar to that observed in our studies of Cr-Ir alloys. There was very little erosion of the crucible and apparently no significant effect on the alloy samples. The nature of this reaction is unknown.

The temperatures indicated by our thermocouples during a solidus determination were in good agreement with temperatures deduced by reference to a plot of furnace current versus temperature provided that care was taken to insure that all operating conditions corresponded closely to those which prevailed during our calibration of furnace current versus temperature.

2. Liquidus Temperatures

The liquidus temperatures were not determined directly but were estimated from the general form of the solidus curves and the location of invariant reactions. Our metallographic examination of solidus samples was also helpful in locating the liquidus through the application of well known principles associated with the lever law. This was done by estimating the relative amounts of residual solid and chilled liquid phases in the microstructures of the partially melted alloys.

3. Other Phase Boundaries

The boundaries of intermediate phases were determined by metallographic studies of alloys annealed at temperatures which would place them in close proximity to the boundary being determined. Alloys annealed within two-phase regions were particularly helpful in determining the location of phase boundaries. By estimating the relative amount of each phase in the microstructure and then applying the lever rule one can estimate the approximate location of the phase boundaries. This is particularly true if one of these boundaries is already known from some independent prior observations.

In the case of the β-phase it was possible to determine the phase boundaries by quantitative electron probe microanalyses of two-phase alloys ($\epsilon + \beta$ and $\beta + \alpha$) annealed at various temperatures. Alloys annealed within the two-phase $\epsilon + \alpha$ region, however, could not be used for electron probe microanalyses due to the presence of a fine precipitate in both the ϵ phase and the α phase regions. These precipitates apparently form during cooling. For these samples, therefore, the primary reliance was placed on metallographic studies in locating the phase boundaries.

The temperature of the peritectoid reaction was determined by annealing the alloy $Cr_{78}Rh_{22}$ at temperatures near the invariant temperature and then examining the microstructure

of the rapidly cooled alloy. Alloys quenched from above the reaction temperature contained a different major phase than alloys quenched from below the reaction temperature and in this manner the invariant temperature was bracketed within the discrete temperature range shown in Fig. 37.

Phase boundaries in the $\gamma + \epsilon$ region were determined by x-ray diffraction studies of powders obtained by first annealing the bulk samples at a given temperature and then removing the alloy powders from these bulk samples with a dental diamond wheel. Diamond powders detached from the wheel during grinding were removed by sieving the powder through a - 325 mesh screen. The alloy powders were then given a "strain-anneal" heat-treatment in high vacuum at the same temperature as that of the "bulk" anneal. X-ray patterns obtained from these powders showed sharp lines with well-resolved K_α doublets at high diffraction angles. It was not feasible to locate phase boundaries by measuring lattice parameter variations since the dependence of the lattice parameters on alloy composition was relatively small and therefore insensitive.

H. Experimental Results

1. General

The proposed constitution diagram for the chromium-rhodium system is shown in Fig. 37. All alloys were examined either metallographically or by x-ray diffraction methods or both. The data obtained by various methods were all in good agreement.

2. Solidus and Liquidus

It was usually possible to detect the first signs of melting in these samples by direct visual observation during slow heating particularly on sharp corners or edges of the sample. Melting usually occurred rapidly at a well-defined temperature and when this occurred, the furnace power was turned off and the

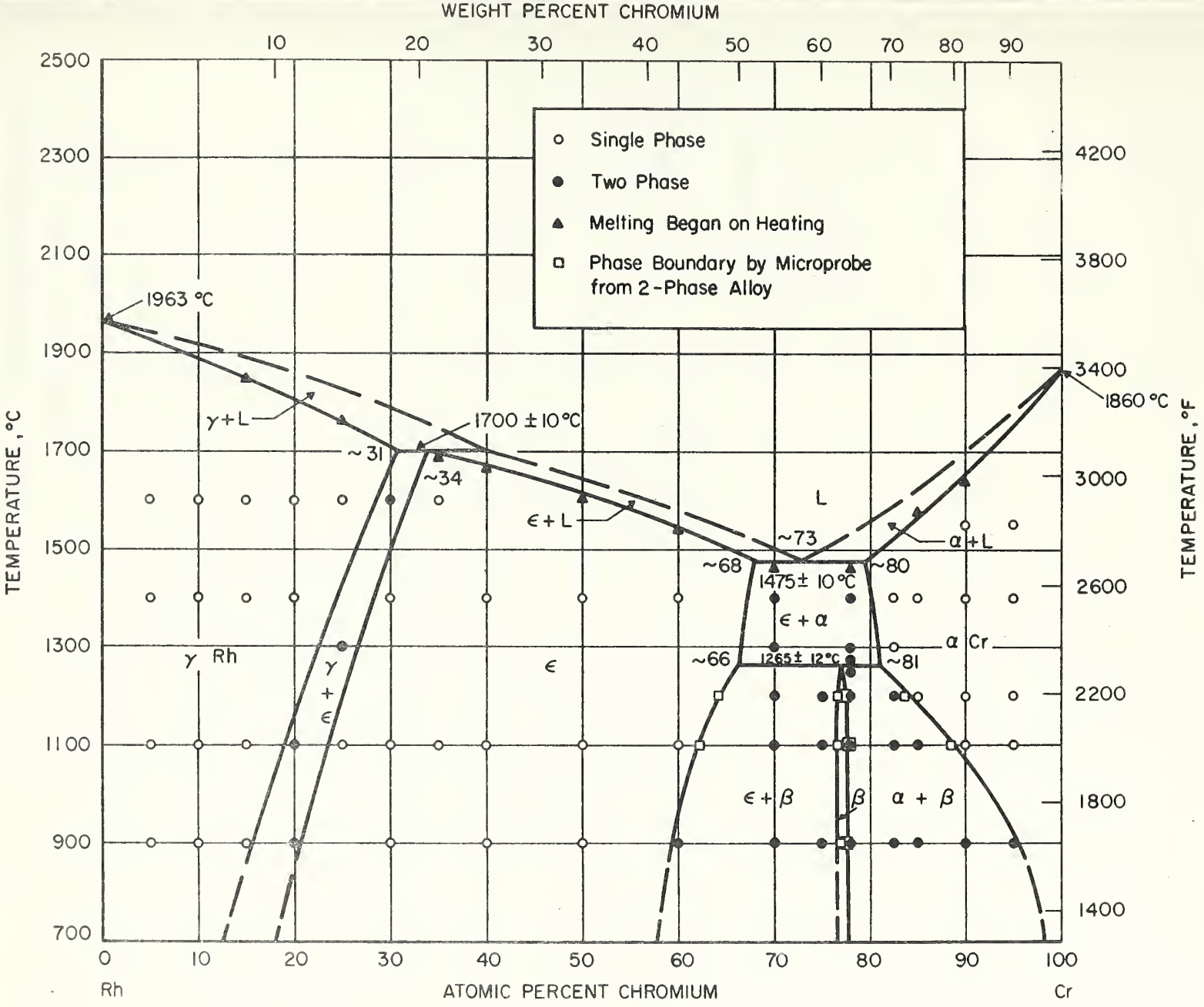

Fig. 37 - The chromium-rhodium constitution diagram.

sample was allowed to cool rapidly in the furnace. The sample was then removed for metallographic examination. In view of the relatively low temperatures and sharp melting which were observed it seems probable that the solidus temperatures have been established to an accuracy of not less than ± 20°C and it is probable that the error did not exceed ± 10°C. The liquidus temperatures are subject to more uncertainty and thermal analyses measurements would be desirable to locate the liquidus temperatures with greater precision.

3. Rhodium Terminal Solid Solution - γ

The solubility of chromium in face-centered cubic rhodium extends to a maximum of about 30 atomic percent chromium at 1700°C but at lower temperatures the solubility decreases rapidly. At 900°C we found a solubility of about 15 atomic percent chromium in face-centered cubic rhodium and this seems to be in disagreement with the solubility of eight atomic percent Cr which Raub and Mahler[1] reported, presumably on the basis of their alloys annealed at 800°C. We were unable to retain the cubic γ phase by rapid cooling of our alloy $Cr_{25}Rh_{75}$ from 1600°C and instead obtained an x-ray pattern of a hexagonal close-packed structure. However, we obtained lines of both the face-centered cubic γ and the hexagonal close-packed ∈ phases from a sample of $Cr_{30}Rh_{70}$ similarly annealed at 1600°C and rapidly cooled. It appears therefore that rapid quenching is needed in order to retain the γ phase in alloys containing more than 20 atomic percent chromium.

The strong temperature dependence of the (γ phase to ∈ phase) transformation in Cr-Rh alloys is in sharp contrast to the behavior of this transformation in Cr-Ir alloys where it is essentially temperature-independent. In this respect, the Cr-Rh alloys resemble the Cr-Co alloys which also show a strong temperature dependence for the (γ phase to ∈ phase) transformation.

It is tempting to speculate that pure rhodium may resemble pure Co in having a low temperature allotropic transformation to a hexagonal close-packed structure. In the case of pure rhodium, however, it would appear that the allotropic transformation

temperature, if it exists, could not be higher than room temperature and it may therefore have escaped detection due to the difficulty of obtaining equilibrium conditions at these relatively low temperatures.

4. Chromium Terminal Solid Solution - α

The maximum solubility of rhodium in body-centered cubic chromium is about 20 atomic percent Rh at the eutectic temperature (1475°C). However, the solubility is strongly temperature dependent below the peritectoid temperature (1265°C) and decreases to less than five atomic percent Rh at 900°C. This strong temperature dependence of the solubility is probably responsible for the precipitation effects which have been observed in α-phase alloys which have been cooled fairly rapidly.

The precipitate particles are needle-like in appearance and the alloy microstructure resembles a Widmanstatten-type structure (Fig. 45a). This structure is also observed in two-phase alloys annealed above the peritectoid temperature and rapidly cooled. The prior α-phase regions in such alloys apparently decompose during cooling (Figs. 41 to 44). The nature of this precipitation reaction is of considerable interest since it is apparently responsible for a significant increase in hardness[1] and may also improve the strength of these alloys.

We have therefore obtained x-ray diffraction data from the surface of a sample containing a sizeable amount of the needle-like precipitate (Fig. 45a). The data so obtained indicate that the precipitate particles possess a hexagonal close-packed structure. This being the case, it would appear that the precipitate is metastable since prolonged annealing of this sample at temperatures from 900°C to 1200°C results in the formation of the cubic β phase and the complete disappearance of the hexagonal close-packed structure (Fig. 44). Even more remarkable, however, is our observation of a lamellar structure in this alloy after a

prolonged anneal (two months) at 900°C. This lamellar structure was found to consist of body-centered cubic α Cr and the cubic β phase. The lamellar structure appears to be consuming the prior needle-like structure (Fig. 43b).

The discovery of this lamellar structure suggested the possible existence of a eutectoid transformation in the Cr-Rh system but a careful study of all our alloys revealed no evidence for the existence of a eutectoid reaction. We have therefore concluded that the lamellar structure results from a low temperature (~900°C) decomposition of the prior metastable needle-like regions. The needle-like regions form within the large primary grains of α Cr during fairly rapid cooling from above the eutectoid temperature (1265°C) or from above the solvus temperature of the α Cr solid solution. It would be of considerable interest to explore the mechanical properties of the Cr-rich alloys having the needle-like precipitate as well as similar alloys annealed at various temperatures so as to produce a variety of microstructures.

5. Intermediate Phase ϵ

The existence of an intermediate phase having a disordered hexagonal close-packed structure in the Cr-Rh system has been reported in the previous investigations.[1, 2] It has also been reported that chromium-rich alloys having this structure show ferromagnetic behavior.[3, 4]

It has been established in the present investigation that the solubility limits of the ϵ phase region have a pronounced temperature dependence. The solubility varies from about 20 atomic percent Cr at 900°C to 68 atomic percent Cr at 1475°C. A plot of the lattice parameters versus composition is shown in Fig. 38.

6. Intermediate Phase β

The existence of an intermediate phase Cr_3Rh having an A15 (β-W) structure was apparently first reported by

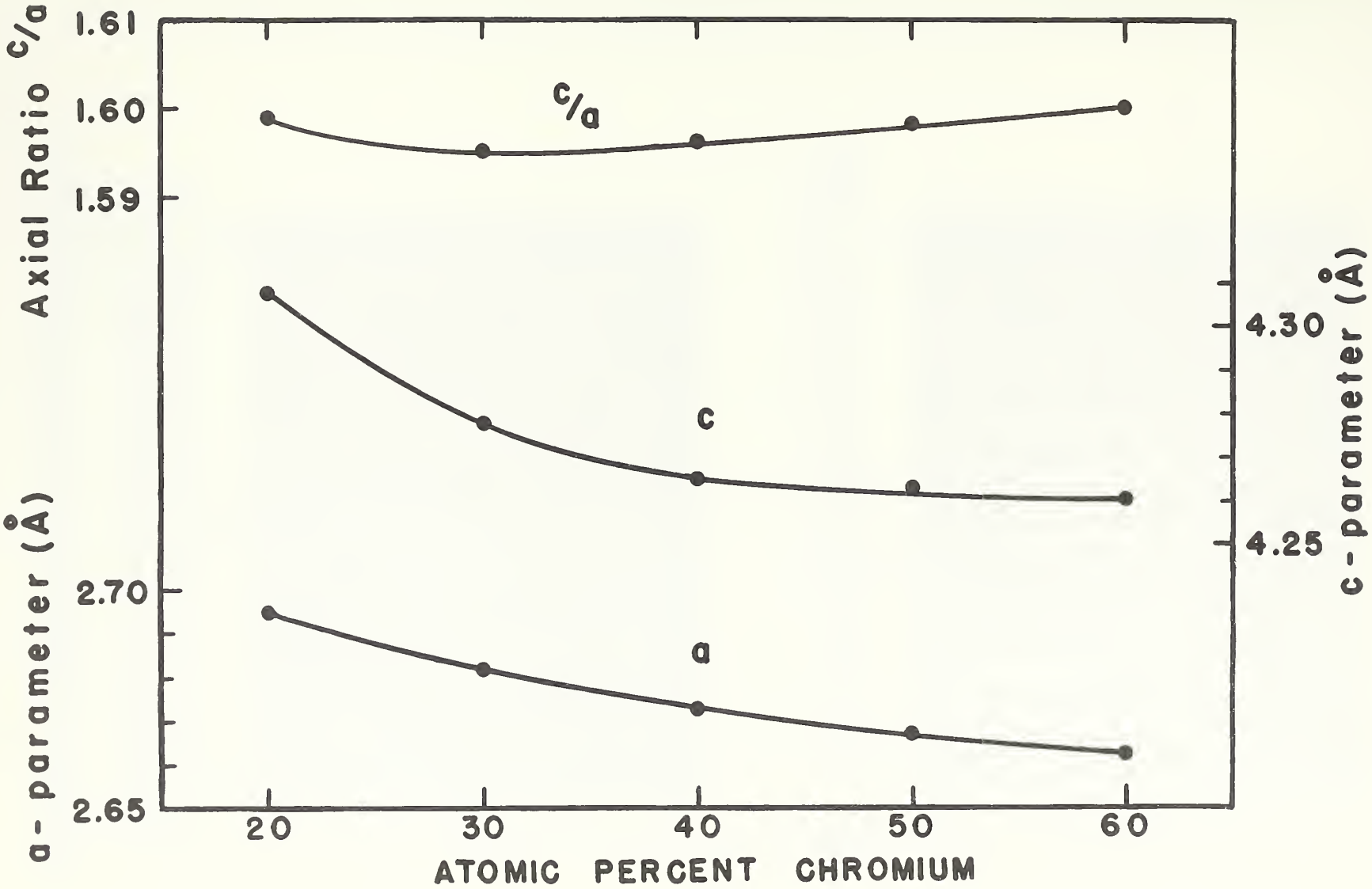

Fig. 38 - Lattice parameters of ϵ phase Cr-Rh alloys.

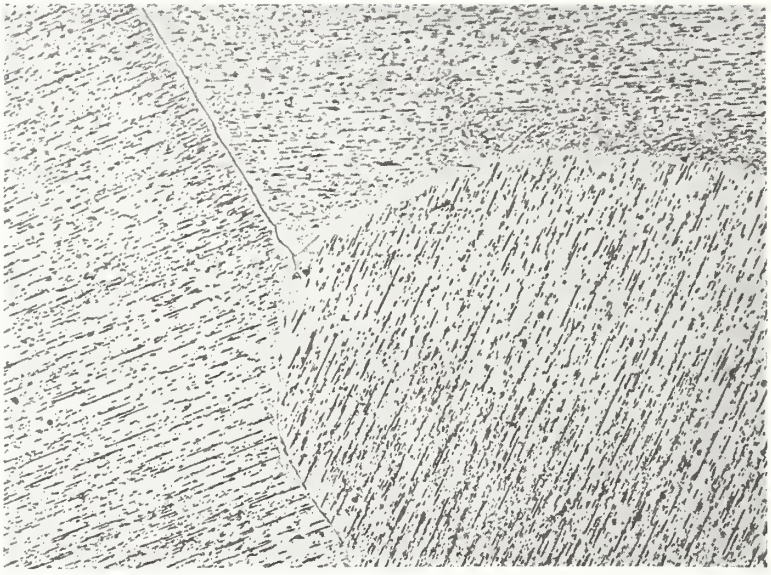

160X (a)

60 at. % Cr, 40 at. % Rh equilibrated at 900°C. Large grains of ϵ phase with precipitated particles of β phase.

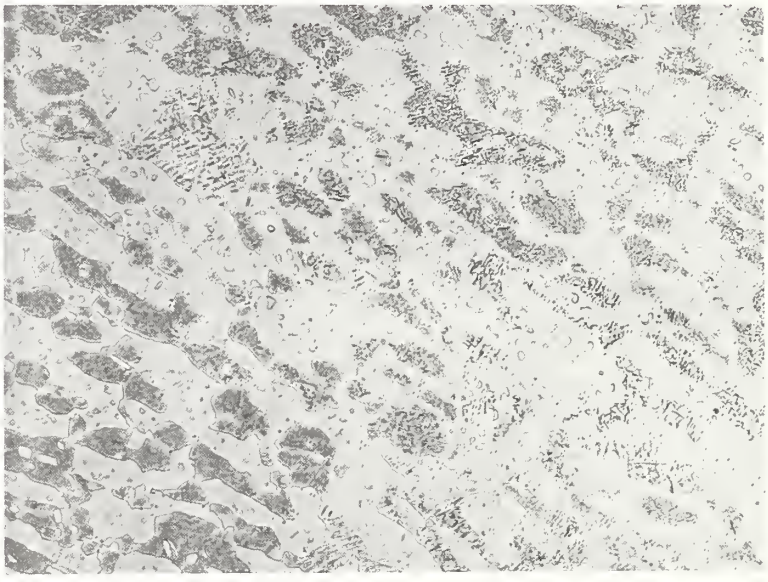

160X (b)

70 at. % Cr, 30 at. % Rh equilibrated at 900°C. The clear matrix is β phase. Darker areas are ϵ phase containing an oriented precipitate of β phase.

Fig. 39 - Microstructures of chromium-rhodium alloys.

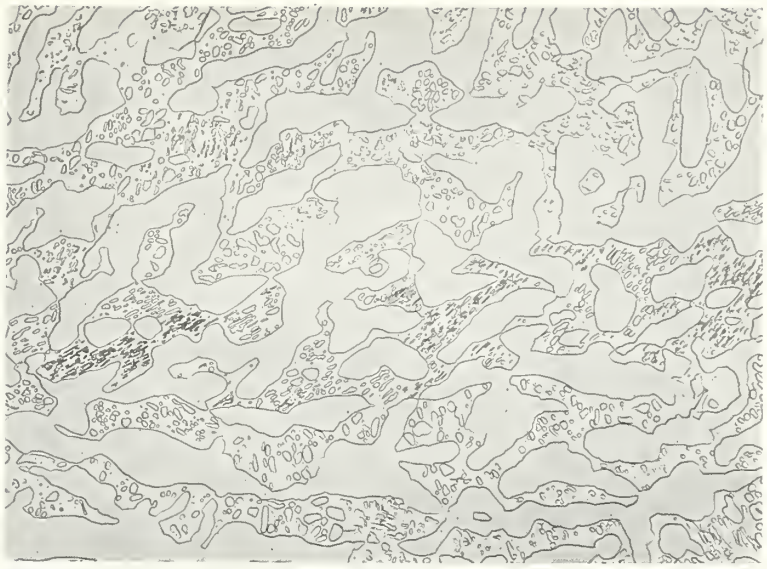

160X (a)

70 at. % Cr, 30 at. % Rh equilibrated at 1100°C. The clear areas are β phase. The ∈ phase regions contain globular particles of β phase.

160X (b)

70 at. % Cr, 30 at. % Rh equilibrated at 1200°C. Clear β phase regions coexisting with grains of ∈ phase which contain some finely precipitated β phase.

Fig. 40 - Microstructures of chromium-rhodium alloys.

160X (a)

70 at. % Cr, 30 at. % Rh equilibrated at 1300°C. The clear matrix is ϵ phase containing some acicular particles of β phase. The dark grains were formerly α Cr but now contain an acicular precipitate.

130X

70 at. % Cr, 30 at. % Rh alloy in the "as-cast" condition. Eutectic structure of ϵ phase and α phase. The α phase regions contain a dark-etching fine precipitate.

Fig. 41 - Microstructures of chromium-rhodium alloys.

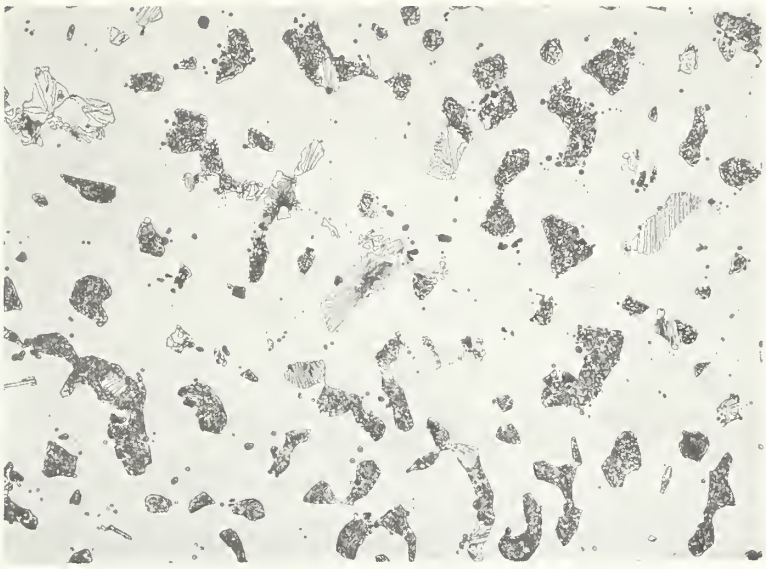

160X (a)

78 at. % Cr, 22 at. % Rh equilibrated at 900°C. The clear matrix is β phase. Darker grains are decomposed αCr.

160X (b)

78 at. % Cr, 22 at. % Rh equilibrated at 1200°C. The matrix is β phase. Darker grains containing an acicular precipitate are decomposed αCr.

Fig. 42 - Microstructures of chromium-rhodium alloys.

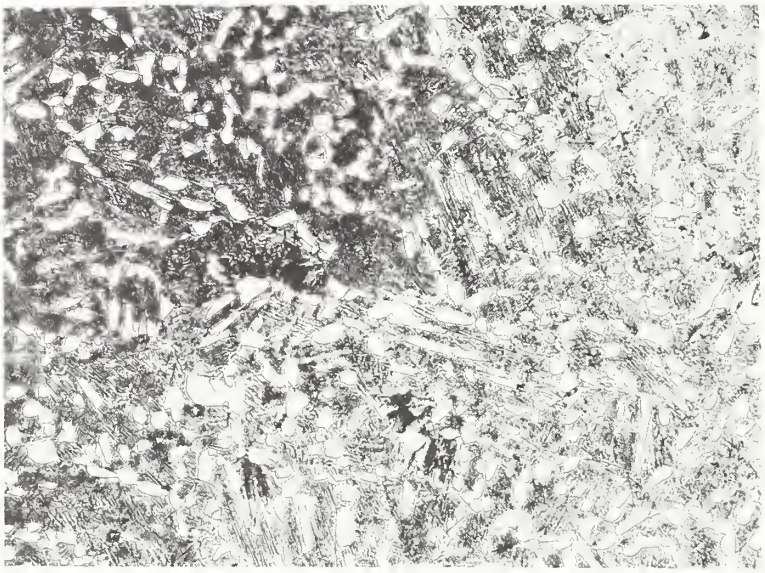

160X (a)

78 at. % Cr, 22 at. % Rh equilibrated at 1275 °C. Dark areas containing an oriented precipitate are decomposed α Cr. Light grains are ∈ phase.

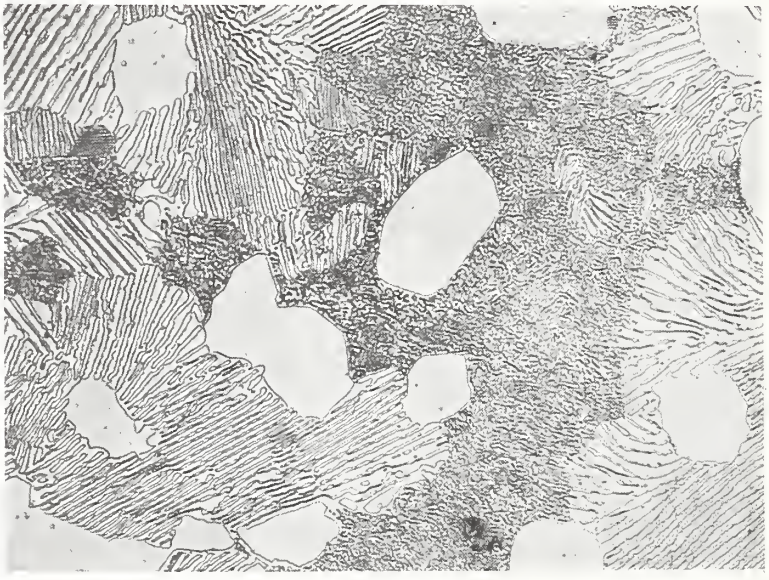

270X (b)

82.5 at. % Cr, 17.5 at. % Rh equilibrated at 900°C. The large clear grains are β phase in a matrix of decomposed α Cr. A lamellar growth of α + β is consuming the finely decomposed α Cr regions.

Fig. 43 - Microstructures of chromium-rhodium alloys.

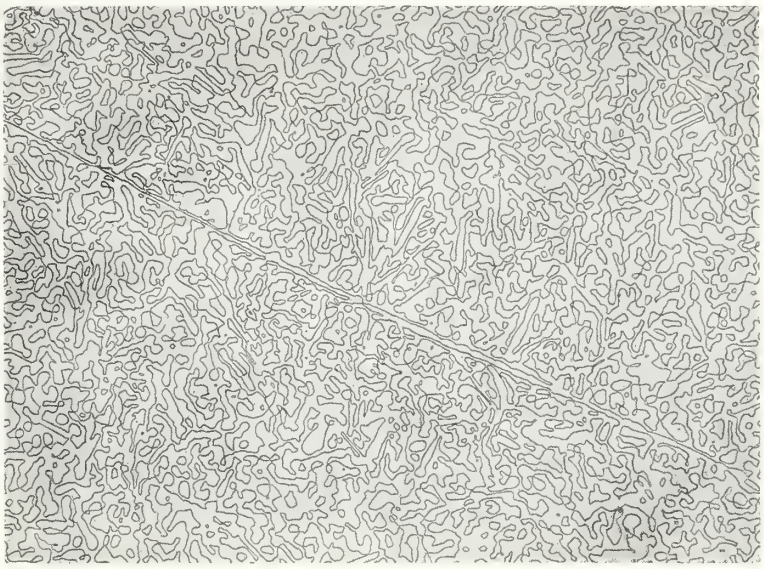

100X (a)

82.5 at. % Cr, 17.5 at. % Rh equilibrated at 1100°C. Two larger prior grains of αCr have decomposed to form a two-phase structure consisting of α + β phases.

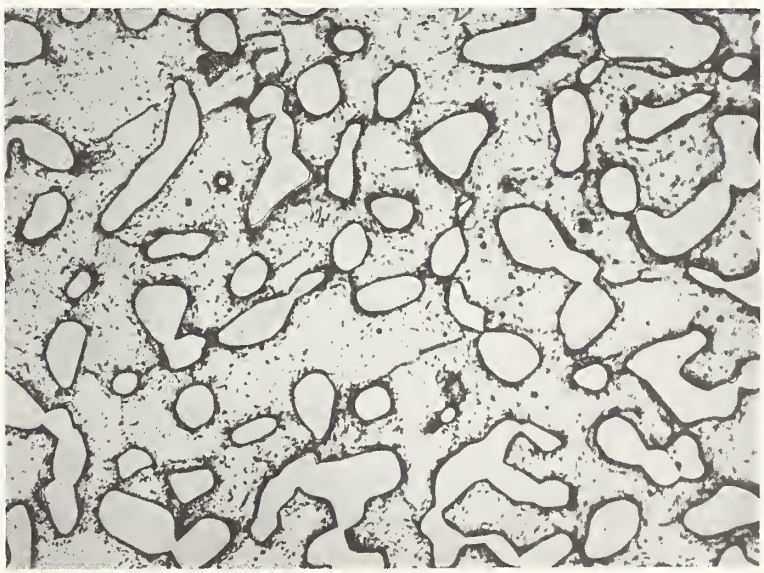

160X (b)

82.5 at. % Cr, 17.5 at. % Rh equilibrated at 1200°C. The matrix is partially decomposed αCr containing an acicular precipitate. The clear grains are β phase.

Fig. 44 - Microstructures of chromium-rhodium alloys.

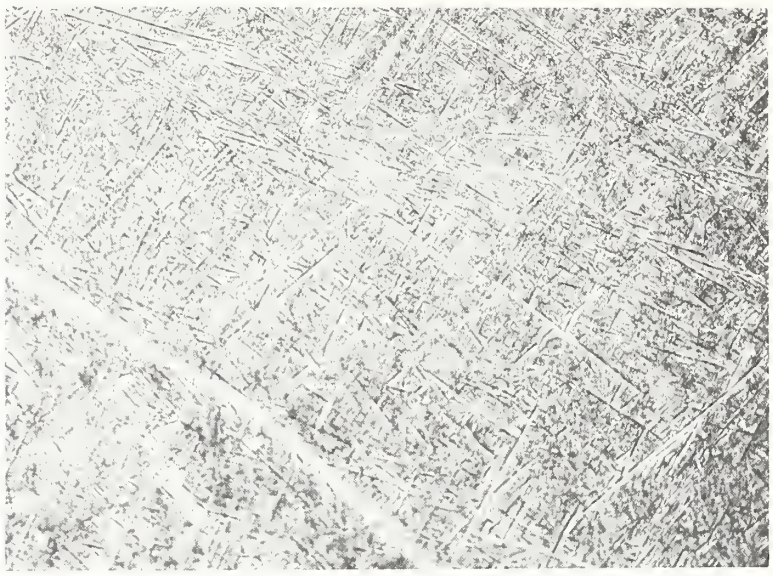

400X (a)

82.5 at. % Cr, 17.5 at. % Rh equilibrated at 1300°C. The large prior grains of αCr have decomposed to form an acicular structure consisting of αCr and an oriented precipitate having a metastable hexagonal close-packed structure .

400X (b)

85 at. % Cr, 15 at. % Rh equilibrated at 900°C. Areas which were formerly αCr contain a lamellar structure of α + β. Clear areas are β phase.

Fig. 45 - Microstructures of chromium-rhodium alloys.

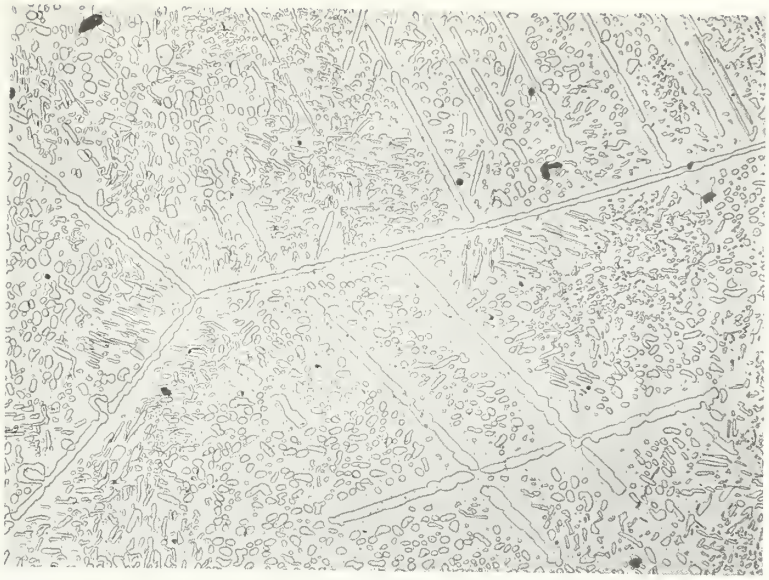

80X (a)

85 at. % Cr, 15 at. % Rh equilibrated at 1100°C. Large grains of prior α Cr containing precipitated globules of β phase.

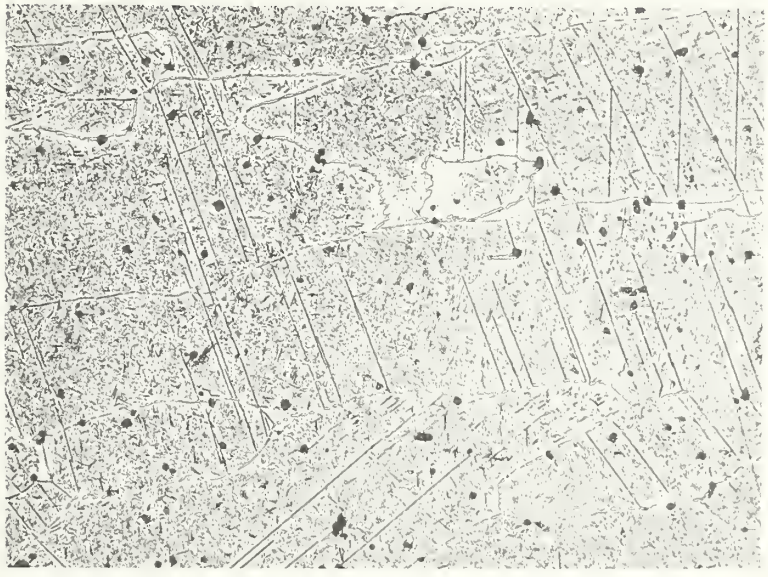

160X (b)

90 at. % Cr, 10 at. % Rh equilibrated at 900°C. Partially decomposed grains of α Cr containing precipitated β phase.

Fig. 46 - Microstructures of chromium-rhodium alloys.

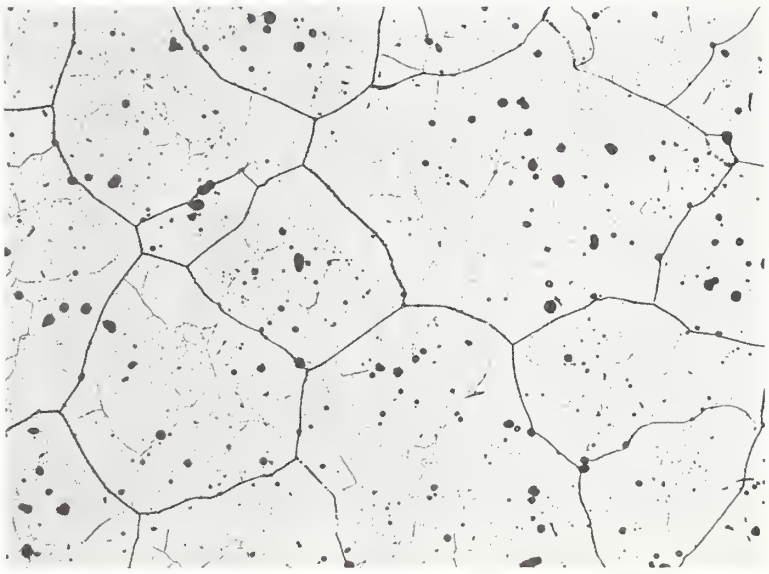

160X (a)

90 at. % Cr, 10 at. % Rh equilibrated at 1550°C. Alloy is single-phase αCr. Large grains show evidence of polyganization. Dark particles are oxide inclusions.

160X (b)

95 at. % Cr, 5 at. % Rh equilibrated at 900°C. Large grains of αCr with a small amount of β phase at the grain boundaries. Dark particles are oxide inclusions.

Greenfield and Beck.[2] It is difficult to understand why Greenfield and Beck have attributed the discovery of this phase to Raub and Mahler* since there is no mention of such a phase in the paper by Raub and Mahler.[1]

The β phase apparently forms via a peritectoid reaction at 1265°C. It has a composition range which varies from about 77 atomic percent Cr to 78 atomic percent Cr. It has been reported to possess incomplete long-range atomic ordering[5] and was found to be a superconductor at temperatures below 0.072 K.[6-8]

7. Peritectic $\gamma + L \rightleftharpoons \epsilon$

The existence of this peritectic reaction was established mainly through measurements of solidus temperatures particularly for the alloy $Cr_{35}Rh_{65}$ which lies close to the peritectic horizontal at 1700 ± 10°C. Alloys annealed in the two-phase $\gamma + \epsilon$ region usually produced x-ray diffraction patterns in which sharp lines of both the face-centered cubic and hexagonal close-packed structure coexisted. However, it was difficult to discern these two phases by metallographic studies since the microstructure of these two-phase alloys appeared to contain only a twinned structure with little or no contrast attributable to the presence of two phases.

8. Eutectic $L \rightleftharpoons \epsilon$

This reaction was established primarily by the observed solidus data and these data indicated a eutectic horizontal at 1475 ± 10°C.

9. Peritectoid $\epsilon + \alpha \rightleftharpoons \beta$

The location of the peritectoid horizontal was established by means of successive annealing treatments for the

---

* A footnote in the paper by Greenfield and Beck states that Raub and Mahler "...identified the same two intermediate phases as described here..." but a careful study of the paper which they referenced shows that only one intermediate phase is mentioned. This was reported as having a hexagonal close-packed structure and therefore corresponds to the ε phase rather than the β phase.

alloy $Cr_{78}Rh_{22}$. The composition of this alloy is such that when it is annealed and quenched from temperatures above the peritectoid temperature its structure contains the α phase as a major constituent with small amounts of the ϵ phase (Fig. 43a). When this same alloy is annealed and quenched from below the peritectoid temperature its major constituent is the β phase with small amounts of the α phase (Fig. 42b). Thus the location of the peritectoid temperature was established by successive heat-treatments which rapidly converged on the desired peritectoid temperature. The use of thermal analysis methods to detect such a transformation may lead to serious errors due to nonequilibrium cooling effects and the present method is therefore more reliable since the alloys are annealed at each temperature for a sufficient time to insure that equilibrium conditions essentially prevail.

REFERENCES

1. Raub, E. and Mahler, W., The Alloys of Chromium with Platinum, Iridium, Rhodium and Ruthenium, Z. Met., 46, 210-215, (1955).

2. Greenfield, P. and Beck, P. A., Intermediate Phases in Binary Systems of Certain Transition Elements, Trans AIME, 206, 265-276, (1956).

3. Raub, E., Metals and Alloys of the Platinum Group, J. Less Common Metals, 1, 3-18, (1959).

4. Matthias, B. T., Geballe, T. H., Compton, V. B., Corenzwit, E. and Hull, G. W. Jr., Superconductivity of Chromium Alloys, Phys. Rev., 128, 588-590, (1962)

5. van Reuth, E. C. and Waterstrat, R. M., Atomic Ordering in Binary A15-Type Phases, Acta Cryst., B24, 186-196, (1968).

6. van Reuth, E. C., Waterstrat, R. M., Blaugher, R. D., Hein, R. A. and Cox, J. E., Superconductivity and Long Range Ordering in A15-Type Structures, Proc. 10th Int. Conf. on Low Temperature Physics (Ed. Malkov, M. P.), 137, (1967).

7. Hein, R. A., Cox, J. E., Blaugher, R. D. and Waterstrat, R. M., Superconducting Behavior of A15 Compounds, Solid State Communications, 7, 381-384, (1969).

8. Blaugher, R. D., Hein, R. A., Cox, J. E. and Waterstrat, R. M., Atomic Ordering and Superconductivity in A15 Compounds J. Low Temperature Physics, 1, 539-561, (1969).

APPENDIX I: METALLOGRAPHIC PROCEDURES

Alloy specimens used for this study were in the form of small pieces which had been removed from the arc-melted buttons by an abrasive cut-off wheel or, in the case of brittle alloys, by breaking the button with a hammer. Sufficient material was usually available to permit the use of separate pieces for the various heat-treatments and consequently, remounting of specimens was seldom necessary. Samples were, therefore, mounted in bakelite. A compressed ball of copper turnings was placed in the bakelite wrapped around the rear of the specimen to produce a good electrical contact. A small hole was then drilled into the mount from behind the specimen and into the region containing the copper turnings but not deep enough to contact the sample directly. This hole served as an electrical contact area for electro polishing or etching.

Grinding operations were performed manually on a Handimet* surface grinder lubricated with cold running water. Silicon carbide papers were used in the grit sequence 240, 320, 400 and 600. The samples were then given a preliminary polish on Microcut paper sheets (Grit 600 soft). Final polishing procedures involved the use of 7 micron size diamond compound on a Struers DUR cloth followed by 1/4 micron size diamond compound on a Struers MOL cloth using the recommended lubricants. In most cases, this was sufficient preparation for electro etching but in some cases a final polish of MgO slurry on a Rayvel cloth was used.

---

* Certain commercial equipment, instruments, or materials are identified in this paper in order to adequately specify the experimental procedure. In no case does such identification imply recommendation or endorsement by the National Bureau of Standards, nor does it imply that the material or equipment identified is necessarily the best available for the purpose.

The alloys used in this study are frequently very resistant to conventional etchants such as hydrochloric or nitric acid and consequently, it was necessary to develop more suitable methods of etching. We have found that in most cases one may obtain satisfactory microstructures on these alloys by electro etching in an aqueous solution of 2% to 10% potassium cyanide using 1 to 2 amperes at an applied AC voltage of up to 30 volts. This method was particularly effective when used with a simultaneous etch-polish technique which tended to reduce any tendency toward pitting. The electrolytic cyanide etch is quite effective in delineating the boundaries of the various phases in these noble-metal alloys and also in revealing grain boundaries or twinning. However, it frequently does not produce a contrasting color within the various phase regions and consequently, it is sometimes difficult to establish the identity of an observed phase. In such cases the use of the electron microprobe was most helpful since we were unable to develop conventional etching procedures which would produce color contrast in alloys having a high noble-metal content.

APPENDIX II: X-RAY DIFFRACTION PROCEDURES

Debye-Scherrer powder patterns were taken of nearly all equilibrated samples. A Phillips 114.6 mm diameter camera was employed for these pictures using nickel-filtered copper radiation. In some cases, it was necessary to obtain an x-ray pattern directly from the surface of a flat sample or to obtain quantitative information on relative intensities. In such cases, an x-ray diffractometer was used and Mr. Howard Swanson of the National Bureau of Standards was most generous in assisting us to obtain this data.

Most of the lattice parameters given in this report were obtained by carefully measuring the Debye-Scherrer films and then applying the usual extrapolation methods in order to obtain higher accuracy. However, the precision obtainable by the methods which we employed is probably not higher than about one part in 1,000 but this seemed adequate for our purposes and limitations in the available time prevented us from extending these measurements using methods of higher precision. In most cases relative intensities were estimated by visual comparison of the lines on the Debye-Scherrer films.

Powder from the brittle alloys could be obtained simply by crushing the alloy fragments in a glazed mullite mortar and pestle but the more ductile alloys could not be crushed in this manner. Powders of the ductile alloys were, therefore, obtained by grinding a sectioned surface of the alloy fragment. Grinding of these surfaces was accomplished using a dental diamond disc (S. S. White #142 or 182) mounted in a horizontal 1/6 H. P. electric motor rotating at 3500 r. p. m. During the grinding process the alloy powders became mixed with diamond particles which had been dislodged from the discs. Fortunately the diamond particles could be almost completely removed from the collected powders by sieving through a 400 mesh screen. The diamond

particles remained on the screen while almost all of the alloy powder passed through the screen. Therefore, differential sieving, whereby the balance of the phase content is altered, was apparently not a significant factor in our x-ray data. If any residual diamond particles remained in the alloy powder, it did not seriously interfere with our interpretation of the powder patterns since the diamond lines were very spotty and readily identified as such. Care was taken to replace the discs before excessive wear had occurred since one would otherwise introduce contamination from the substance used in bonding the diamond powder to the metal disc.

Alloy powders obtained in this manner were highly strained and contained much residual cold work. This would produce considerable x-ray line broadening and such patterns would be unsuitable for accurate lattice parameter measurements. It was, therefore, necessary to remove the residual cold work by means of a high-temperature annealing treatment. This was done by placing the powder in a container of either Ta foil, alumina or thoria, depending on the alloy composition, and then heating the powder in our vacuum furnace at a pressure of less than 10^{-5} mm for a few seconds to several minutes depending on alloy composition and annealing temperature. In all cases the annealing temperature used for the powders was identical to that used in the last equilibration treatment for the bulk sample from which the powder had been obtained. After the annealing treatment, the powders were rapidly cooled by turning off the furnace power. Excessive annealing resulted in a partial sintering of the powders and, therefore, the minimum annealing time needed to effectively remove the internal strains is usually employed. Satisfactory x-ray diffraction patterns were obtained using these procedures as shown in Fig. 21.

APPENDIX III: ELECTRON MICROPROBE ANALYSIS

The electron microprobe is an instrument capable of focusing a beam of electrons on a spot approximately one micron (0.00004 inch) in diameter. These electrons excite x-rays, characteristic of the elements irradiated, which can be analyzed to yield a quantitative chemical analysis of the spot irradiated. The probe is equipped with an optical microscope and the electron beam is focused in the desired areas. The wave lengths emitted by the elements in the specimens are separated by diffraction from an analyzing crystal, and their intensities are recorded by radiation counters. By comparing the observed intensity of characteristic radiation from the sample with that of a pure element as a standard, a quantitative analysis can be obtained for the irradiated spots.

The characteristic intensities for a given element in the sample and in the standard are first corrected for pulse coincidence losses and background. From this data one obtains an intensity ratio for the sample relative to the standard. The percentage of a given element necessary to produce such an intensity ratio is calculated by either of the programs COR or MULTI8 on a digital computer. This introduces corrections for x-ray absorption, atomic number differences and secondary x-ray fluorescence. The calculations are checked by analyzing alloys of known composition which have been chemically analyzed. A comparison of compositions obtained by the microprobe with chemically analyzed compositions for several single-phase platinum-chromium alloys is shown on the next page. The alloy samples were analysed for both elements and the analytical totals varied from about 99 to 101%.

Electron probe analysis atomic % Cr	Chemical analysis atomic % Cr
28.8	29.7
39.0	39.5
49.2	49.7
59.1	59.4

Phase identity was readily established for each sample by operating the probe as a scanning electron microscope. This permits one to establish which of the two phases has the highest average atomic number as revealed by differences in brightness of the specimen image on an oscilloscope screen. This was particularly helpful in our alloys since the identity of each phase could not usually be clearly established by chemical etching methods but differences in the atomic numbers were quite large. The determination of phase diagrams using annealed two phase alloys is particularly efficient when each individual phase can be chemically analyzed. Since the phases are in equilibrium with one another, the phase boundary compositions are given directly by the compositions of the two phases. This permits a great saving in the number of samples needed. Only one sample is required for each equilibration annealing temperature in a given two phase region. Conventional methods of metallographic examination usually require the preparation of many different alloy compositions in order to obtain an identical amount of information by bracketing the phase boundary. The use of the electron microprobe also provides valuable information on the equilibrium status of the alloys and the effectiveness of quenches, since it very quickly reveals composition gradients or precipitation of a third phase.

We were particularly careful in searching for fine precipitated particles in our samples since a representative microprobe analysis will not be obtained when such precipitates occupy an area smaller than the diameter of the electron beam. In several cases, fine precipitates were suggested as being responsible for erratic results during microprobe analysis. The presence of these precipitates was later verified by optical microscopy. It is not possible to obtain an accurate quantitative analysis from phase regions containing such fine precipitates.

APPENDIX IV: HIGH TEMPERATURE VACUUM FURNACE

The furnace with which most of this work was carried out contains four strips of tantalum sheet arranged in a square configuration and heated by a high current (up to 500 amps.) at a relatively low voltage (up to about 25 volts) in a vacuum chamber evacuated to a pressure of about 10^{-6} mm Hg. A schematic diagram of this apparatus is shown below:

Fig. 48 -

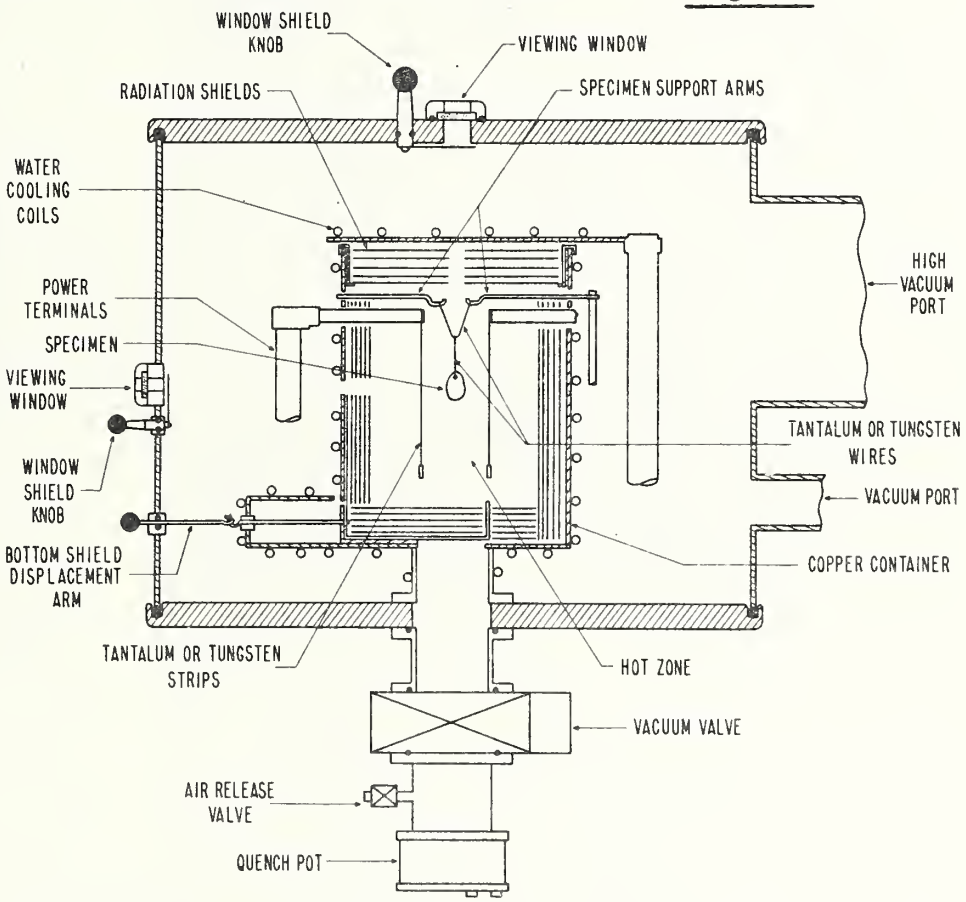

The furnace hot zone has a 2" square cross-section and is about 5" long with a zone of relatively constant temperature (±10°C) about 1" long in the center of the hot zone. The four tantalum heater strips are connected at the bottom to a common tantalum connector strip while at the top each strip is connected to its own power terminal by means of four separate tungsten arms. This design permits unrestrained lateral and vertical thermal expansion of the

heating elements resulting in better heat distribution and longer element life as compared to the cylindrical type of heating elements.

When this furnace is used for a solidus determination, the apparatus of Fig. 2 is suspended within the hot zone and the tungsten-rhenium thermocouple extends vertically to a vacuum connection which replaces the top viewing window.

This furnace may be operatured at temperatures above 2500°C by replacing the tantalum-strip heating element with a tungsten-mesh heating element having a similar square configuration. Tantalum radiation shields are similarly replaced with tungsten shields. In this manner the furnace has been operated up to the melting point of pure tantalum (about 3000°C). This required a heating element current of about 700 amps at an applied voltage of about 20 volts in each leg of the heater circuit. There are two legs in the heater circuit and the power is applied pairwise to the four strips resulting in a total power input of about 30 KVA. The furnace is shown in actual operation in the accompanying photograph.

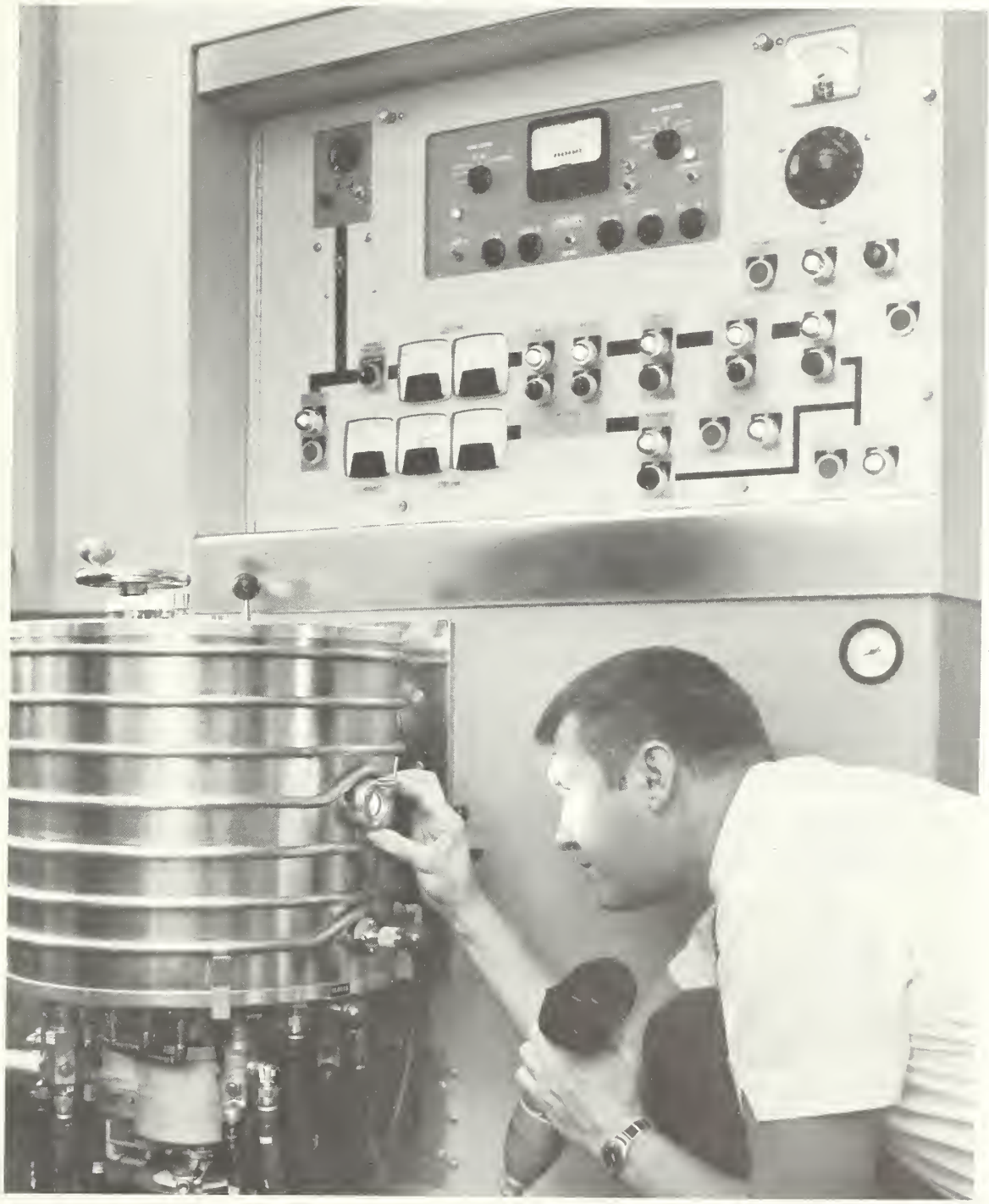

Fig. 49 - High-temperature vacuum furnace in operation.

APPENDIX V: ATOMIC VOLUME RELATIONSHIPS

It is sometimes desirable to compare the unit cell dimensions for each of the various phases which occur in a given alloy system. In order to make such a comparison it is necessary to bring the unit cell dimensions to a common basis. This is done by plotting the lattice parameter data in the form of atomic volumes (volume of the unit cell divided by the number of atoms per unit cell) as a function of composition. If one draws a straight line between the atomic volumes of each elemental component, then it is possible to determine whether any net expansion or contraction has occurred in the various intermediate phases, i.e., whether there is a positive or negative departure from a "volume Vegard's Law" relationship.

Plots of atomic volume vs. composition have, therefore, been constructed for the phases occurring in each of the four binary systems explored in this investigation. These plots are shown on the following pages. It is noteworthy that volume expansions occur in the Cr-Pt, Cr-Ir and Cr-Rh systems whereas in the V-Pt system, one observes a volume contraction. It is not yet possible to establish the reasons for this behavior.

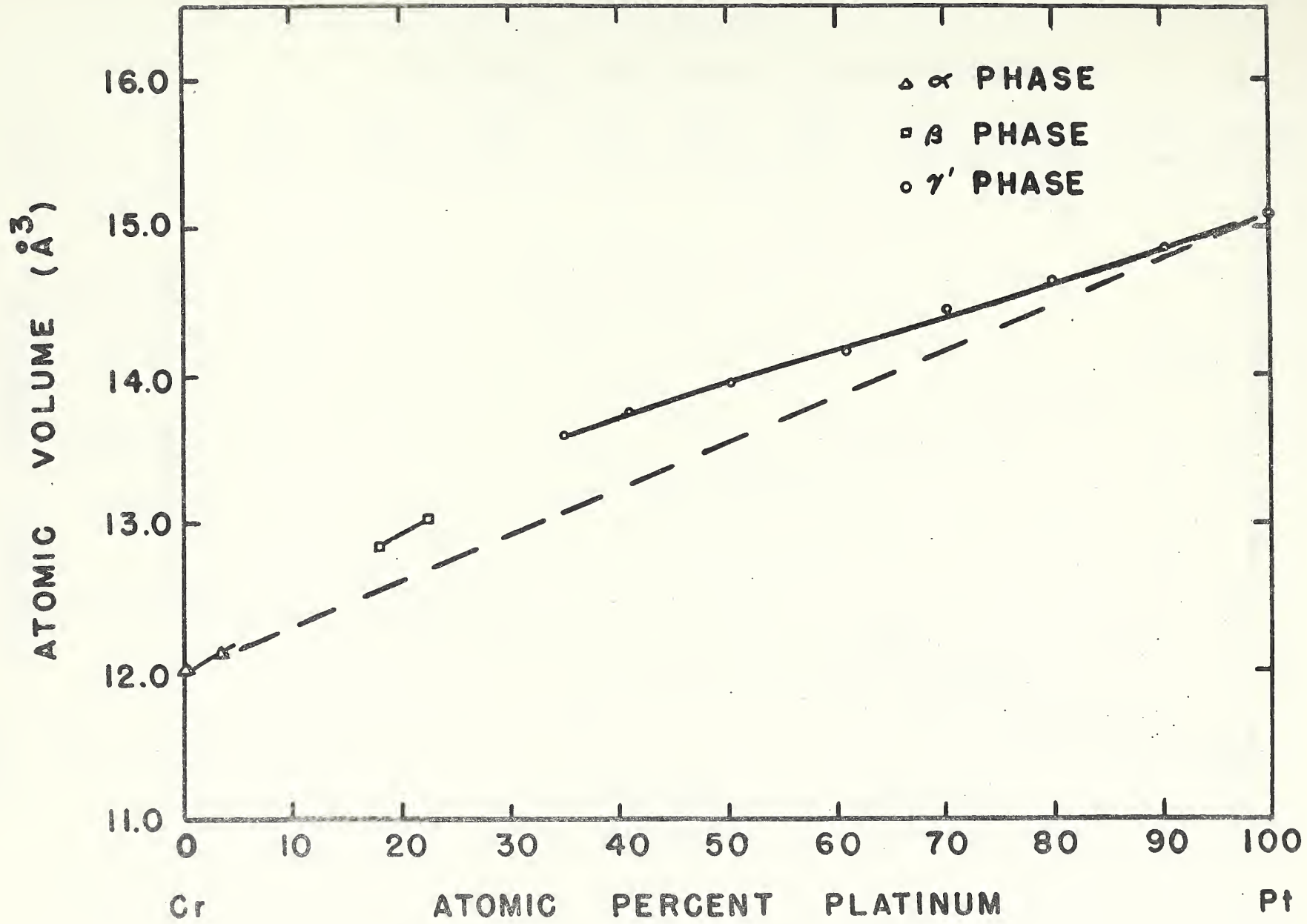

Fig. 50- Atomic volumes of Cr-Pt alloys.

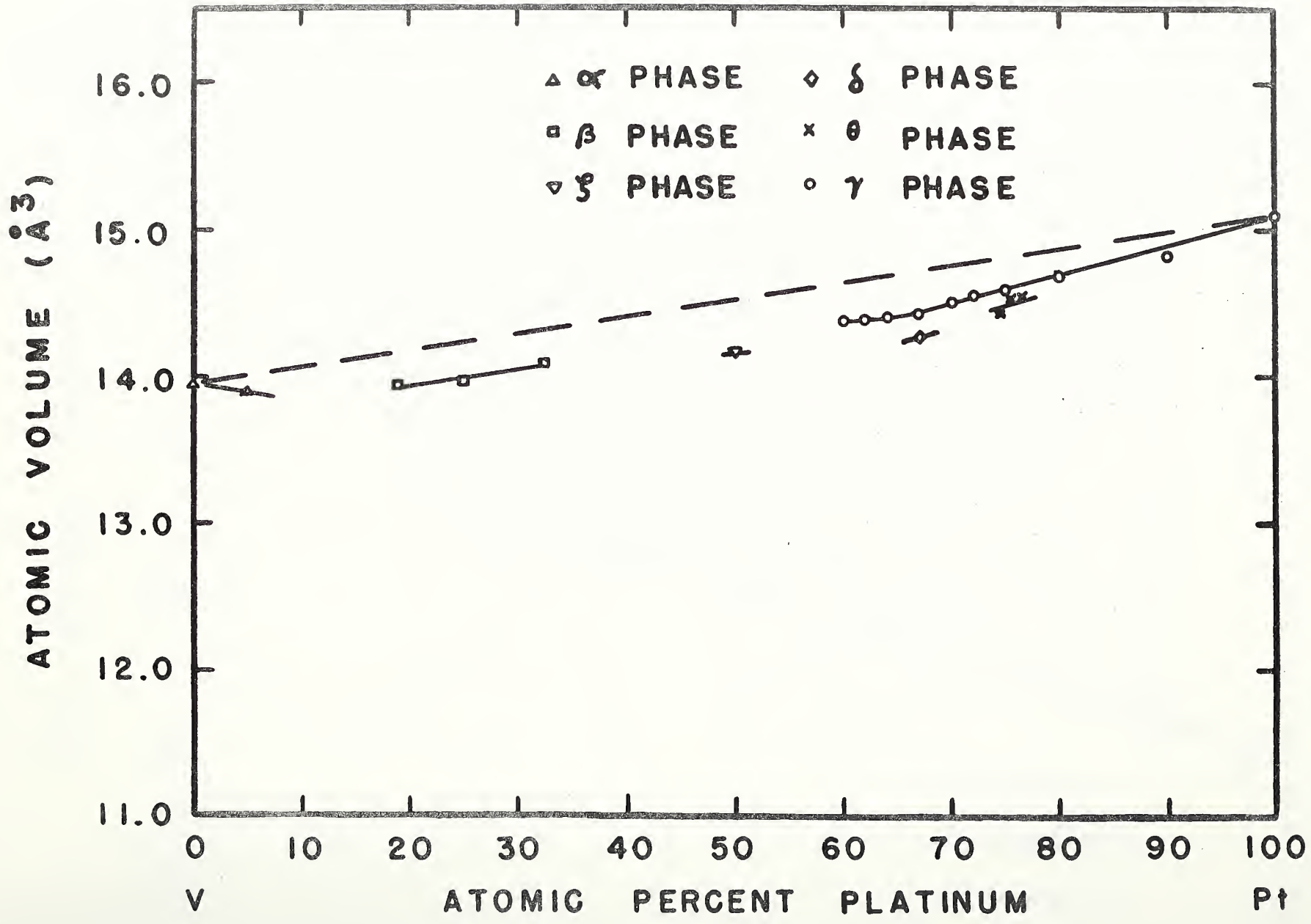

Fig. 51 - Atomic volumes of V-Pt alloys.

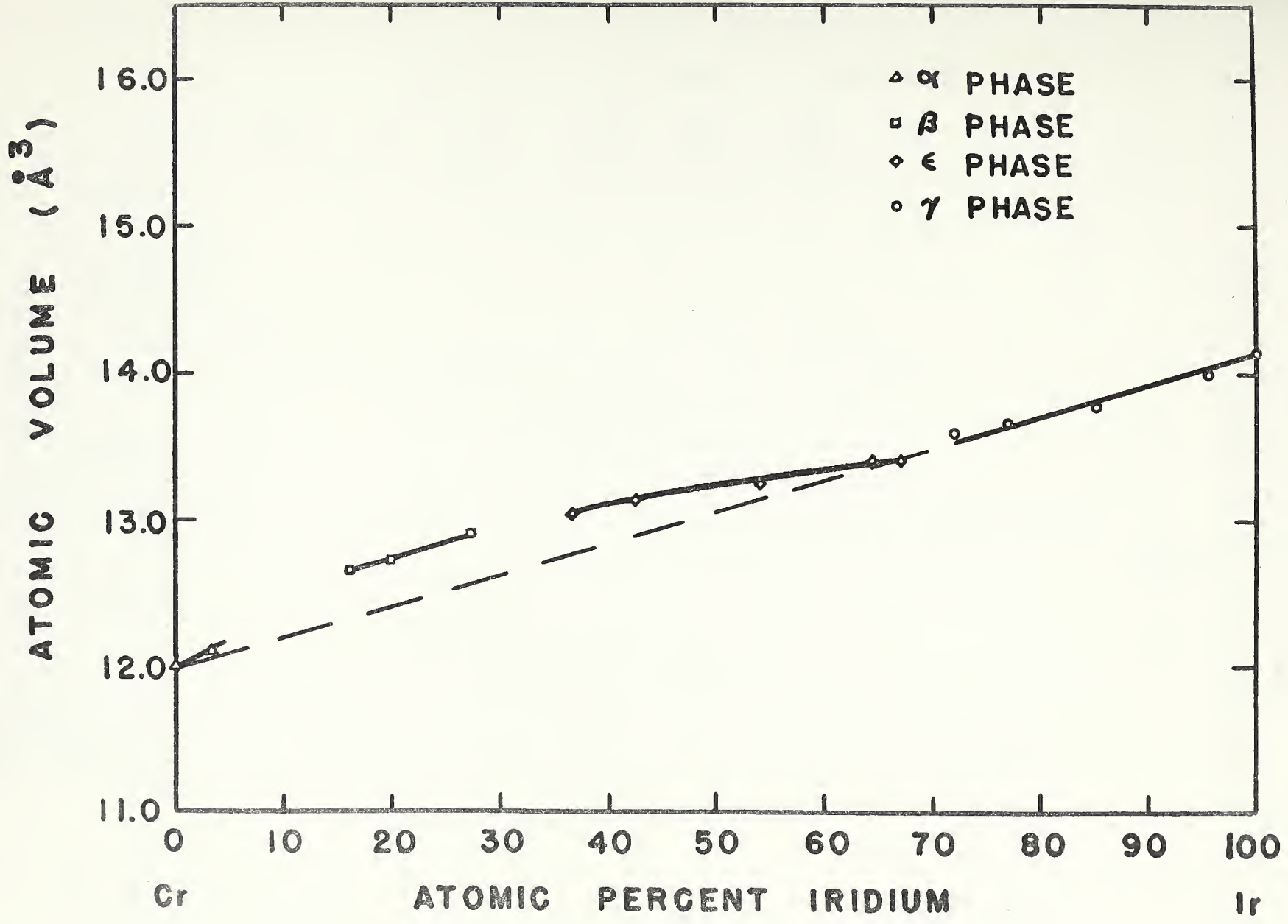

Fig. 52 - Atomic volumes of Cr-Ir alloys.

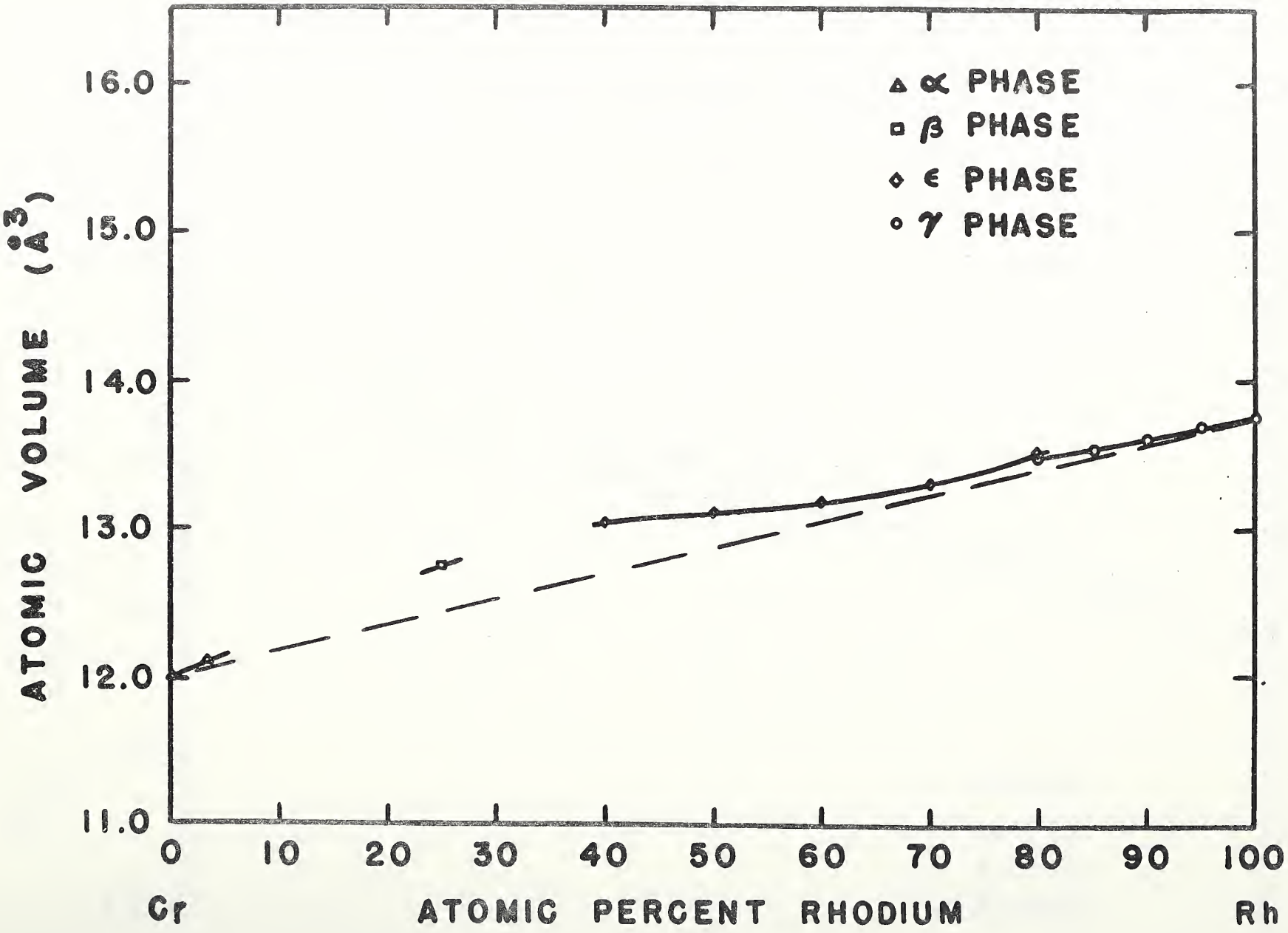

Fig. 53 - Atomic volumes of Cr-Rh alloys.


DEPARTMENT OF COMMERCE
NATIONAL BUREAU OF STANDARDS